A New Approximation of Fermi-Dirac Integrals of Order 1/2 by Prony's Method and Its Applications in Semiconductor Devices

by

Ahmed AlQurashi

A thesis
presented to the University of Waterloo
in fulfillment of the
thesis requirement for the degree of
Master of Applied Science
in
Electrical and Computer Engineering

Waterloo, Ontario, Canada, 2017

AUTHOR'S DECLARATION

I hereby declare that I am the sole author of this thesis. This is a true copy of the thesis, including any required final revisions, as accepted by my examiners.

I understand that my thesis may be made electronically available to the public.

Abstract

Electronic devices are vital for our modern life. Semiconductor devices are at the core of them. Semiconductor devices are governed by the transport and behavior of electrons and holes which in turn are controlled by Fermi-Level or the Quasi-Fermi Level. The most frequently used approximation for the population of electrons and holes based on the Boltzmann approximation of Fermi-Dirac distribution. However when the Fermi-level is closer to the majority carrier band edge, by less than 3kT, it causes significant errors in the number of the carriers. This in turn causes errors in currents and other quantities of interest. In heavily doped semiconductors, it is desirable to use Fermi-Dirac Integral itself. However this is a tabulated function and therefore approximations are developed. Most of the approximation are mathematically cumbersome and complicated and they are not easily differentiable and integrable.

Although several approximations have been developed, some with very high precision, these are not simple nor are they sufficiently useful in semiconductor device applications. In this thesis after exploring and critiquing these approximations, a new set of approximations is developed for the Fermi-Dirac integrals of the order 1/2. This analytical expression can be differentiated and integrated, still maintaining high accuracy. This new approximation is in the form of an exponential series with few terms using Prony's method. Application of this approximation for semiconductor device calculations are discussed. Substantial errors in carrier densities and Einstein relation are shown when compared with Boltzmann approximation. The efficacy of the approximation in the calculation of Junctionless transistor quantities is demonstrated as an example.

Acknowledgements

First and foremost, I would like to express my gratitude and thanks to Allah for providing me the blessings and the strength to complete this work. All the praises are due to Allah for giving me the honor of helping the humanity by contributing to enrich its knowledge.

Also, I would like to express my sincere gratitude and appreciations to my esteemed supervisor Professor. Chettypalayam Selvakumar, for his significant support, help, and guidance through my journey to obtain my master degree. The knowledge and experience I gained under Professor Selvakumar's supervision have not only developed my academic life, but they also improved my personality.

This thesis would not have been in its current without the assistance of many people. I would like to express my deepest gratitude to all my friends at University of Waterloo whom have helped me to achieve my academic goals. Special appreciations to AbdulAziz AlMutairi, Mohammed Aldosari, Nizar Alsharif, Abdulrahman Aloraynan, Hassan Alrajhi, Dawood Alsaedi, Khalfan AlMarzouqi, and all my friends whom make my life meaningful and delightful.

Undeniably, I owe my deepest gratitude and thanks to my parents, my brothers, and my sisters for their supports, prayers, and patience, and I would not have reached this stage without you. Special thanks to my mother, Fawziah, for giving me motivation and love when I needed them through the difficult times, and my brother Mohammed for taking my duties in my family.

I would like to express my genuine appreciation and gratitude to the person who is my source of patience and inspiration, my beloved wife, Duaa. She has been always supportive and patient.

I would like to thank Professor William Wong and Professor. Youngki Yoon for being the readers of my thesis.

In addition, I would like to thank University of Umm AlQura and Saudi Arabian Cultural Bureau for giving me this opportunity to get masters and PhD degrees and supporting me financially during my journey.

Dedication

This thesis is dedicated to my lovely parents, sisters, brothers, and my beloved wife

Table of Contents

List of Figures

List of Tables

List of Abbreviations

E_C : The Conduction Band

E_V : The Valence Band

E_f : The Fermi-level

m_n : The Effective Mass of Electrons

m_p : The Effective Mass of Holes

$g_C(E)$: The Density of States in the Conduction Band

$g_v(E)$: The Density of States in the Valence Band

k : Boltzmann's Constant $= 8.6173 * 10^{-5}\ eV.K^{-1}$

h : Planck's Constant $= 6.6261 * 10^{-34}\ J.s^{-1}$

T : The Temperature ($°K$)

$f(E)$: The Fermi Distribution Function

η : The Normalized Fermi-level Energy

m_0 : The Free Electron Mass $=\ 9.1094 * 10^{-31}\ kg$

$n(E)$: The Electron Density

$p(E)$: The Hole Density

N_C : The Effective Density of States in the Conduction Band

N_V : The Effective Density of States in the Valence Band

$D_{n,p}$: Diffusion Coefficients

μ_n : The Electron Mobility

μ_p : The Hole Mobility

n (in the Figures): the Normalized Fermi-level Energy (because of inability to write η in Matlab)

Chapter 1
Fermi-Dirac Integrals and Its Importance in Electronics

1.1 Preface

Integrated circuits (ICs) have been developed for the last fifty years and have transformed our modern life. Primarily, ICs have evolved by realizing ever smaller size devices achieving better performance from the reduced sizes. This has been possible by employing a set of coordinated Scaling Laws. One important consequence of the Scaling Laws is the increase in doping densities in the various semiconductor regions. As a result of this increased doping densities, a number of equations currently used in many textbooks and simulations cannot be considered accurate enough. The doping concentration plays a significant role in semiconductor devices since it changes the semiconductor devices from non-degenerate to degenerate conditions.

The degeneracy of the material depends on the Fermi-level position, and the Fermi-level position can be adjusted by varying the doping concentration levels. By increasing the number of donors or acceptors atoms in the semiconductor devices, the Fermi-level will move towards the conduction or valence bands. When Fermi-levels are very close to the conduction or the valence bands, the commonly used approximations are not valid as cannot be used to calculate carrier densities in semiconductor devices. For instance, the Boltzmann distribution has been extensively applied in most of the semiconductor devices equations, however the Boltzmann distribution is only useful if the doping concentration is below $10^{18}\ cm^{-3}$.

1.2 The Importance of Fermi-Dirac Integrals

The electron and hole densities in the semiconductor devices are crucial quantities in the semiconductor devices since most of the behaviour of semiconductor devices equations rely on them. In order to calculate the electron density at a given temperature at any given energy level, the density of states, which is the number of available states that can be occupied by an electron, is required and is depicted in Figure 1.1.a and calculated as follows:

$$g_C(E) = \frac{8\,\pi\sqrt{2}}{h^3} m_n^{*\frac{3}{2}} \sqrt{E - E_C} \qquad (1.1)$$

The density of states depends on the square root of the energy above the conduction band edge and the effective mass of the electron. While the density of states describes the energy states available, the probability that any given energy level is occupied by the Fermi-Dirac distribution law as follows:

$$f(E) = \frac{1}{1+e^{\frac{E-E_f}{kT}}} \qquad (1.2)$$

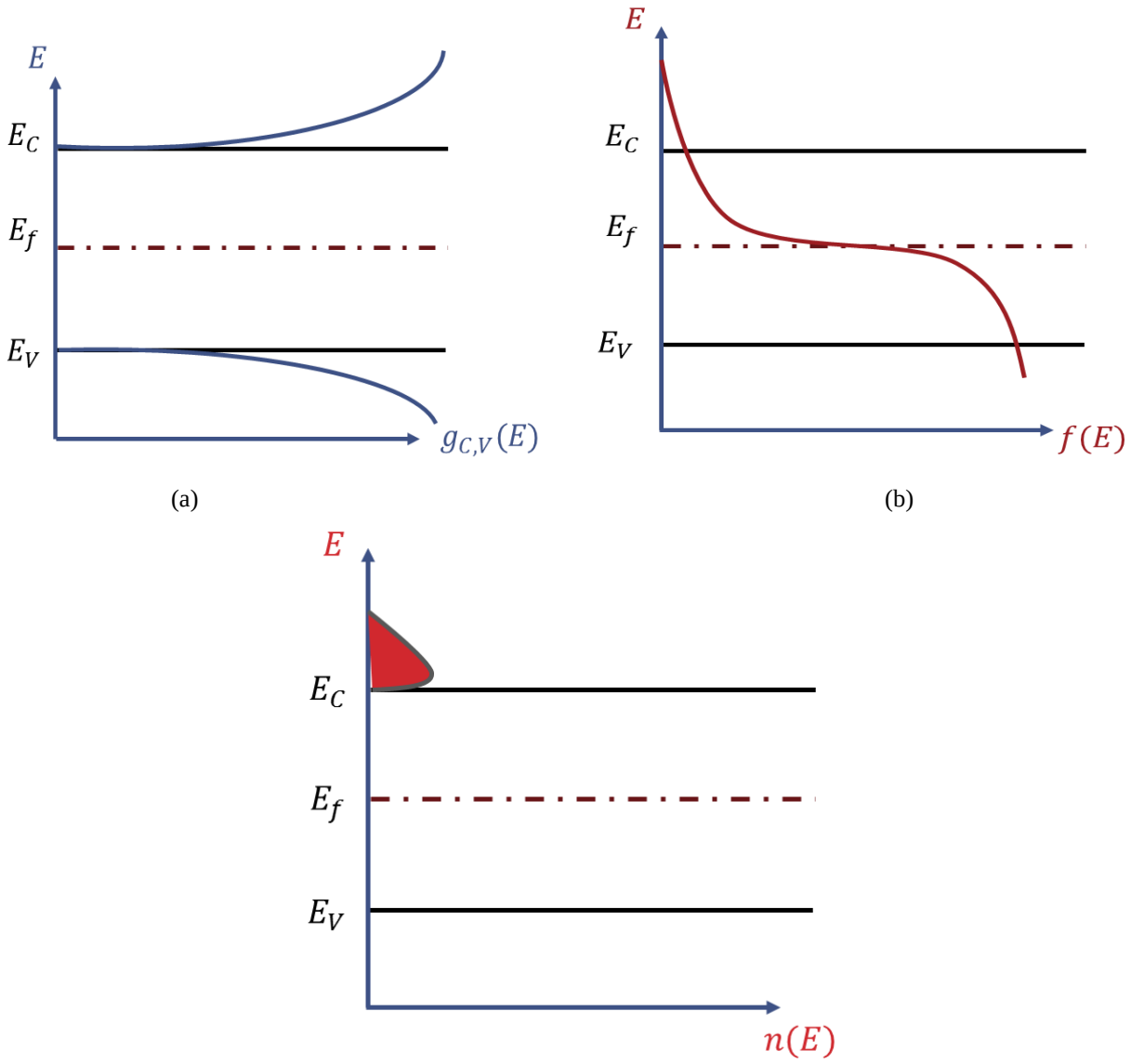

(a) (b)

(c)

Figure 1.1 (a) The Density of States in the Conduction and Valence Bands. (b) Fermi-Dirac Probability Distribution. (c) The Electron Density in the Conduction Band

The Fermi-Dirac distribution law is described in Figure 1.1.b. The electron density at each given energy level can be thus determined by multiplying the density of states by the Fermi-Dirac distribution. By integrating the density of electrons in the whole conduction band, one can determine the total density of electrons in the whole conduction band as shown in Figure 1.1.c.

$$n = \int g_C(E) f(E) \tag{1.3}$$

$$n = \left(\frac{4\sqrt{2}\pi m_n}{h^2}\right)^{\frac{3}{2}} \int_{E_C}^{E_{C,top}} \sqrt{E\_E_C}\ \frac{1}{1+e^{\frac{E-E_f}{kT}}}\, dE \tag{1.4}$$

The integral in equation (1.4) can be transformed and expressed as follows:

$$n = 2\left(\frac{2\pi m_n kT}{h^2}\right)^{\frac{3}{2}} \int_0^{\infty} \frac{t^{\frac{1}{2}}}{1+e^{t-x}}\, dt \tag{1.5}$$

Equation (1.5) includes an integral that is called one of the Fermi-Dirac Integrals (FDI), $F_{\frac{1}{2}}(\eta)$ where, $\eta = \frac{E_f - E_C}{kT}$ is the normalized Fermi level. The Fermi-Dirac Integrals have a general form, which is expressed as follows for any order:

$$F_j(x) = \int_0^{\infty} \frac{t^j}{1+e^{t-x}}\, dt \tag{1.6}$$

In semiconductor devices, the order j in the equation (1.6) is usually equal to 1/2. Instead of the use of Fermi-Dirac Integrals oftentimes, an exponential function, which is the result of Boltzmann approximation, is used to express the electron density as follows:

$$n = N_C\, e^{\frac{E_f - E_C}{kT}} \tag{1.7}$$

where $N_C = 2\left(\frac{2\pi m_n kT}{h^2}\right)^{\frac{3}{2}}$ is the effective density of states in the conduction band.

Boltzmann's approximation is an excellent one when the Fermi-level is more than 3kT away from the majority carrier band. However, when the Fermi level is less than $3kT$ away from the majority carrier band, which means the device region is a degenerate semiconductor due to the heavy doing condition, serious error results in carrier densities. Thus, we are required to use $F_{\frac{1}{2}}(\eta)$, and it has an important role in determining other significant quantities in semiconductor devices along with the electron density, hole density and the Einstein relation, which is defined as the ratio of diffusivity to mobility. In the degenerate doping level, the electron and hole densities and the Einstein Relation can be expressed as follows using FDI.

$$\mathrm{n} = N_C\ * F_{\frac{1}{2}}\left(\frac{E_f - E_C}{kT}\right) \tag{1.8}$$

$$\mathrm{p} = N_V\ * F_{\frac{1}{2}}\left(\frac{E_V - E_f}{kT}\right) \tag{1.9}$$

$$\frac{D_{n,p}}{\mu_{n,p}} = \frac{1}{q} * \frac{n,p}{\frac{dn,p}{dE_{fn,p}}} \tag{1.10}$$

The FDI is an important function in determining several characteristics in several semiconductor devices such as transistors, diodes, solar cells, Nano-devices, and in the field of particle physics. Nevertheless, the

FDI does not have a convenient closed form solution to be implemented directly in semiconductor devices. FDIs are at present either numerically evaluated or analytically approximated.

1.3 Numerical Evaluation and Tabulated Values

While the FDI does not have a closed form solution, there have been many attempts made to compute the FDI. One of the early attempts to extend the general form of FDI has been proposed by Sommerfeld, which is an asymptotic series expansion [89]. In order to obtain accurate values of FDI, there have been many numerical evaluations performed by using numerical integration of the general form of FDI [11, 96], using a pair of extrapolation procedures [28], or with quadratures of the integrand [5, 42, 61, 76]. In addition, FDI has been numerically evaluated by applying Chebyshev approximations for different ranges [29] and for different orders [94]. Where Levin-like transforms have been used to approximate the Fermi-Dirac Integrals [15], Lin *et al*. have developed two approximations based on the contour integral representations and multiple representations of simple pole [58].

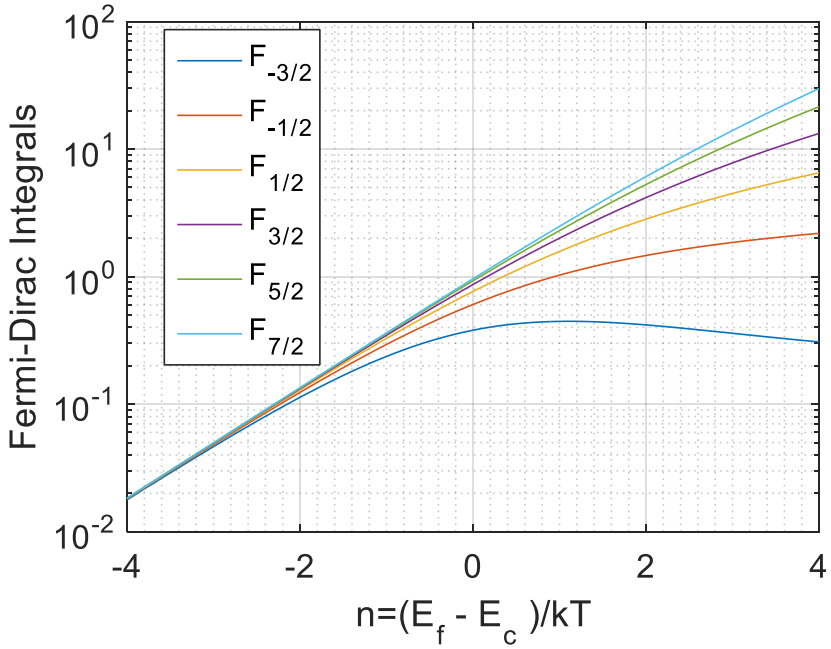

Figure 1.2 A Plot of Blakemore's Tabulated Family of FDI

With well-known integration methods, FDI has been numerically evaluated using approaches such as, the Trapezoidal method with pole corrections [41, 73, 74]. A few of the other attempts of integrating FDI have been a double series [33] and a single series [79]. In the next chapter, a few of the recent numerical evaluations will be discussed in detail.

Unlike the previous numerical evaluations, a few of the earlier computations of FDI have been tabulated in order to be used as reference values for analytical expressions. McDougall and Stoner presented one of the earlier numerical approaches to determine the Fermi-Dirac Integrals by dividing the values of η to three different ranges in order to create an approximation for each range [64]. Therefore, they formed a series representation for $F_j(\eta)$ for the range $\eta \leq 0$, and used Euler-Maclaurin numerical integration method for the ranges $0 < \eta < 3$, and $\eta \geq 3$ achieving accuracies of the order of 10^{-6} to 10^{-8}. Furthermore, Dingle [33] and Rhodes [79] published their tables of different orders of Fermi-Dirac Integrals based on the numerical methods that they developed; however, both tables were for integer orders which are not useful in semiconductor device calculations of our interest. Another set of computations of FDI, proposed and tabulated by Blakemore [16], are the ones used in this thesis as a reference. Figure 1.2 shows the family of the tabulated Fermi-Dirac Integrals computed by Blakemore.

1.4 Mean Absolute Error (MAE)

Since the approximations we are seeking should have reasonable accuracy, a method of determining the error should be applied. Two of the common methods used in evaluating accuracies of models in these studies are, Relative Root Mean Square Error (RMSE) and Mean Absolute Error (MAE). Since the number of the tried points is large, Mean Absolute Error gives smaller error than Relative Root Mean Square Error (RMSE) [20]. The two ways of determining the error are shown in equations (1.11) and (1.12)

$$MAE = \frac{1}{n}\sum_{i=1}^{n}\left|\frac{(Actual)_i-(Approximated)_i}{(Actual)_i}\right| \qquad (1.11)$$

$$RMSE = \sqrt{\frac{1}{n}\sum_{i=1}^{n}\left(\frac{(Actual)_i-(Approximated)_i}{(Actual)_i}\right)^2} \qquad (1.12)$$

1.5 Boltzmann Distribution

The numerical evaluations of FDI are not useful in providing insightful semiconductor device calculations. Therefore, an analytical approximation of FDI with sufficient accuracy is required. Some of the important previous analytical approximations will be discussed in the next chapter. We find that the earlier analytical approximations are either too complicated, hard to differentiate and integrate, or of poor accuracy. The commonly used analytical expression of FDI that is used in semiconductor devices employs Boltzmann's approximation, which is an exponential function that can be easily differentiated and integrated. Equation (1.13) defines the FDI by using Boltzmann's distribution; however, the resulting

values of FDI are not accurate enough for the modern semiconductor devices where the doping concentration levels are high. For example, in Silicon, for doping densities greater than about $5 * 10^{17} cm^{-3}$:

$$F_{\frac{1}{2}}(\eta) = e^{\eta} = e^{\frac{E_f - E_C}{kT}} \tag{1.13}$$

The Boltzmann's approximation results in reasonable accuracy where the difference between the Fermi level and the majority carriers' band's edge is larger than 3kT. The Boltzmann's approximation results in the simplest form of FDI since the form is integrable and differentiable. Figure 1.3 shows the approximated values of FDI using Boltzmann's approximation compared to the tabulated values of FDI by Blakemore.

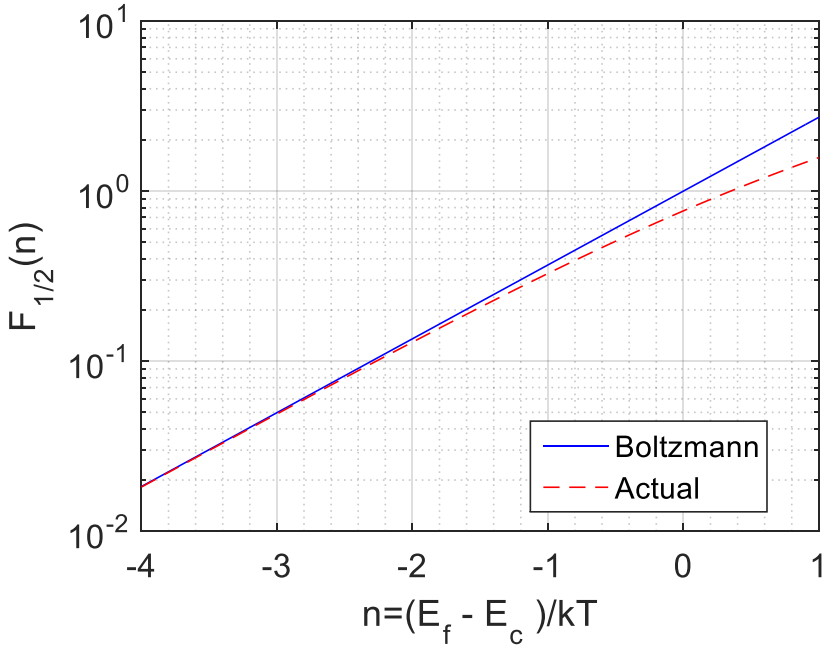

Figure 1.3 FDI using Boltzmann's Approximation compared with the actual values (Blakemore's)

As can be seen from Figure 1.3, Boltzmann's approximation of FDI holds good up to about 3kT away from the majority carrier band but results in poor accuracy when the Fermi level moves closer to the conduction band. The mean absolute error over the range shown in Figure 1.3 is 16.61%, and the mean absolute error of the range from -4 to +4 is 122.49%. Figure 1.4 shows the relative error values of each normalized Fermi level position. Consequently, Boltzmann's approximation of FDI is not accurate enough for semiconductor devices where larger doping densities are employed as a result of scaling down of the vertical dimensions.

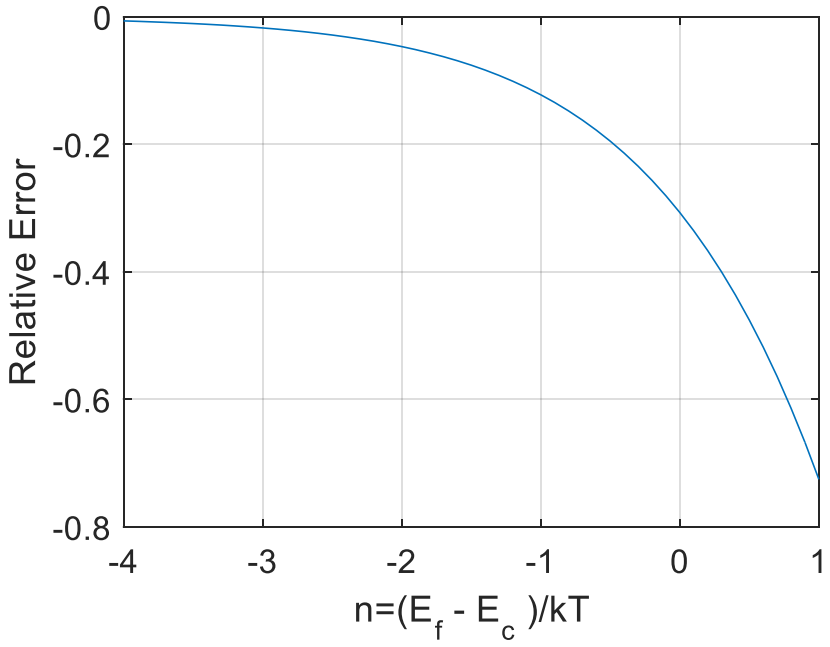

Figure 1.4 The Relative Error values of Boltzmann's Approximation of FDI

1.6 The Objectives of the Thesis

The Boltzmann's approximation of FDI is the simplest of expressions of FDI, and it has been extensively applied in semiconductor devices due to its simplicity. In this thesis we endeavor to develop approximations to FDI, which are similar to Boltzmann's approximations in their simplicity and use. As a result, we endeavor to seek a sum of exponential terms to approximate the FDI. We seek this sum of exponential terms as an approximation such that the exponents and the pre-exponential constants are chosen *systematically* to result in the minimum errors. The systematic method we employ is the Prony's method [48].

1.7 Details of the Objectives

This research has several objectives that can be classified as follows:

- Surveying and studying some of the important existing analytical approximations employed in semiconductor device applications and are simple in terms of their abilities to be calculated with measuring the mean absolute error for each.

- Forming an analytical expression of FDI in a way that can hold adequate accuracy and be differentiated and integrated without using any numerical software to make a bridge between the approximated form and its differentiation and integration.
- Applying the proposed approximation on crucial semiconductor device equations that can be significantly affected by changes in FDI and on new devices that are highly doped.

1.8 Thesis's Outline

The thesis has five chapters as follows:

- Chapter 2 investigates a few numerical and analytical approximations of FDI in terms of their accuracies and their ability to be useful in semiconductor devices equations.
- Chapter 3 provides an introduction about the Prony's method that is used to approximate the FDI in the thesis, indicating the advantages of using the Prony's method and showing the steps for approximating FDI by Prony's method.
- Chapter 4 shows the effectiveness of the new approximation of FDI in a number of semiconductor device quantities and its use in new semiconductor devices.
- Chapter 5 concludes and summarizes the proposed approximation and its use in electronic devices and discusses further work that can be done based on the proposed expression of FDI.

Chapter 2
Previous Expressions of FDI

2.1 Introduction

Since 1928 several numerical evaluations of Fermi-Dirac Integrals and analytical approximations of FDI have been developed. Some of these have been used in calculating semiconductor device quantities. This chapter will not cover some of the analytical expressions which are derived using some numerical methods such as Fourier series since they are complicated and have large errors [3, 93].

2.2 Numerical Evaluations of FDI

Accuracy is an important factor in numerical evaluations or analytical approximations of FDI, however the numerical evaluations aim to achieve very high accuracies. Numerical evaluations have been typically developed with high accuracies by using different numerical integration methods or programming languages. A few of the recent numerical evaluations with high accuracies have been proposed by Fukushima [36-39]. The four papers of Fukushima have aimed to accomplish numerical evaluations of FDI that can achieve high precisions (16 digits – 20 digits) with different orders.

Fukushima has proposed an analytical computation of generalized FDI by rewriting the first 11 terms of the Sommerfeld expansion [39] where it only covers the large values of η that are larger than the threshold values in Sommerfeld expansion , ($\eta = 12.3, 11.0, 9.75, and\ 9.0$ when the orders $j = -\frac{1}{2}, \frac{1}{2}, \frac{3}{2}, and \frac{5}{2}$, respectively). The Sommerfeld expansion will result in poor accuracy for the values less than the threshold values and the direct numerical quadrature integration can be used in this case. In addition, the proposed computational evaluation method is 10-80 times faster than the direct numerical quadrature integration.

In a different approach, Fukushima has computed the generalized of FDI by means of extending the method of McDougall and Stoner [38]. For the values of $\eta \leq 0$, he computed $F(\eta)$ by its direct numerical integration. On the other hand, the $F(\eta)$ has been computed for the values of $\eta > 0$ by splitting the integration intervals into three sub-intervals $[0, \eta)$, $[\eta, 2\eta)$and $[2\eta, \infty)$ as:

$$F(\eta) = P(\eta) + Q(\eta) + C(\eta) \tag{2.1}$$

where:

$P(\eta) = \int_0^{\eta} \frac{f(x)}{\exp(x-\eta)} dx$

$$Q(\eta) = \int_{\eta}^{2\eta} \frac{f(x)}{\exp(x-\eta)} dx$$

$$C(\eta) = \int_{\eta}^{\infty} \frac{f(x)}{\exp(x-\eta)} dx$$

The cost of the computation decreases as the value of η increases, while the computation of FDI by using Chebyshev polynomial expansion is independent on η. As a result, the proposed computation is not useful in the semiconductor devices since it results in large errors for small values of η.

A fast and precise computation of FDI of integer and half integer orders by piecewise minimax rational approximation has also been developed by Fukushima [36]. The minimax computation is a combination of the previous computation using McDougall and Stoner method [36], piecewise shortened Chebyshev expansion series [80], and the reflection formula for $F_k(\eta)$ of integer orders and positive arguments [79]. Furthermore, the proposed computation tends to use less CPU time and runs 16-30 times faster than the piecewise Chebyshev polynomial approximations [61]. In 2015, Fukushima introduced a fast and piecewise computation of the inverse of FDI order ½ by minimax rational function approximation [37].

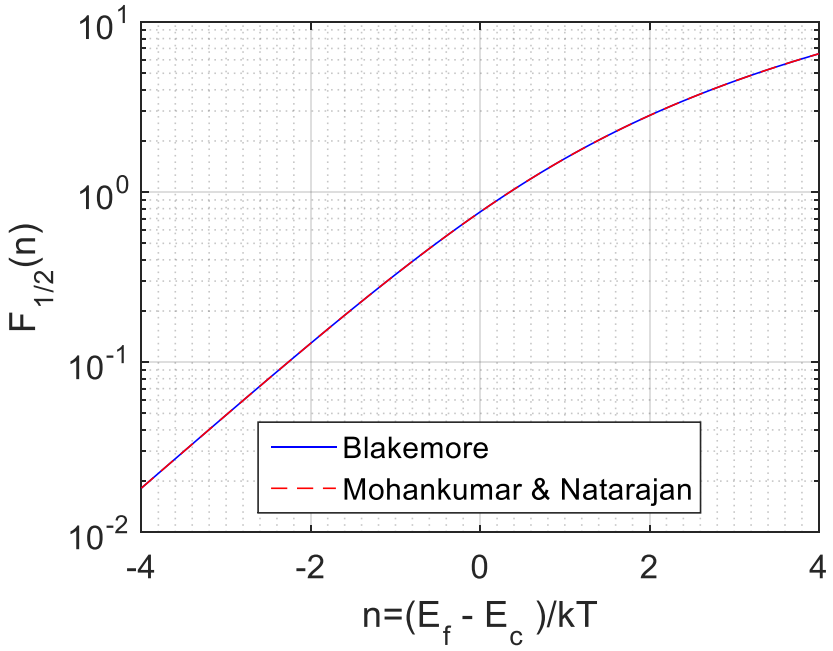

Figure 2.1 The Numerical Evaluations of FDI by Mohankumar and Natarajan compared to Blakemore's Tabulated Values

Mohankumar and Natarajan [72] proposed one of the most recent numerical evaluations, using an algorithm which uses Double Exponential, Trapezoidal and Gauss–Legendre quadratures. They proposed two different evaluations of generalized FDI for the large values of η. The first evaluation offers values

with near double precision accuracy (~ 22 digits) while the second evaluation offers the values of generalized FDI with very high accuracy (achieving relative error $< 10^{20}$). By comparing the most recent numerical evaluation of FDI proposed by Mohankumar and Natarajan, with one of the early numerical evaluations offered by Blakemore, the mean absolute error we calculated is less than $6 * 10^{-5}$, and Figure 2.1 shows the two evaluations are very close to each other.

Even though the numerical evaluations of FDI are offering high accuracy and very high precision, they are not readily usable in determining the semiconductor devices quantities of our interest; thus an analytical expression of FDI is needed to be applicable and useable in semiconductor devices equations. In the next sections, a few complicated and simple expressions of FDI are discussed in terms of the simplicity and the ability of the expression to be efficiently employed in the equations of semiconductor devices.

2.3 Complicated Analytical Expression

The accuracy of approximating FDI is a significant goal that researchers have been seeking along with the simplicity of the expression. However, few attempts of approximating FDI have achieved both accuracy and simplicity. An approximation has used McDougall and Stoner tables to acquire an accurate approach of half-order of Fermi-Dirac Integrals with a set of rational functions, but the range of the approximation is divided into two ranges ($4 \leq \eta \leq 0$, and $0 \leq \eta \leq 20$), which cannot be an approximation for all heavily doped devices [51]. Jones used rational Chebyshev approximations to acquire an expression of FDI as follows:

$$F_{\frac{1}{2}}(\eta) = \mathrm{e}^{\eta} R_{33}; [-4 \leq \eta \leq 0] \tag{2.2}$$

$$R_{33}(\eta) = b_0 + \frac{e_1}{\eta + f_1} + \frac{e_2}{\eta + f_2} + \frac{e_3}{\eta + f_3}$$

$$F_{\frac{1}{2}}(\eta) = R_{53}; [0 \leq \eta \leq 20] \tag{2.3}$$

$$R_{53}(\eta) = b_0 + b_1\eta + b_2\eta^2 + \frac{e_1}{\eta + f_1} + \frac{e_2}{\eta + f_2} + \frac{e_3}{\eta + f_3}$$

The coefficients in the equations (2.2) and (2.3), b's and f's, are being used based on the tabulated values in Jones' paper. The expression of FDI below zero involves an exponential term, which is an expression of FDI by using Boltzmann's approximation, so the approximated form is an attempt to develop an expression of FDI that is similar to the simplest form of FDI. Jones has offered different expressions of FDI with different coefficients based on the range and the order. A few analytical expressions have been

developed using the plasma dispersion function by applying the binomial expansion theorem and the gamma functions [62, 66]. One of the recent attempts to develop an expression that holds high accuracy was proposed by Guseinov and Mamedov [45]. They developed two expressions of FDI for the regions below and above zero. The expression of FDI for the range above zero can be formed as follows:

$$\mathrm{F}_{\frac{1}{2}}(\eta) = \frac{\eta^{\frac{3}{2}}}{\frac{3}{2}} + \lim_{\mathrm{N}\to\infty} \sum_{\mathrm{i}=1}^{\mathrm{N}} \mathrm{f_i}(-1)\mathrm{K_i}\left(\frac{1}{2},\eta\right) + \lim_{\mathrm{N'}\to\infty} \sum_{\mathrm{j}=1}^{\mathrm{N'}} \mathrm{f}_j(-1)\mathrm{e}^{\eta(1+\mathrm{j})} \frac{\Gamma(\frac{3}{2},\ \eta(\mathrm{j}+1))}{(\mathrm{j}+1)^{\frac{3}{2}}} \tag{2.4}$$

$$K_i\left(\frac{1}{2},\eta\right) = e^{-\eta i} \sum_{k=0}^{\infty} \frac{\eta^{\frac{3}{2}+k}}{(\frac{3}{2}+k)\Gamma(k+1)} i^k \tag{2.5}$$

$$f_i(m) = \frac{(-1)^i\, \Gamma(i-m)}{i!\, \Gamma(-m)} \tag{2.6}$$

Another expression of FDI for values below zero has been developed, but it requires calculating equations (2.5) and (2.6).

The complicated expressions of FDI have achieved high accuracies however, they are not useful for implementation in semiconductor device equations because they are not easy to differentiate or integrate.

2.4 Simple Analytical Approximations

The complicated expressions of FDI are not easily usable in semiconductor device calculations and are not easily differentiable and integrable, and hence we are seeking an expression of FDI that is accurate enough and easy to differentiate and integrate and to be employed in semiconductor device calculations. In this section, a few analytical approximations of FDI are presented in terms of simplicity and accuracy of each expression.

2.4.1 Joyce and Dixon's Approximation

In order to avoid repeated numerical evaluation of the Fermi-Dirac Integral during typical electrical characterizations of semiconductor devices under different operating conditions, a few attempts have been proposed to approximate the normalized Fermi-level position. One famous approximation introduced by Joyce and Dixon is expressed as follows [52]:

$$\eta_C = \ln\left(F_{\frac{1}{2}}(\eta_C)\right) + a_1 F_{\frac{1}{2}}(\eta_C) + a_2\left(F_{\frac{1}{2}}(\eta_C)\right)^2 + a_3\left(F_{\frac{1}{2}}(\eta_C)\right)^3 + a_4\left(F_{\frac{1}{2}}(\eta_C)\right)^4 \tag{2.7}$$

where $a_1 = 0.35355, a_2 = -4.9501 * 10^{-3}, a_3 = 1.4839 * 10^{-4}, a_4 = -4.4256 * 10^{-5}$

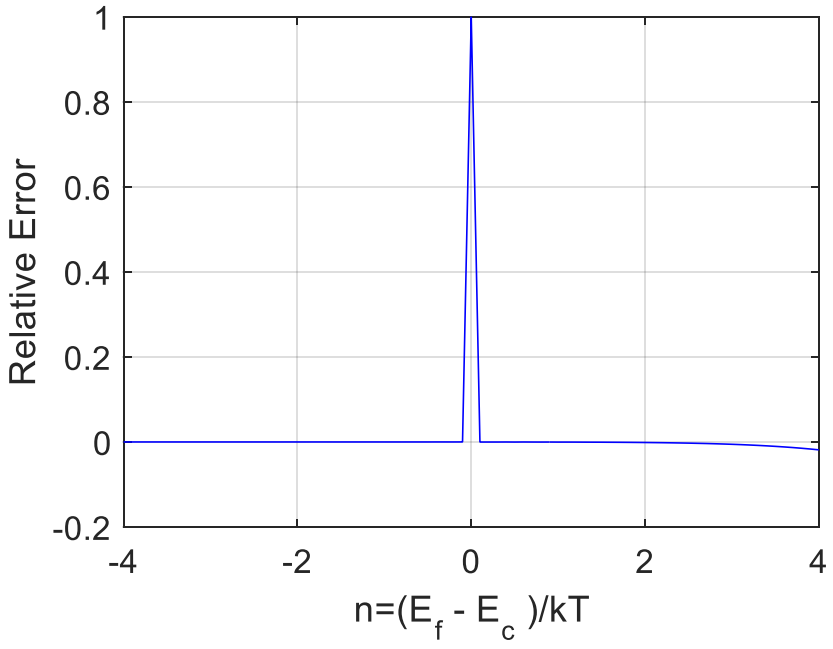

Figure 2.2 The Relative Error of Joyce and Dixon's approximated values of normalized Fermi-level positions

For calculating $F_{\frac{1}{2}}(\eta_C)$, they used the formula of electron density $n = N_C F_{\frac{1}{2}}(\eta_C)$. Joyce and Dixon's expression consists of a polynomial function. Figure 2.2 shows the relative errors of Joyce and Dixon's approximation. The mean absolute error of Joyce and Dixon's approximation is 0.0143, which is accurate enough to be employed in a semiconductor device. Therefore their expression has been applied to determine the Qusai Fermi-level of $GaAs - Al_xGa_{1-x}As$ double-heterostructure lasers [18], the current density of GaAs: (Al, Ga)As heterostructure [10], the small single junction voltage of semiconductor laser diode [47], and the Fermi-level position of high performance p-type field-effect transistors that is based on a single layered WSe_2 [35]. Another attempt proposed an approximation of $F_{-\frac{1}{2}}(\eta)$ in terms of $F_{\frac{1}{2}}(\eta)$ based on Joyce and Dixon's approximation [22].

2.4.2 Abidi and Mohammed's Approximation

Based on Joyce and Dixon's form, Abidi and Mohammed developed another approximation of normalized Fermi-level position as follows [1]:

$$\eta_C = \beta \ln\left(F_{\frac{1}{2}}(\eta_C)\right) + b_0 + b_1 F_{\frac{1}{2}}(\eta_C) + b_2\left(F_{\frac{1}{2}}(\eta_C)\right)^2 + b_3\left(F_{\frac{1}{2}}(\eta_C)\right)^3 + b_4\left(F_{\frac{1}{2}}(\eta_C)\right)^4 \qquad (2.8)$$

where $\beta = 0.9985, b_0 = -1.048 * 10^{-4}, b_1 = 35.4625 * 10^{-2}, b_2 = -4.958417 * 10^{-3},$

$b_3 = 1.199012 * 10^{-4}, b_4 = -1.532784 * 10^{-6}.$

The improvement that Abidi and Mohammed acquired is realized when the Fermi-level is above the conduction band by 3kT because of adding new terms (β, b_0). Figure 2.3 is displaying the relative error of the Abidi and Mohammed's approximation while the mean absolute error over the whole range is 0.0139, which is more accurate than Joyce and Dixon's approximation is.

Mohammed and Abidi used their approximation of Fermi-level position to determine properties of binary compound polar semiconductors with nonparabolic energy bonds [71]. Abidi and Mohammed's approximation was used to study the electric field dependence of room temperature electrotransmittance in $In_{0.53}Ga_{0.47}As$/ $In_{0.52}Al_{0.48}As$ single quantum wells [32]. Halkias used Abidi and Mohammed's approximation in order to optimize strained Si channel SiGe/Si n-MOSFET [46].

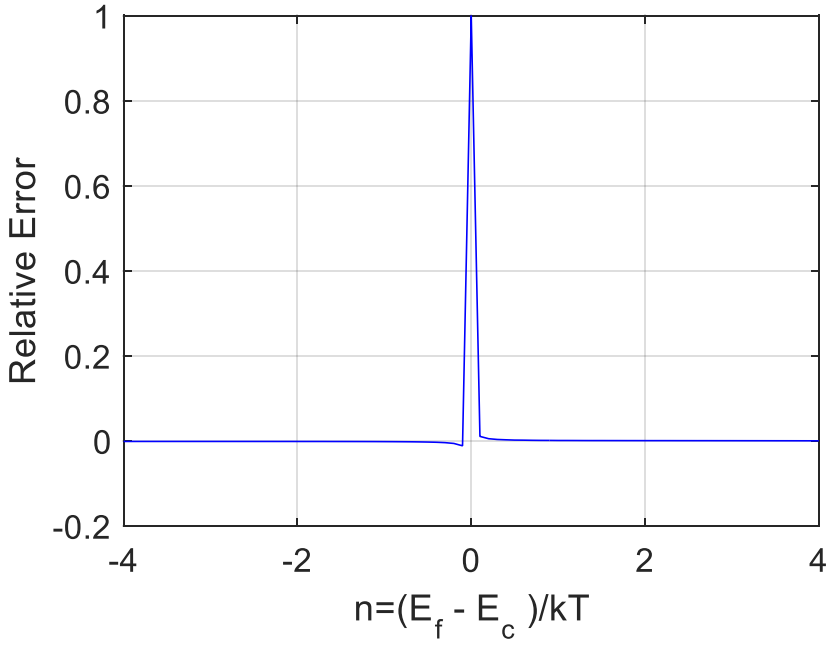

Figure 2.3 The Relative Error of Abidi and Mohammed versus Normalized Fermi-level Positions

2.4.3 Bednarczyks Approximation

Bednarczyk. D and Bednarczyk. J [12] introduced an analytical expression of $F_{\frac{1}{2}}(\eta)$ for a range $\infty < \eta < \infty$ that can be expressed as follows:

$$F_{\frac{1}{2}}(\eta) = \frac{1}{2}\sqrt{\pi}\left[\frac{3}{4}\sqrt{\pi}\left(a(\eta)\right)^{-\frac{3}{8}} + e^{-\eta}\right]^{-1} \quad (2.9)$$

where $a(\eta) = \eta^4 + 33.6\eta\left(1 - 0.68e^{-0.17(\eta+1)^2}\right) + 50$

The Bednarczyks' expression is one of the earlier attempts to obtain an analytical expression of $F_{\frac{1}{2}}(\eta)$by expanding the approximation of $F_{\frac{1}{2}}(\eta)$ by using Boltzmann's Approximation. Even though their expression has the simplest form of FDI, the expression has a polynomial equation that involves another exponential term. The accuracy of the Bednarczyks' approximation is not adequate to semiconductor device equations since the accuracy of the approximation varies based on the region as shown in Figures 2.4 and 2.5. The mean absolute error of Bednarczyk's approximation is 103.13%.

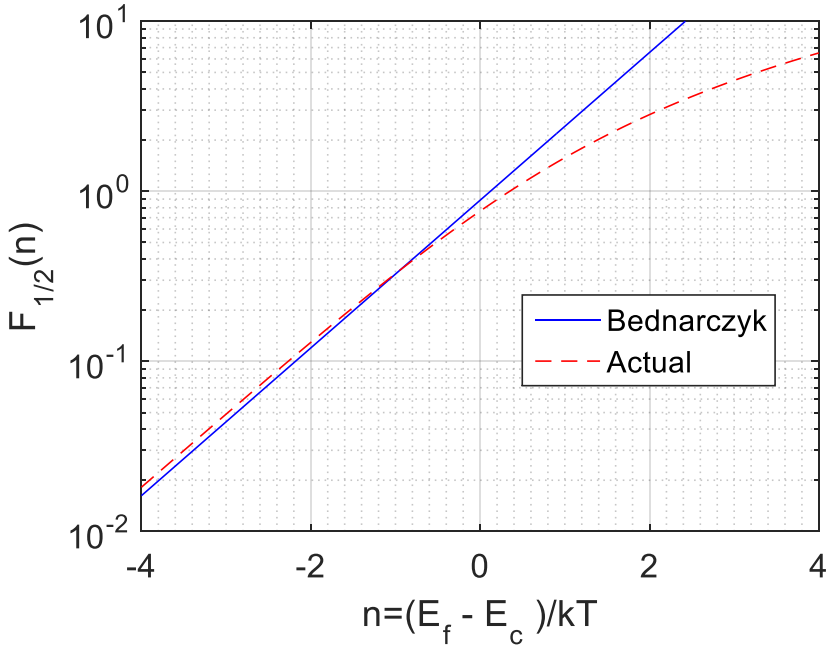

Figure 2.4 Bednarczyk's Approximated Values Compared to the Actual Values

The expression of FDI cannot be differentiated or integrated without using a numerical tool because of the complexity of the approximation. The inaccuracy in the differentiation of the approximation may cause large error in important semiconductor quantities such as the Einstein relation.

Bednarczyks' approximation has been applied to calculate the free electron concentration in the conduction band of the bulk material single quantum well [17], to determine the electric potential in GaAs nanowires [25], and to determine the band parameters in heterostructure semiconductor devices [57, 60]. Johnson and

McCallum have presented Bednarczyks' approximation as the most accurate approximation in order to be used it in numerical calculations of carrier concentrations [50]. Gao et al. computed the volume electron density and 1D electron density of quantum dots by using Bednarczyks' approximation of FDI [40].

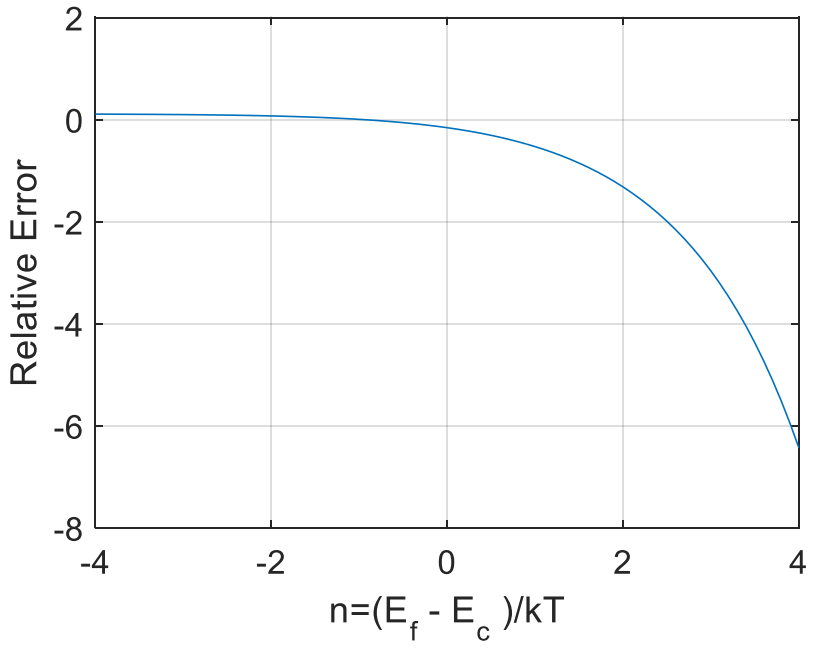

Figure 2.5 The Relative Error Profiles of Bednarczyk's Approximation

2.4.4 Aymerich-Humet, Serra-Mestres, and Millan Approximation

Aymerich-Humet et al. was trying to develop an expression that is comparable to the simplest form of FDI and is easy to be employed in semiconductor device calculations. In 1981, they proposed an analytical expression of FDI of orders (j =1/2, 3/2) that is simpler than Bednarczyk's approximation and is expressed as follows [7]:

$$F_j(\eta) = \left(\frac{(j+1)2^{j+1}}{\left[b+\eta+(|\eta-b|^c+a)^{\frac{1}{c}} \right]^{j+1}} + \frac{e^{-\eta}}{\Gamma(j+1)} \right)^{-1} \qquad (2.10)$$

For $j = \frac{1}{2}, a = 9.6, b = 2.13, c = \frac{12}{5}$.

Although their approximation is simple compared to Bednarczyks' approximation, yet their approximation requires the help of a numerical tool to differentiate and integrate the expression. As can been noticed from

Figure 2.6, Aymerich-Humet et al. approximation holds an acceptable range of the accuracy between negative 1 and zero compared to the other regions.

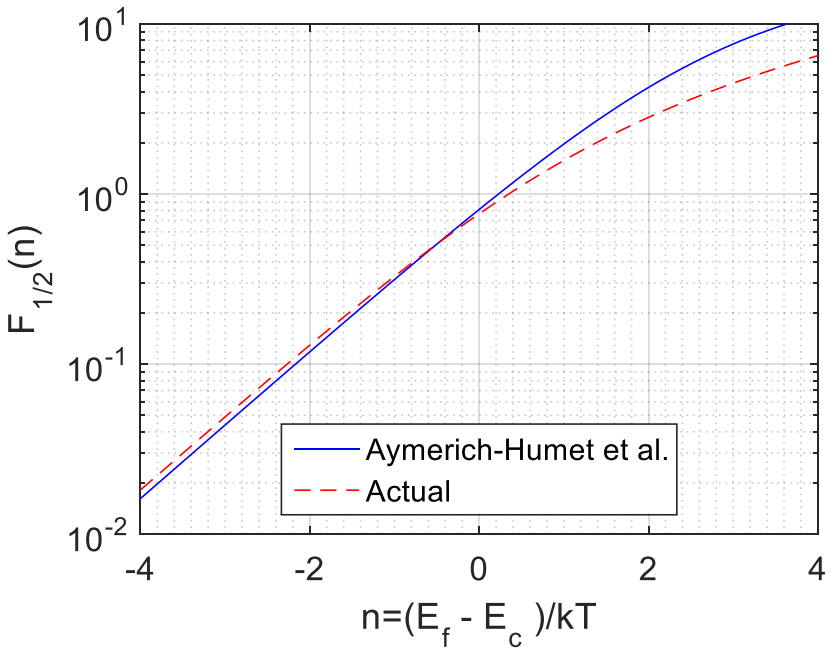

Figure 2.6 Aymerich-Humet et al. (1981) Approximated Values with the Actual Values

The mean absolute error of Aymerich-Humet et al. approximation of FDI (1981) is 0.2721. Wang et al. used Aymerich-Humet et al. approximation of FDI to evaluate Einstein relation in n-CdSe/p-ZnTe based wide band-gap light emitters [101]. Aymerich-Humet et al. approximation of FDI has been employed instead of FDI statistics to calculate the electron density of metal/insulator/AlGaN/GaN heterostructure capacitors [69] and to obtain a quantum mechanical simulation of charge distribution in Silicon MOSFETs [2]. Ramayya and Knezevic calculate the electron line density in Silicon nanowires by using Aymerich-Humet et al. approximation [78]. Lami and Hirlimann used Aymerich-Humet et al. approximation of FDI to compute the normalized carriers of CdS devices in order to determine the temperatures and the chemical potentials of the thermalized electrons (T_e, μ_e) and holes T_h, μ_h) [55]. Wang et al. calculated the current density of AlGaN/GaN high electron mobility transistors (HEMTs) by using Aymerich-Humet et al. approximation instead of FDI statistics [100].

After two years, Aymerich-Humet et al. proposed a generalized approximation of FDI that has a similar form to their previous approximation but with a different set of the coefficients (a, b, c) [8]. The coefficients in the new approximation are expressions based on the FDI's order as follows:

$$a = \left(1 + \frac{15}{4}\,(j+1) + \frac{1}{40}\,(j+1)^2\right),$$

$$b = 1.8 + 0.61j,$$

$$c = 2 + \left(2 - \sqrt{2}\right)2^{-j}.$$

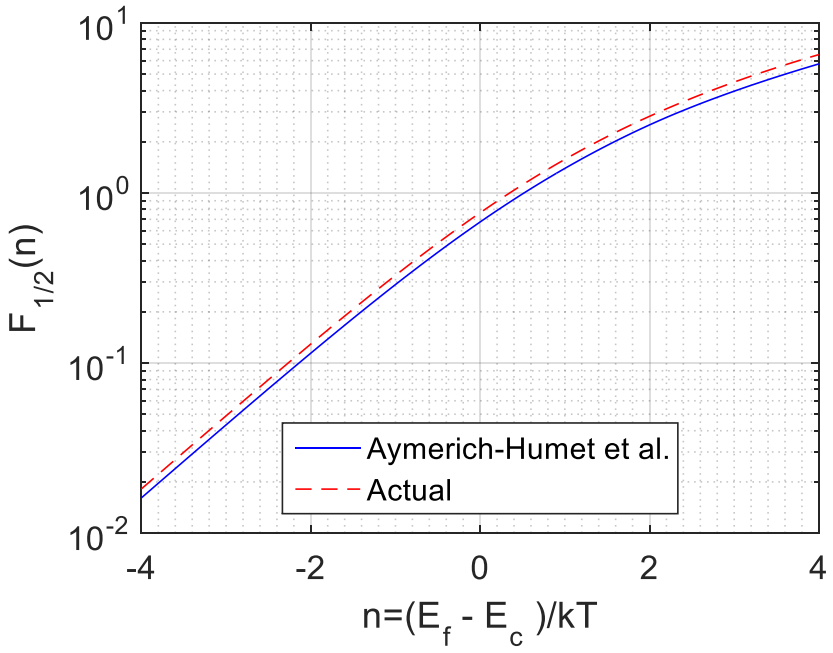

Figure 2.7 Aymerich-Humet et al. (1983) Approximated Values with the Actual Values

Their new approximation's mean absolute error is 0.1155, which is more accurate than their previous approximation. Their new approximation of FDI is graphically shown in Figure 2.7 comparing it to the Actual values of FDI. As can be seen from Figure 2.7, the shape of the approximated values is similar to the shape of actual values with shifting down.

Sherwin and Drummond used Aymerich-Humet et al. (1983) approximation to obtain the linear density of electrons in AlGaAs/GaAs quantum wires [86], and Szmyd, Hanna, and Majerfeld calculated the Fermi-level position in GaAs:Se by using Aymerich-Humet et al. (1983) approximation [91]. Szmyd et al. have acquired the screening length of heavily doped GaAs: Se devices by using Aymerich-Humet et al. (1983) approximation of FDI [92]. Idrish Miah used the Aymerich-Humet et al. (1983) approximation in order to calculate the diffusion coefficient of spin-sensitive electronics [67, 68]. Aymerich-Humet et al. (1983) approximation of FDI has been used to determine the mobile charge density of ballistic nanowire transistors [24]. The surface potential of double-gate tunnel-FETs has been determined by using

Aymerich-Humet et al. (1983) approximation instead of FDI statistics [105]. Wan et al. have obtained the carrier density of graphene field effect transistors by using Aymerich-Humet et al. (1983) approximation of FDI [99].

Figure 2.8 shows the relative errors of both Aymerich-Humet et al. approximation of FDI where the later approximation offers small relative errors compared to the old approximation.

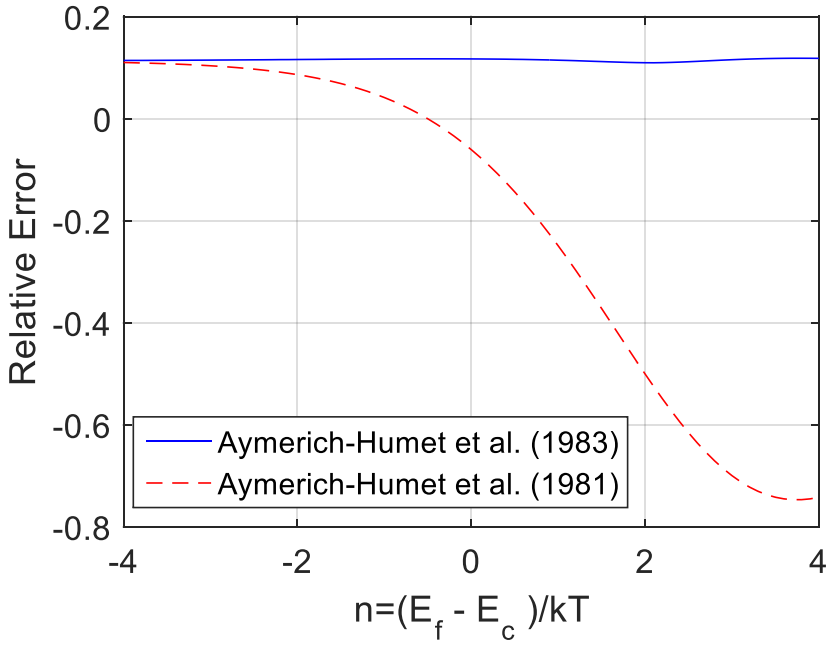

Figure 2.8 The Relative Error Profiles of Both Approximations Compared to the Actual Values

2.4.5 Marshak, Shibib, Fossum, and Lindholm Approximation

Marshak et al. proposed one of the most accurate approximations of FDI which combines the FDI approximation of Boltzmann in the numerator and the denominator as follows [63]:

$$F_{\frac{1}{2}}(\eta) = \frac{e^{\eta}}{1+C(\eta)e^{\eta}} \qquad (2.11)$$

$$C(\eta) = -4.4 * 10^{-2}\eta + 3.1 * 10^{-1} \qquad \text{For } (\eta \leq 2)$$

$$C(\eta) = e^{8.6*10^{-3}\eta^2 - 3.2*10^{-1}\eta - 8.8*10^{-1}} \qquad \text{For } (2 < \eta \leq 12)$$

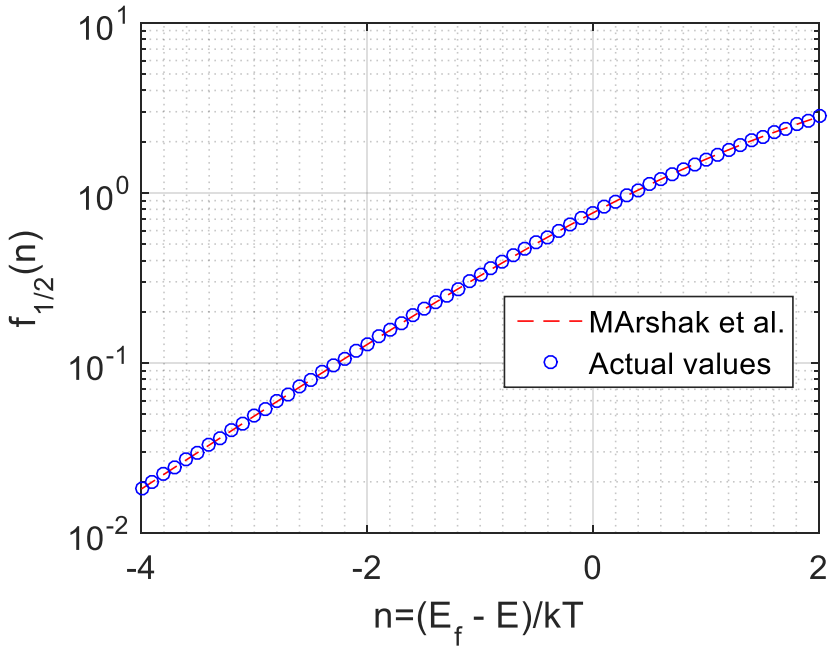

Figure 2.9 Marshak et al. Approximation Compared to the Actual Values

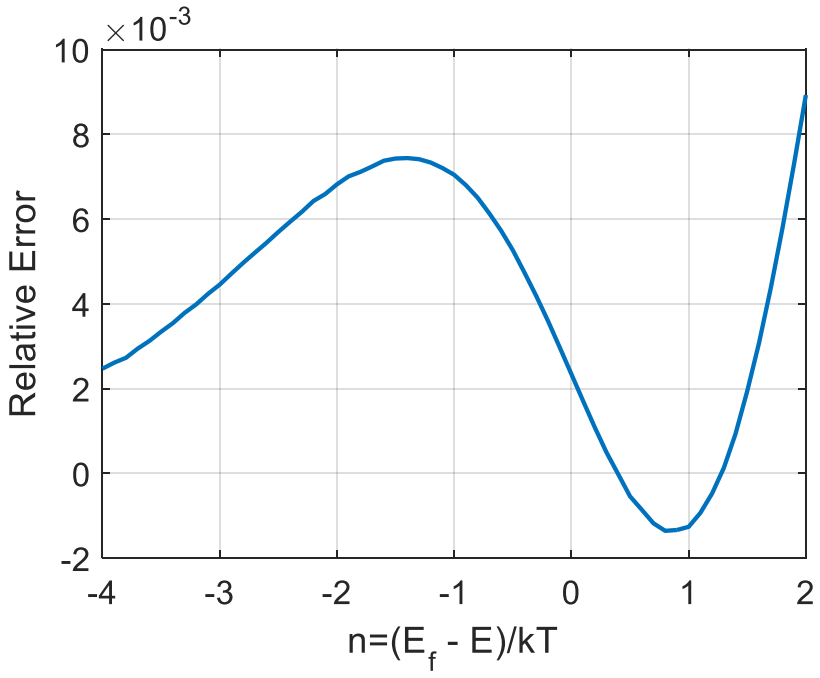

Figure 2.10 The Relative Error of Marshak et al. Approximation versus Fermi Level Position

The approximation uses a pre-exponential function, which is a polynomial function but the function varies with the range, one polynomial for η below two and an exponential function for the range between two and twelve. The Marshak et al. approximation will be like FDI by using Boltzmann's approximation when the pre-exponential function equals to zero. Figure 2.9 shows Marshak et al. approximated values, which cannot be clearly seen because they are fitting pretty close to the actual values.

The differentiation and the integration of Marshak et al. approximation cannot be achieved without using a numerical tool. The relative errors of the approximation are shown in Figure 2.10 compared to the actual values, and the mean absolute error is 0.0043.

Marshak et al. used their approximation of FDI to determine the semiconductor device quantities such as current density and Einstein relation [63]. De et al. introduced an expression of effective intrinsic carrier density in heavily doped InGaAsP devices [31].

2.4.6 Selvakumar's Approximation

Another attempt to approximate FDI has been proposed by Selvakumar, which is an exponential function with a seven term polynomial in the exponent [85]:

$$F_{\frac{1}{2}}(\eta) = e^{g(\eta)} \tag{2.12}$$

where $g(\eta) = \sum_{k=0}^{7} a_k \eta^k$

$a_0 = -0.269951, a_1 = 0.780032, a_2 = -0.061577, a_3 = -2.60578 * 10^{-3},$

$a_4 = 8.37333 * 10^{-4}, a_5 = -1.90326 * 10^{-5}, a_6 = -4.1397 * 10^{-6}, a_7 = 2.085 * 10^{-7}$

The approximation is easy to differentiate but difficult to integrate. Selvakumar's approximated values are graphically shown in Figure 2.11 with the actual values where the approximated values are almost sitting on the actual values. Figure 2.12 shows the relative errors of Selvakumar's approximation and the mean absolute error is 0.0051. Kozhukhov et al. used Selvakumar's approximation of FDI in order to determine the current of gate induced drain leakage [54].

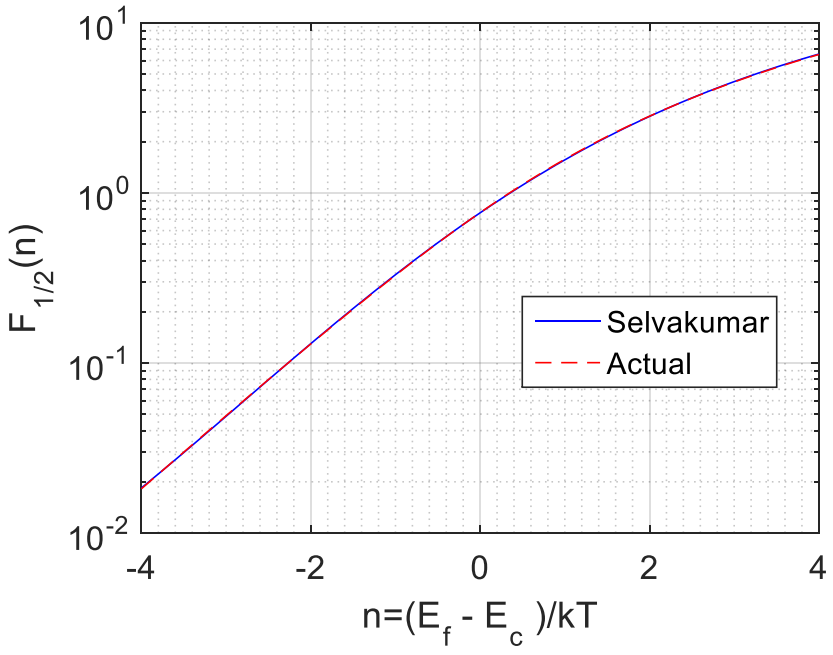

Figure 2.11 The Approximation of Fermi-Dirac Integrals by Selvakumar

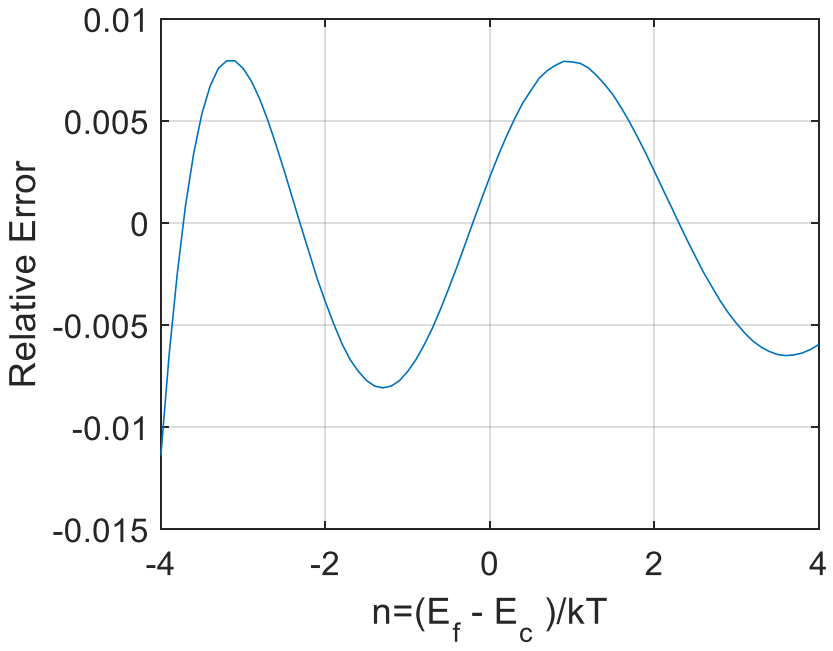

Figure 2.12 The Relative Error Profiles of Selvakumar's Approximation

2.4.7 Van Halen and Pulfrey Approximation

One of the well-known approximations we examine in this thesis has been developed by Van Halen and Pulfrey [97]. They proposed approximations for the whole family of FDIs with dividing the range into two separate ranges. Their approximation of FDI has two different expressions for the order 1/2 where the range above zero has two different sets of coefficients as follows:

$$F_{\frac{1}{2}}(\eta) = \sum_{r=1}^{7}(-1)^{r+1}a_r e^{r\eta} \quad \text{, For } \eta \leq 0 \qquad (2.13)$$

$$F_{\frac{1}{2}}(\eta) = \sum_{r=1}^{7} a_r \eta^{r-1} \quad \text{, For } \eta > 0 \qquad (2.14)$$

The coefficients of each expression and the mean square error for each range are presented in Table 2.1. Their approximation for the values below zero is an attempt to improve the simplest approximation of FDI by summing the seven terms of exponential functions multiplying by pre-exponential coefficients. The expression of FDI beyond zero is a seven polynomial function that has two sets of coefficients based on the range. Both expressions are easy to differentiate and integrate, however the accuracy of the approximation is not adequate to be useful in semiconductor device equations. Figure 2.13 shows the three ranges of the approximation compared to the actual values. The relative errors of Van Halen and Pulfrey approximation are shown in Figure 2.14 where the accuracy of each range is separated.

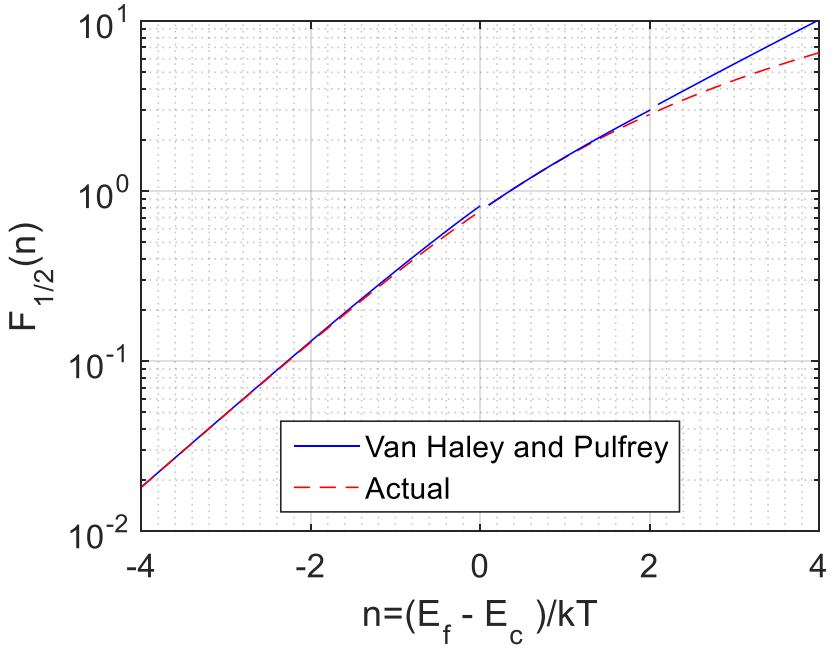

Figure 2.13 The Approximations of Van Haley and Pulfrey for Different Ranges

Table 2.1 Coefficients and Mean Absolute Errors (MAE) for Van Haley and Pulfrey Approximations

The Coefficient	$-4 \leq \eta \leq 0$	$0 < \eta \leq 2$	$2 < \eta \leq 4$
a_1	1	0.765147	0.777114
a_2	0.250052	0.604911	0.581307
a_3	0.111747	0.189885	0.206132
a_4	0.064557	0.020307	0.01768
a_5	0.040754	0.004380	0.006549
a_6	0.020532	0.000366	0.000784
a_7	0.002108	0.000133	0.000036
MAE	0.0215	0.0152	0.2836

Due to the simplicity of the Van Halen and Pulfrey approximation of FDI, Chu and Pulfrey used Halen and Pulfrey approximation of FDI to calculate the electron current and the net hole tunnel current in metal-insulator semiconductor tunnel junction [26]. The mobility of heavily doped GaAlAs devices has been determined by using Halen and Pulfrey approximation of FDI [14]. Venugopal et al. presented a simulation of quantum transport in nanoscale transistors where the 3D electron density is calculated by using Halen and Pulfrey approximation of FDI [98].

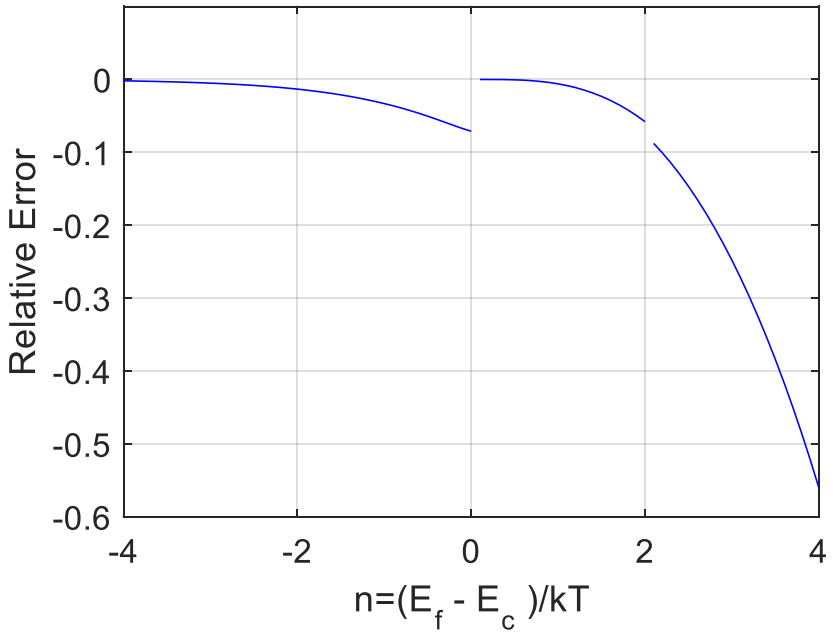

Figure 2.14 The Relative Errors of Different Ranges of Van Haley and Pulfrey Approximation

2.4.8 Abdus Sobhan and NoorMohammad Approximation

In 1985, Abdus Sobhan and NoorMohammad proposed an approximation of FDI that has a form similar to Marshak et al. approximation as follows [88]:

$$F_{\frac{1}{2}}(\eta) = \frac{e^{\eta}}{1+C(\eta)e^{\eta}} \tag{2.15}$$

where $C(\eta) = \sum_{v=0}^{7} a_v \eta^v$ and the coefficients of $C(\eta)$:

$a_0 = 0.307098, a_1 = 0.118985, a_2 = 0.0166708, a_3 = -0.371322 * 10^{-2}, a_4 = 0.863507 * 10^{-3},$

$a_5 = -0.340475 * 10^{-4}, a_6 = -0.524534 * 10^{-6}, a_7 = 0.199866 * 10^{-6}$

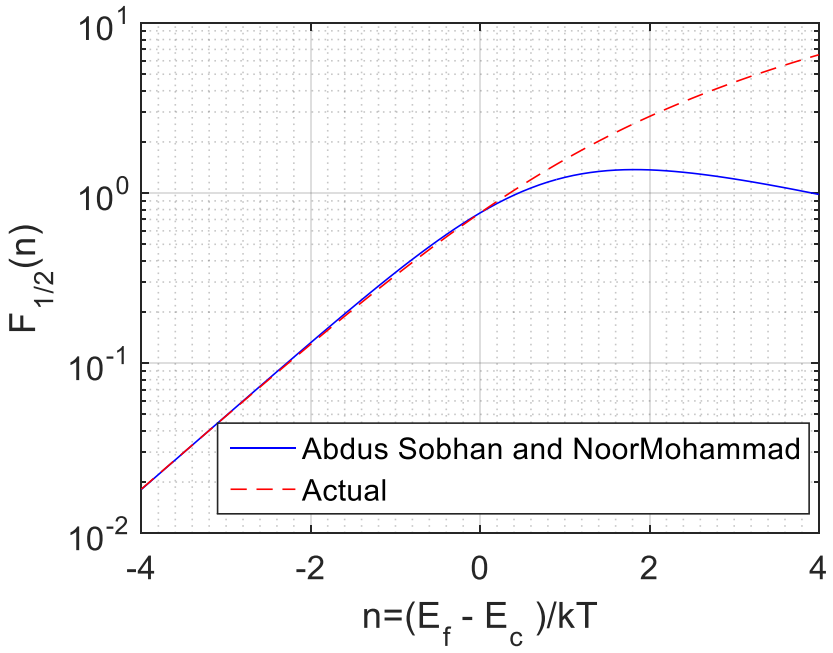

Figure 2.15 Approximation of Abdus Sobhan and NoorMohammad with the Actual Values

The pre-exponential function is a polynomial function that has seven terms. The mean absolute error is 0.2478. As can be seen from Figure 2.15, the error is starting to accumulate for the values beyond zero; therefore, their approximation cannot be useful where the Fermi-level is above the conduction band. The relative errors of the approximation are shown in Figure 2.16 for the range between negative four and positive four where the non-degenerate and degenerate semiconductors are covered.

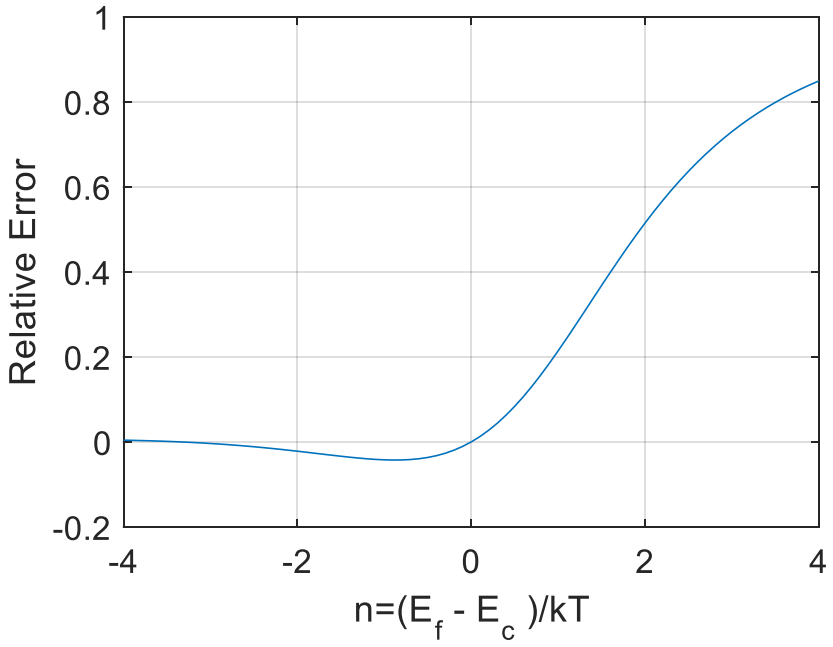

Figure 2.16 The Relative Error Profiles as a Function of Normalized Relative Fermi-Level

2.5 Summary

In this chapter, several important analytical approximations of Fermi-Dirac Integrals have been discussed in terms of complexity of the form and the accuracy of the approximation. In addition, a few of tabulated approaches have been reviewed comparing them to the actual values that based on Blakemore's tabulations. Then, a number of simple analytical approximations have been presented and studied in terms of how precise the approximation is and how amenable approximations are to be differentiated and integrated. We have computed the mean absolute error for every approximation discussed.

Chapter 3
Approximation of Fermi-Dirac Integrals of Order 1/2 by Prony's Method

3.1 Introduction

This chapter describes the Prony's method that has been chosen to be used in the new proposed approximation. This new approximation lends itself for easy differentiation and integration.

3.2 Prony's Method

Prony proposed a method of approximating a function as a sum of exponential functions through a series of data values at equally spaced points [77]. Prony's method is a way to solve a series of nonlinear equations by generating a series of linear equations. It had been used in order to approximate some functions such as the two-step Diffusion profiles [84] and the average probability of transmission error in the digital communication instead of Fourier series [59]. The Prony's method is explained analytically in the next part of this section.

Some of the steps of the Prony's method lead to finding the coefficients of Prony's main equation: forming a series of linear equations, using an algebraic equation, and then multiplying the actual values of the function by suitable coefficients. These steps are discussed in this chapter.

3.2.1 Prony's Method Components

The symbols that are used in Prony's method should be defined before introducing the steps in the Prony's method [48]. N is the number of equally spaced chosen points. The quantity n is the number of terms in Prony's approximation. The quantity C is the coefficient multiplying the exponential term in the function, and a is an exponent. Secondly, the general form of Prony's function is:

$$f(x_k) = \sum_{i=1}^{n} C_i e^{-a_i * x_k} \qquad (3.1)$$

where k=1,2,…,N and i=1,2,…,n.

In order to simplify the form during computations, the general form of Prony's function can be written as:

$$f(x_k) = \sum_{i=1}^{n} C_i \mu_i^{x_k} \qquad (3.2)$$

where $u_i = e^{-a_i}$

3.2.2 Steps of Prony's Method

The first step towards finding the coefficients C's is forming the N equations using the actual values of $f(x_k)$ in the following order:

$$C_1 + C_2 + \cdots + C_n = f_0 \quad (3.3.1)$$

$$C_1\mu_1 + C_2\mu_2 + \cdots + C_n\mu_n = f_1 \quad (3.3.2)$$

$$C_1\mu_1^2 + C_2\mu_2^2 + \cdots + C_n\mu_n^2 = f_2 \quad (3.3.3)$$

.

.

.

.

$$C_1\mu_1^{N-1} + C_2\mu_2^{N-1} + \cdots + C_n\mu_n^{N-1} = f_{N-1} \quad (3.3.N)$$

The Prony's set of equations can be solved directly if μ_i values are known, and equal to the number of the terms. However, if $N > n$, the least square technique could be used in order to solve the Prony's set of equations. The Prony's method can solve the Prony's set of equations if $N > n$ and μ_i values are to be determined. After forming the N equations, the next step is letting $\mu_1, \ldots\ldots, \mu_n$ to be the roots of an algebraic equation as follows:

$$\mu^n + \alpha_1\mu^{n-1} + \alpha_2\mu^{n-2} + \cdots + \alpha_{n-1}\,\mu + \alpha_n = 0 \quad (3.4)$$

so that it can be expressed as follows:

$$(\mu - \mu_1)(\mu - \mu_2)\ldots(\mu - \mu_n)$$

In order to determine $\alpha_1, \ldots\ldots, \alpha_n$, the first actual value f_0 should be multiplied by α_n, second actual value f_1 should be multiplied by α_{n-1}, and nth actual value should be multiplied by 1. Thus, the result is seen to be of the form:

$$f_n + \alpha_1 f_{n-1} + \alpha_2 f_{n-2} + \cdots + \alpha_n f_0 = 0 \quad (3.5)$$

Then, a set of $N - n - 1$ additional equations of similar type is obtained in the same way by starting instead successively with the second, third, …, $(N - n)$th equations. Therefore, equations (3.3) and (3.4) imply a set of $N - n$ linear equations.

$$f_n + \alpha_1 f_{n-1} + \alpha_2 f_{n-2} + \cdots + \alpha_n f_0 = 0 \quad (3.6.1)$$

$$f_{n+1} + \alpha_1 f_n + \alpha_2 f_{n-1} + \cdots + \alpha_n f_1 = 0 \quad (3.6.2)$$

.

.

.

.

$$f_{N-1} + \alpha_1 f_{N-2} + \alpha_2 f_{N-3} + \cdots + \alpha_n f_{N-n-1} = 0 \qquad \text{(3.6.N-n-1)}$$

Since the actual values of f_k are known, this set of equations can be solved directly if $N = 2n$, or solved approximately by the least squares technique if $N > 2n$. After determining $\alpha's$, $\mu's$ can be real or imaginary roots of equation (3.4). Then, the set of equations (3.3) can be linear equations in the C's, with known coefficients, and the way to determine the n number of C's is applying the least squares technique. A key transformation is the conversion of a set of non-linear equation to a set of linear equation through the algebraic equation (3.4).

3.2.3 Special Cases of Prony's Method

When $f(x_k)$ tends to a finite limit as $x \to \infty$, the approximation:

$$f(x_k) \approx C_0 + C_1 e^{a_1 x_k} + \cdots + C_n e^{a_n x_k}$$

is appropriate where $a's$ are expected to have negative real parts. Furthermore, the equations (3.6) can be modified by replacing each f_k by the difference $\Delta f_k = f_{k+1} - f_k$ since the previous approximation implies that:

$$\Delta f(x_k) \approx C_1' e^{a_1 x_k} + \cdots + C_n' e^{a_n x_k}$$

where the coefficients C_n' is unknown constants which is related to the unknown C_n. Then, $\alpha's$ and $\mu's$ are determined as before. Moreover, the equations (3.3) are being modified by insertion of the unknown C_0 in each left-hand member, and at least $N = 2n + 1$ independent data are needed for this case.

The second case is when one or more of the $\mu's$ values are not real and $\mu_k = \rho_k e^{i\beta}$,where ρ and β are real and ρ is positive; therefore, the polar $\rho e^{i\beta}$ and its conjugate $\rho e^{-i\beta}$ should be involved because the coefficients in equation (3.4) are assumed to be real. The corresponding part of equation (3.2) can be written as $\rho^x\left(A_1 e^{i\beta x} + A_2 e^{-i\beta x}\right)$ where $A_1 = \frac{C_1 - iC_2}{2}$ and $A_2 = \frac{C_1 + iC_2}{2}$ which are constants. Consequently, the corresponding parts can be expressed in the following form:

$$\rho^x(C_1 cos\beta x + C_2 sin\beta x) = e^{x log\rho}(C_1 cos\beta x + C_2 sin\beta x)$$

Before the set of equations (3.3) are formed and solved for the coefficients of the approximating functions, $\mu's$ are determined from (3.4) and (3.6).

3.2.4 Advantages of Using Prony's Method

Since the Prony's method is based on a series of exponential terms in the main case or cosine and sine terms in the particular case, it can be easily differentiated and integrated. As a result, Prony's method can be used

to approximate certain functions in electronic devices which need to be differentiated or integrated this is sometimes needed in the computation of some quantities such as the use of the half integer Fermi-Dirac function in the charge density equation. The first and second derivation forms of Prony's general form can be expressed as:

$$\frac{df(x_k)}{dx_k} = \sum_{i=1}^{n} C_i * a_i e^{a_i x_k} \quad (3.7)$$

$$\frac{d^2 f(x_k)}{dx_k^2} = \sum_{i=1}^{n} C_i * a_i^2 e^{a_i x_k} \quad (3.8)$$

In addition, the Prony's approximation can be integrated as shown in followed forms

$$f'(x_k) = \int f(x_k)\, dx = \sum_{i=1}^{n} \frac{C_i}{a_i} e^{a_i x_k} + constant \quad (3.9)$$

$$f''(x_k) = \int f'(x_k)\, dx = \sum_{i=1}^{n} \frac{C_i}{a_i^2} e^{a_i x_k} + constant \quad (3.10)$$

Furthermore, the steps of the Prony's method can be easily followed, and the coefficients of the Prony's method can be determined in few steps.

3.3 The New Proposed Approximation of Fermi-Dirac Integrals of Order ½

As seen in the literature review, the positive half integer of Fermi-Dirac can have a major impact on the highly doped region of the semiconductor devices. For example one can consider the current density, electron or hole density, and the Quasi-Fermi level position. Therefore, a simple way to approximate the exact values is needed in order to be used in explicit expressions. Moreover, the ability to differentiate and integrate the approximated form is often needed and have been aimed at this work. As a result, the Pony's method was chosen to approximate the Fermi-Dirac Integrals of positive half order. In the first part of this section, parameters of the approximation are introduced. Next, steps of approximating the Fermi-Dirac Integral are proposed. Last part of this section shows the differentiation and integration of the resulting approximation.

3.3.1 Components of the Approximation

$f_{\frac{1}{2}}(x_k)$ values for a specific range (-4 to +12) have been tabulated by Blakemore (1961) (See the Blakemore's table at the Appendix A), so the actual values used in this thesis are taken from these tabulated values. First, we select a range of values of x_k that is from (-2) to (+4) with the interval (0.1) because the degenerate semiconductor has the highest deviation from the Boltzmann's values. Thus, we select this region and use a value of N unit 61 points. In addition, the number of chosen terms of the exponentials is four (n=4). Even though a large number of terms might imply a good approximation, by using different

number of terms for this approximation (n=6, 8, and 10) the accuracy of the approximation turns out to be similar and not significantly improved.

3.3.2 Steps of the Approximation

The general form of the proposed approximation can be expressed in the following form:

$$f_{\frac{1}{2}}(x_k) = \sum_{i=1}^{4} C_i e^{a_i x_k} = C_1 e^{a_1 x_k} + C_2 e^{a_2 x_k} + C_3 e^{a_3 x_k} + C_4 e^{a_4 x_k}$$

$$f_{\frac{1}{2}}(x_k) = \sum_{i=1}^{4} C_i \mu_i^{x_k} = C_1 \mu_1^{x_k} + C_2 \mu_2^{x_k} + C_3 \mu_3^{x_k} + C_4 \mu_4^{x_k}$$

where $\mu_i = e^{a_i}$.

The first step to take towards approximating the Fermi-Dirac Integral is forming 61 equations by using the actual values of Fermi-Dirac Integral values from the tabulated values:

$$C_1 \mu_1^{x_1} + C_2 \mu_2^{x_1} + C_3 \mu_3^{x_1} + C_4 \mu_4^{x_1} = f_0$$
$$C_1 \mu_1^{x_2} + C_2 \mu_2^{x_2} + C_3 \mu_3^{x_2} + C_4 \mu_4^{x_2} = f_1$$
$$C_1 \mu_1^{x_3} + C_2 \mu_2^{x_3} + C_3 \mu_3^{x_3} + C_4 \mu_4^{x_3} = f_2$$
$$C_1 \mu_1^{x_4} + C_2 \mu_2^{x_4} + C_3 \mu_3^{x_4} + C_4 \mu_4^{x_4} = f_3$$
$$C_1 \mu_1^{x_5} + C_2 \mu_2^{x_5} + C_3 \mu_3^{x_5} + C_4 \mu_4^{x_5} = f_4$$

.

.

.

.

$$C_1 \mu_1^{x_{61}} + C_2 \mu_2^{x_{61}} + C_3 \mu_3^{x_{61}} + C_4 \mu_4^{x_{61}} = f_{60}$$

Since each equation has four terms, the $\mu's$ can be roots of the algebraic equation

$$\mu^4 + \alpha_1 \mu^3 + \alpha_2 \mu^2 + \alpha_3 \mu + \alpha_4 = 0$$

so, the left-hand side of this equation is identified with:

$$(\mu - \mu 1)(\mu - \mu_2)(\mu - \mu_3)(\mu - \mu_4)$$

To find $\alpha_1, \alpha_2, \alpha_3, \alpha_4$, we multiply α_4 by f_0, α_3 by f_1, α_2 by f_2, and α_1 by f_3, so the first equation will be formed as

$$f_4 + \alpha_1 f_3 + \alpha_2 f_2 + \alpha_3 f_1 + \alpha_4 f_0 = 0$$

By applying the same condition on the rest of the equations, the equations can be formed in the following way

$$f_4 + \alpha_1 f_3 + \alpha_2 f_2 + \alpha_3 f_1 + \alpha_4 f_0 = 0$$
$$f_5 + \alpha_1 f_4 + \alpha_2 f_3 + \alpha_3 f_2 + \alpha_4 f_1 = 0$$
$$f_6 + \alpha_1 f_5 + \alpha_2 f_4 + \alpha_3 f_3 + \alpha_4 f_2 = 0$$
$$f_7 + \alpha_1 f_6 + \alpha_2 f_5 + \alpha_3 f_4 + \alpha_4 f_3 = 0$$
$$f_8 + \alpha_1 f_7 + \alpha_2 f_6 + \alpha_3 f_5 + \alpha_4 f_4 = 0$$

.

.

.

.

$$f_{60} + \alpha_1 f_{59} + \alpha_2 f_{58} + \alpha_3 f_{57} + \alpha_4 f_{56} = 0$$

Since $N > 2n$, we use least squares technique and the resulting form is

$$\alpha_4 \sum_{i=0}^{56} f_i + \alpha_3 \sum_{i=0}^{56} f_{i+1} + \alpha_2 \sum_{i=0}^{56} f_{i+2} + \alpha_1 \sum_{i=0}^{56} f_{i+3} + \sum_{i=0}^{56} f_{i+4} = 0$$

By differentiating previous equation with respect $\alpha_1, \alpha_2, \alpha_3, and\ \alpha_4$, four equations are being formulated as shown in equations

$$\alpha_4 \sum_{i=0}^{56} f_i^2 + \alpha_3 \sum_{i=0}^{56} f_i * f_{i+1} + \alpha_2 \sum_{i=0}^{56} f_i * f_{i+2} + \alpha_1 \sum_{i=0}^{56} f_i * f_{i+3} = -\sum_{i=0}^{56} f_i * f_{i+4}$$

$$\alpha_4 \sum_{i=0}^{56} f_i * f_{i+1} + \alpha_3 \sum_{i=0}^{56} f_{i+1}^2 + \alpha_2 \sum_{i=0}^{56} f_{i+1} * f_{i+2} + \alpha_1 \sum_{i=0}^{56} f_{i+1} * f_{i+3} = -\sum_{i=0}^{56} f_{i+1} * f_{i+4}$$

$$\alpha_4 \sum_{i=0}^{56} f_i * f_{i+2} + \alpha_3 \sum_{i=0}^{56} f_{i+1} * f_{i+2} + \alpha_2 \sum_{i=0}^{56} f_{i+2}^2 + \alpha_1 \sum_{i=0}^{56} f_{i+2} * f_{i+3} = -\sum_{i=0}^{56} f_{i+2} * f_{i+4}$$

$$\alpha_4 \sum_{i=0}^{56} f_i * f_{i+3} + \alpha_3 \sum_{i=0}^{56} f_{i+1} * f_{i+3} + \alpha_2 \sum_{i=0}^{56} f_{i+2} * f_{i+3} + \alpha_1 \sum_{i=0}^{56} f_{i+3}^2 = -\sum_{i=0}^{56} f_{i+3} * f_{i+4}$$

Meanwhile, there are four equations in four unknowns, and these equations can be solved directly. The resulting $\alpha's$ are:

$\alpha_1 = -3.49404$

$\alpha_2 = \ \ 4.57663$

$\alpha_3 = -2.66342$

$\alpha_4 = \ \ 0.58106$

Now, the algebraic equation can be formed since the α values are known

$$\mu^4 - 3.49404\mu^3 + 4.57663\mu^2 - 2.66342\mu + 0.58106 = 0$$

By solving this algebraic equation, the values of $\mu's$ become known:

$\mu_1 = 0.90556$

$\mu_2 = 0.89495$

$\mu_3 = 0.85224$

$\mu_4 = 0.84129$

After finding the $\mu's$, the first equation of the desired approximation can be written as

$$C_1(0.90556)^{x_1} + C_2(0.89495)^{x_1} + C_3(0.85224)^{x_1} + C_4(0.84129)^{x_1} = f_0$$

Moreover, by introducing $\mu's$ in the other equations of the approximation, the resulting general form can be expressed as

$$C_1\sum_{k=1}^{61}(0.90556)^{x_k} + C_2\sum_{k=1}^{61}(0.89495)^{x_k} + C_3\sum_{k=1}^{61}(0.85224)^{x_k} + C_4\sum_{k=1}^{61}(0.84129)^{x_k} = \sum_{k=1}^{61} f_{\frac{1}{2}}(x_k)$$

C's can be determined by differentiating the error equation and equating them to zero in order to get the best accuracy. The equation of Relative mean square error can be expressed as shown in the equation

$$Relative\ mean\ square\ error = \frac{1}{N}\sqrt{\sum_1^N \frac{\left(f_{actual} - f_{approximated}\right)^2}{f_{actual}}} \qquad (3.11)$$

The left-hand member is the approximated value, and the right-hand member is the actual value. In order to minimize the error, the previous equation should be differentiated and equal to zero, the four resulting equations are formed as following

$$C_1\sum_{k=1}^{61}\mu_1^{2x_k} + C_2\sum_{k=1}^{61}(\mu_1\mu_2)^{x_k} + C_3\sum_{k=1}^{61}(\mu_1\mu_3)^{x_k} + C_4\sum_{k=1}^{61}(\mu_1\mu_4)^{x_k} - \sum_{k=1}^{61}\mu_1^{x_k} f_{\frac{1}{2}}(x_i) = 0$$

$$C_1\sum_{k=1}^{61}(\mu_1\mu_2)^{x_k} + C_2\sum_{k=1}^{61}\mu_2^{2x_k} + C_3\sum_{k=1}^{61}(\mu_2\mu_3)^{x_k} + C_4\sum_{k=1}^{61}(\mu_2\mu_4)^{x_k} - \sum_{k=1}^{61}\mu_2^{x_k} f_{\frac{1}{2}}(x_k) = 0$$

$$C_1\sum_{k=1}^{61}(\mu_1\mu_3)^{x_k} + C_2\sum_{k=1}^{61}(\mu_2\mu_3)^{x_k} + C_3\sum_{k=1}^{61}\mu_3^{2x_k} + C_4\sum_{k=1}^{61}(\mu_3\mu_4)^{x_k} - \sum_{k=1}^{61}\mu_3^{x_k} f_{\frac{1}{2}}(x_k) = 0$$

$$C_1\sum_{k=1}^{61}(\mu_1\mu_4)^{x_k} + C_2\sum_{k=1}^{61}(\mu_2\mu_4)^{x_k} + C_3\sum_{k=1}^{61}(\mu_3\mu_4)^{x_k} + C_4\sum_{k=1}^{61}\mu_4^{2x_k} - \sum_{k=1}^{61}\mu_4^{x_k} f_{\frac{1}{2}}(x_k) = 0$$

After calculating these four equations, the resulting C values are

$C_1 = 5.7955 * 10^3$

$C_2 = -8.3584 * 10^3$

$C_3 = 7.0383 * 10^3$

$C_4 = -4.4747 * 10^3$

Moreover, the a's values can be calculated by using the following formula $\mu_i = e^{a_i}$

$a_1 = -0.0992$

$a_2 = -0.1110$

$a_3 = -0.1599$

$a_4 = 0.1728$

Finally, the approximated form of Fermi-Dirac Integrals of positive half order can be written as follows:

$$f_{\frac{1}{2}}(x_k) = 5.7955 * 10^3 e^{-0.0992x_k} - 8.3584 * 10^3 e^{-0.111x_k}$$
$$+7.0383 * 10^3 e^{-0.1599x_k} - 4.4747 * 10^3 e^{-0.1728x_k} \quad (3.12)$$

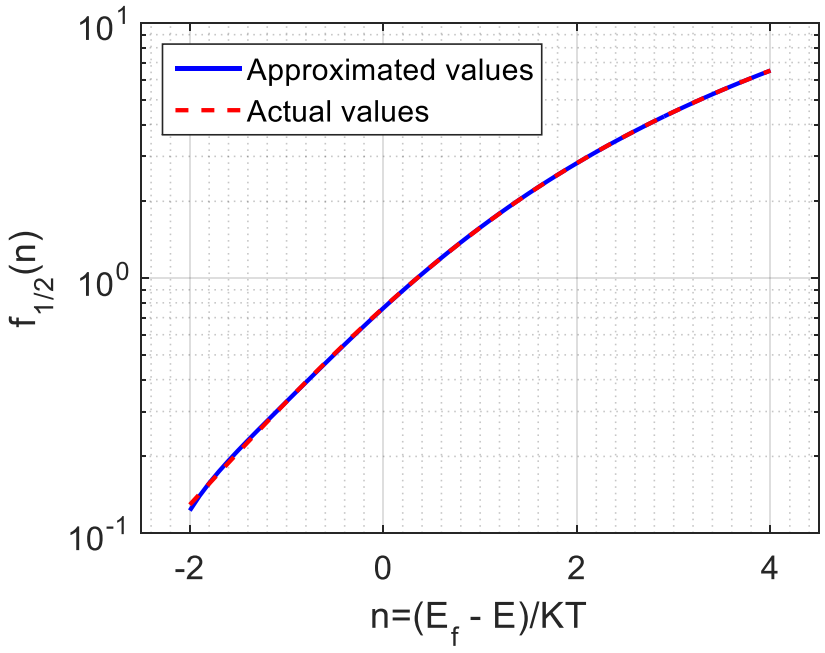

Figure 3.1 Approximated and Actual Values of Fermi-Dirac Positive Half-Integral

Since the actual values of Fermi-Dirac Integrals are known, this approximation can be calculated and compared to the actual values. Thus, a Matlab code has been used to program this method, and the results can be seen in Figure 3.1

As shown in Figure 3.1, the approximated values are mostly comparable to the actual values; consequently, the average relative mean square error has been calculated.

$RMSE = 0.0038$

Our goal is not focused on exclusively achieving the smallest error but much more about achieving the simplest approximation of Fermi-Dirac Integrals with as good an accuracy as possible which can be used effectively in books and software programs. Also, the relative mean error for each point has been computed as shown in Figure 3.2

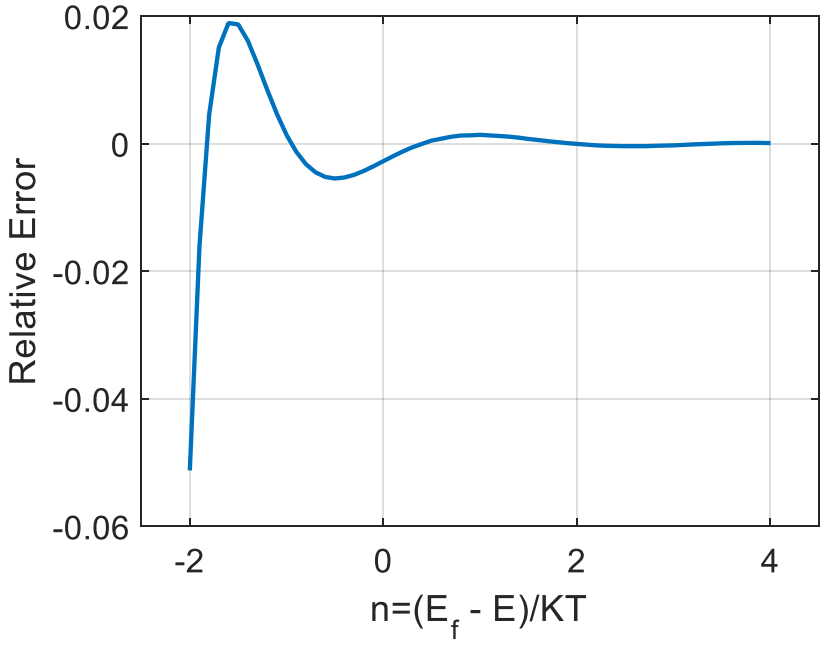

Figure 3.2 Relative Mean Square Error of the Approximation for Different Fermi Level Positions

Table 3.1 Summarized Components of Our Approximation

	1	**2**	**3**	**4**
$\boldsymbol{\alpha}$	-3.49404	4.57663	-2.66342	0.58106
$\boldsymbol{\mu}$	0.90556	0.89495	0.85224	0.84129
a	-0.0992	-0.1110	-0.1599	0.1728
C	$5.7955 * 10^3$	$-8.3584 * 10^3$	$7.0383 * 10^3$	$-4.4747 * 10^3$

Even though Figure 3.2 indicates that there is a significant error around negative two, the approached values are still more accurate than Boltzmann's approximated values.

3.4 Differentiation and Integration of the New Proposed Approximation

In this section, we examine the accuracy of the differentiated and integrated forms of the approximation by comparing them to actual values of the functions.

3.4.1 Differentiation

To examine how good the approximation is, we calculate the first and second differentiated expressions of the approximation. Then, the evaluation of the differentiated functions are being compared to the actual tabulated values based on the following equation:

$$f_{j-1}(x_k) = \frac{df_j}{dx_k} \tag{3.13}$$

Since the value of j in our approximation is $j = \frac{1}{2}$, the first derivative of the equation is $f_{-\frac{1}{2}}(x_k) = \frac{df_{\frac{1}{2}}}{dx_k}$; moreover, the resulting form of the derived function is:

$$f_{-\frac{1}{2}}(x_k) = -1.1253 * 10^3 e^{-0.0992x_k} + 773.2507e^{-0.111x_k} + 927.5932e^{-0.1599x_k} - 574.9186e^{-0.1728x_k} \tag{3.14}$$

The previous function has been calculated at each x point and compared to actual tabulated $f_{-\frac{1}{2}}(x_k)$. The approximated and actual functions have been plotted as shown in Figure 3.3. Then, the average relative mean square error for the derived function has been determined. Further, Figure 3.4 shows the relative mean square error at each point, and it can be noticed that the differentiated function has large errors for the values of η around negative two, which also has occurred for the original approximation. It should be stated that the average relative mean square error of derived function is larger than the average relative mean square error of the original approximation because of the sufferers after the differentiation.

$RMSE = 0.0215$

Table 3.2 Summarized Components of First Derivative Function

	1	**2**	**3**	**4**
a	-0.0992	-0.1110	-0.1599	0.1728
C	$-1.1253 * 10^3$	773.2507	927.5932	-574.9186

The second derivative function can be analytically calculated by differentiating the approximation twice ($f_{-\frac{3}{2}}(x_k) = \frac{d^2 f_{\frac{1}{2}}(x_k)}{dx_k^2}$), and the results can be compared to tabulated $f_{-\frac{3}{2}}(x_k)$; thus, the approached form is

$$f_{-\frac{1}{2}}(x_k) = 179.9299e^{-0.0992x_k} - 133.6301e^{-0.111x_k} - 102.9464e^{-0.1599x_k} + 57.0347e^{-0.1728x_k} \tag{3.15}$$

Figure 3.5 shows the values of the twice differentiated function compared to the actual tabulated values for each position of the Fermi level. Also, the average relative mean square error is

$RMSE = 0.1019$

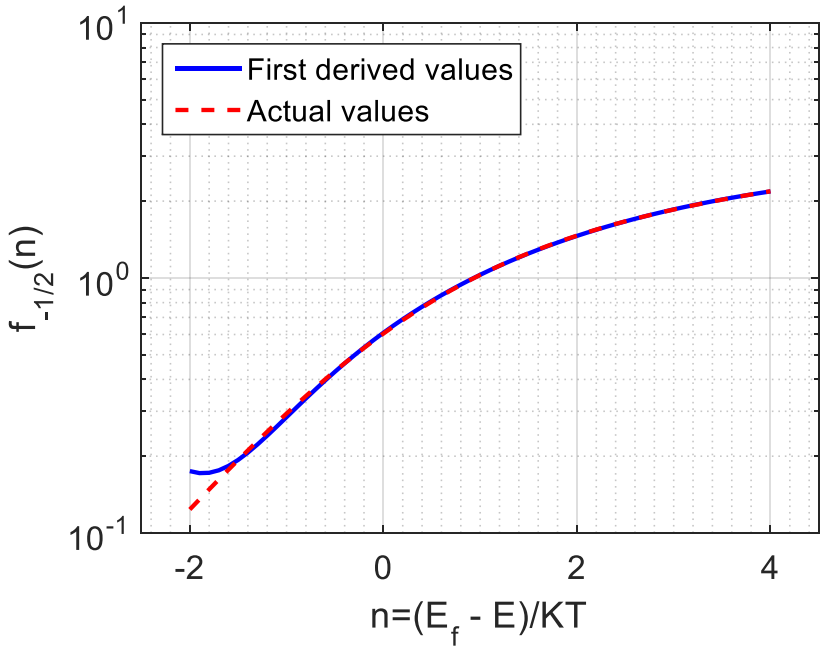

Figure 3.3 The First Derivative Function and Actual Values of Fermi-Dirac Negative Half-Integral $(-\frac{1}{2})$

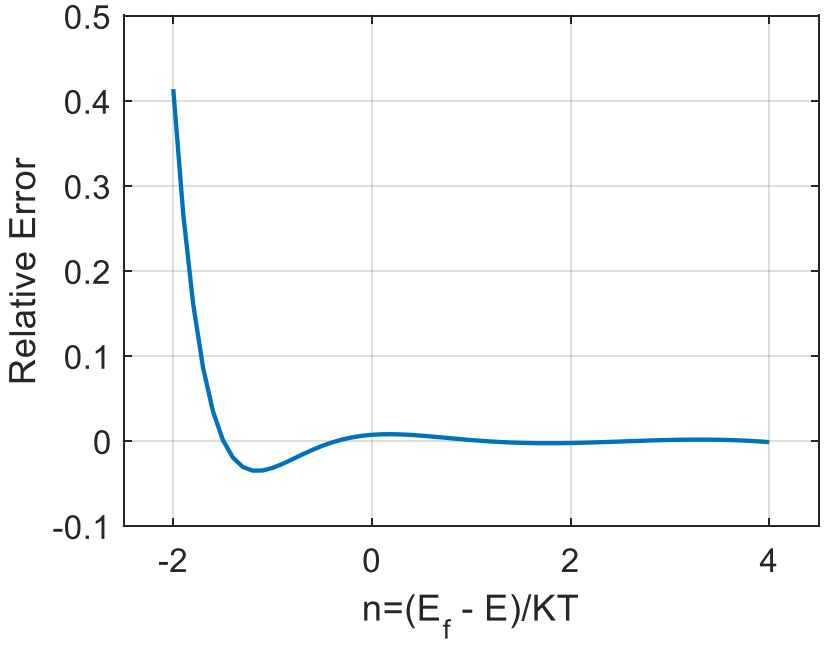

Figure 3.4 Relative Mean Square Error Profiles of the Once-Differentiated Function

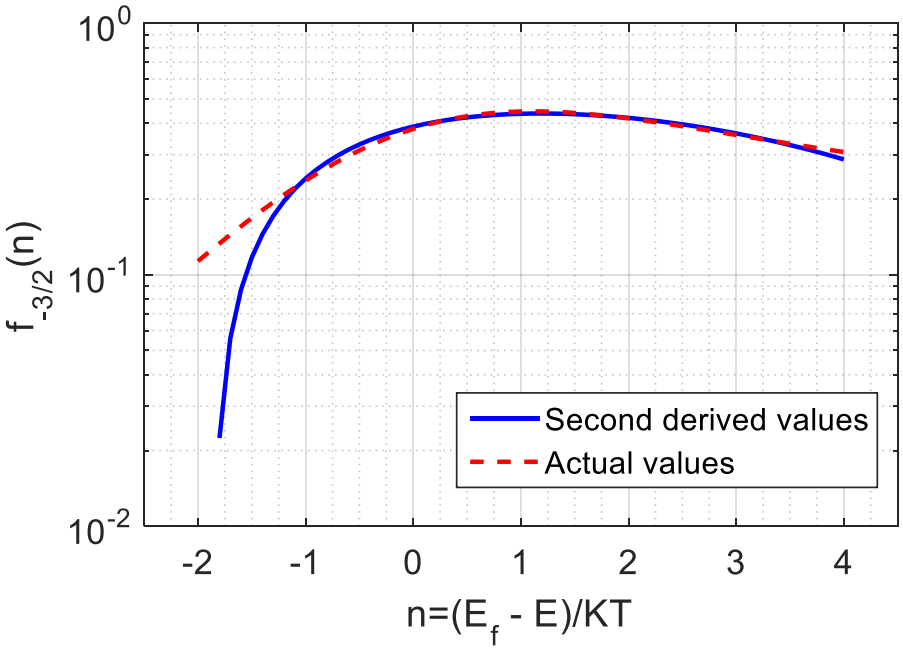

Figure 3.5 The Twice Differentiated Approximation and the Actual Values of Fermi-Dirac Negative One and Half-Integral ($-\frac{3}{2}$)

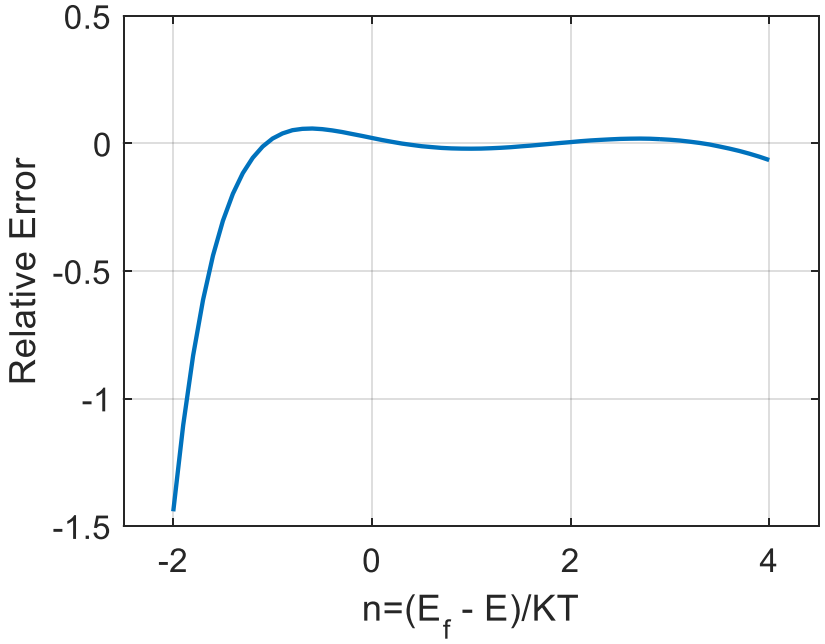

Figure 3.6 Relative Mean Square Error Profiles of the Twice Differentiated Function

As can be seen from Figure 3.5, the values of η that are between negative two and negative one have a bigger error due to the losses after the second differentiation. Further, the average relative mean square error of the second derived function is two order of magnitudes larger than the average relative mean square. However, the average relative mean square errors of the first and the second derivative functions still seem to be reasonable since the accuracy is not the chief goal of this approximation as much as the easiness of using it. The relative mean square error profiles of the values are shown in Figure 3.6

Table 3.3 Summarized Components of Twice Derivative Function

	1	**2**	**3**	**4**
a	-0.0992	-0.1110	-0.1599	0.1728
C	179.9299	-133.6301	-102.9464	57.0347

3.4.2 Integration

In order to examine the effectiveness of the approximation, the approximation can easily be integrated and evaluated. The integration of the approximation can be done based on the following equation:

$$\int f_j(x_k)dx_k = f_{j+1}(x_k) \tag{3.16}$$

Thus, the first integrated function can be compared to $f_{\frac{3}{2}}(x_k)$, and the resulting formula is

$$f_{\frac{3}{2}}(x_k) = -4.4017 * 10^4 e^{-0.0992x_k} + 2.5891 * 10^4 e^{-0.111x_k} + 7.5310 * 10^4 e^{-0.1599x_k}$$
$$-5.8417 * 10^4 e^{-0.1728x_k} + constant \tag{3.17}$$

The appearance of the constant is normal since it appears in the general form of the integration, so the values of the integration without counting the constant were compared to the actual values in order to determine the best choice of the constant. Thus, the constant is the median of the sum of the differences between the actual values and the integrated values ($constant = 1233.8648$). Additionally, the average relative mean square error of the first integrated function is

$RMSE = 9.5425 * 10^{-4}$

As can be noted, the average relative mean square error of the integration is more accurate than the average relative mean square error of the differentiated function.

The first integrated function provides more accurate results than the initial approximation since the integration is the area under the curve as shown in Figure 3.7. Also, the relative mean square error profiles of the Fermi level position can be seen in Figure 3.8

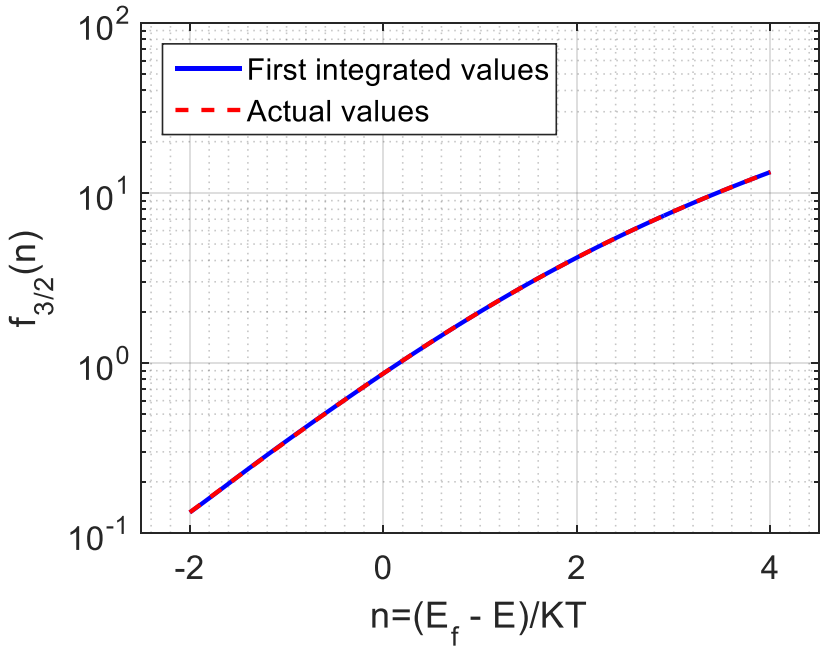

Figure 3.7 The First Integrated and Actual Values of Fermi-Dirac Positive One and Half-Integral ($+\frac{3}{2}$)

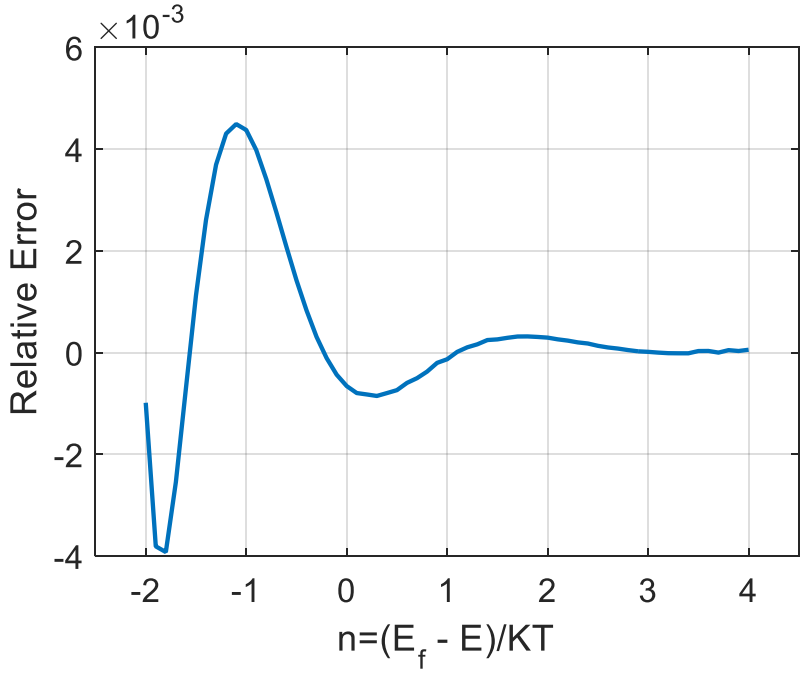

Figure 3.8 Relative Mean Square Error Profiles of the Once Integrated function

Table 3.4 Summarized Components of the First Integrated Function

	1	2	3	4
a	-0.0992	-0.1110	-0.1599	0.1728
C	$-4.4017 * 10^4$	$2.5891 * 10^4$	$7.5310 * 10^4$	$-5.8417 * 10^4$

With $constant = 1233.8648$

By twice integrating the approximate function, one can assess how good the original approximation is. The twice second integrated function can be expressed as follows:

$$f_{\frac{3}{2}}(x_k) = 2.7529 * 10^5 e^{-0.0992x_k} - 1.4982 * 10^5 e^{-0.111x_k} - 6.7857 * 10^5 e^{-0.1599x_k}$$

$$+5.8885 * 10^5 e^{-0.1728x_k} + 1233.8648 * x_k + constant \qquad (3.18)$$

By using the same criteria which were used with the first integrated function, the constant can be determined as ($constant = -35748.68618$).

Figure 3.9 shows how close the twice integrated function is to the tabulated $f_{\frac{5}{2}}(x_k)$. The average relative mean square error is being calculated to be:

$RMSE = 9.3129 * 10^{-4}$

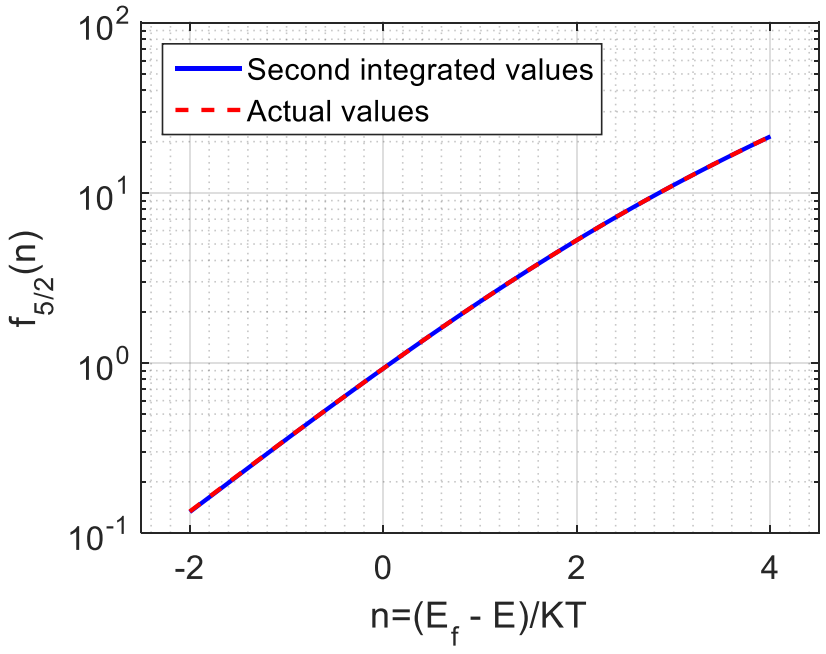

Figure 3.9 The Second Integrated Function of the Approximation and the Actual Values of the Fermi-Dirac Positive Two and Half-Integral ($+\frac{5}{2}$)

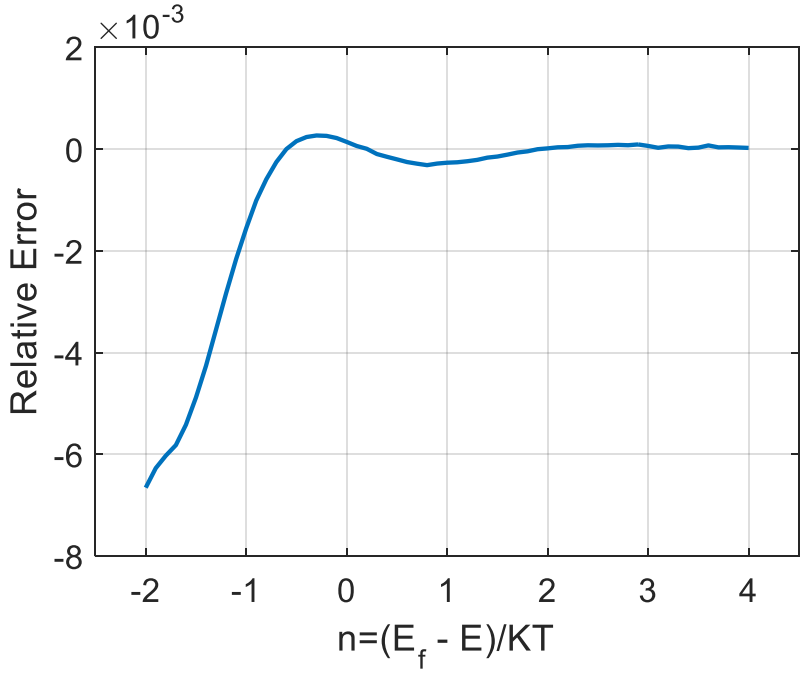

Figure 3.10 Relative Mean Square Error Profiles of the Second Integrated function

Moreover, the relative mean square error of each Fermi level position has been determined and plotted in Figure 3.10

Table 3.5 Summarized Components of Second Integrated Function

	1	**2**	**3**	**4**
a	-0.0992	-0.1110	-0.1599	0.1728
C	$2.7529 * 10^5$	$-1.4982 * 10^5$	$-6.7857 * 10^5$	$5.8885 * 10^5$

With using $1233.8648 * x_k$ from the first integrated and $constant = -35748.68618$

3.5 Summary

In this chapter, the Prony's method has been successfully used to approximate the Fermi-Dirac positive half-integral. Prony's method has been chosen for two reasons: its ability to be differentiated and integrated easily and the simplicity of determining the coefficients of the Prony's equation. In order to examine how good the form of the approximation is, the approximated function was differentiated and integrated once and twice and compared with tabulated actual values. These exercises show that not only that the magnitudes of the values given by the approximation are good, the nature of variation, as indicated by the differentiated functions show, are also very good.

Chapter 4
Applications of the New Approximation

4.1 Introduction

In the previous chapter, I had discussed a new approximation that can be applied to several applications in electronic devices due to its simplicity and the ability to be differentiated and to be integrated. Although the Fermi-Dirac Integrals play a significant role in the electronics, a simple enough approximation of Fermi-Dirac Integrals had not been proposed in the literature other than Boltzmann Approximation with limitation of accuracy. In this chapter, I elaborate how the new approximation can be applied effectively to a few semiconductor devices' equations and how it is simple enough to be used in the calculations.

The first section of this chapter presents previous research on using other approximations of Fermi-Dirac Integrals in the calculation of electron density. Next, I show the application of the new approximation to the calculation of the electron density and also for different temperatures. The hole density calculations are also studied using Fermi-Dirac Integrals approximation, including the new approximation. The third section discusses the Einstein Relation and the importance of obtaining a good approximation for it. Since the new approximation can be applied in the electronic devices, some devices that use heavily doped regions as active region such as Junctionless transistors can use the Fermi-Dirac integrals in some of their characteristics. The last section of this chapter will provide some other applications other than semiconductor devices such as heat thermodynamic and particle physics, to illustrate the usefulness of the developed approximation.

4.2 Electron and Hole Densities

Electron and Hole densities in 3D materials, which are per unit volume, can be expressed as shown in equations (4.1) and (4.2)

$$n = \int_{E_C}^{\infty} g_C(E) f(E) dE \qquad (4.1)$$

$$p = \int_{-\infty}^{E_V} g_V(E)(1 - f(E)) dE \qquad (4.2)$$

When $g_C(E)$ and $g_V(E)$ are the density of available states (DOS) in Conduction Band and Valence Band respectively and $f(E)$ is the Fermi-Dirac Distribution law, which gives the probability of occupation of an energy level E. The equations (4.1) and (4.2) compute the density of free electrons *n* and density of free holes *p* in Conduction Band and Valence band respectively at equilibrium. In this section, Silicon (Si) and

Gallium Arsenide (GaAs) devices are considered which have high doping. The density states equation for three-dimensional Si and GaAs, can be written as follows:

$$g_C(E) = \frac{8\pi\sqrt{2}}{h^3} m_n^{*\frac{3}{2}} (E - E_C)^{\frac{1}{2}} \quad (4.3)$$

$$g_V(E) = \frac{8\pi\sqrt{2}}{h^3} m_p^{*\frac{3}{2}} (E - E_V)^{\frac{1}{2}} \quad (4.4)$$

where m_n^*, m_p^* is the effective mass of electrons and holes

By substituting density of states equations and Fermi-Dirac distribution, the electron and hole densities can be as follows:

$$n = N_C F_{\frac{1}{2}}(E) \quad (4.5)$$

$$p = N_V F_{\frac{1}{2}}(E) \quad (4.6)$$

where N_C and N_V are the "effective density" of states in the conduction band and the "effective density" of states in the valence band, respectively. In addition, $F_{\frac{1}{2}}(E)$ is the positive half integer of Fermi-Dirac Integrals. By choosing three different temperatures ($50\ K, 300\ K, 1000\ K$), the N_C and N_V have been calculated by using the following equations, where it is assumed that the effective masses are temperature-independent.

$$N_C = 2\left(\frac{2\pi m_n^* kT}{h^2}\right)^{\frac{3}{2}} \quad (4.7)$$

$$N_V = 2\left(\frac{2\pi m_p^* kT}{h^2}\right)^{\frac{3}{2}} \quad (4.8)$$

Table 4.1 Calculated N_C and N_V at different temperatures

Material	$\boldsymbol{m_n^*\ (kg)}$	$\boldsymbol{m_p^*\ (kg)}$	$\boldsymbol{N_C\ (cm^{-3})}$			$\boldsymbol{N_V\ (cm^{-3})}$		
			50 *K*	**300 *K***	**1000 *K***	**50 *K***	**300 *K***	**1000 *K***
Si	$1.18m_0$ [75]	$0.81m_0$ [75]	$2.189 * 10^{18}$	$3.217 * 10^{19}$	$1.958 * 10^{20}$	$1.245 * 10^{18}$	$1.829 * 10^{19}$	$1.113 * 10^{20}$
GaAs	$0.067m_0$ [75]	$0.53m_0$ [75]	$2.961 * 10^{16}$	$4.352 * 10^{17}$	$2.649 * 10^{18}$	$6.588 * 10^{17}$	$9.683 * 10^{18}$	$5.893 * 10^{19}$

As shown in Table 4.1, N_C and N_V have been calculated for different temperatures by using the density of effective masses from reference [75]. The electron and hole densities can be calculated directly by using equations (4.5) and (4.6) since the actual values of Fermi-Dirac Integrals have been tabulated. Thus, Figure 4.1 and Figure 4.2 show the electron and hole densities for different temperatures.

As can be seen from the Figures 4.1 and 4.2, the Fermi level positions vary for each temperature. However, the Fermi-Dirac Integrals is itself temperature-dependent. Another factor to be taken into consideration is the temperature has an impact on energy bandgap as well and because of that the Fermi-Dirac Integrals will give rise to a different probability distribution and E_f between conduction and valence bands.

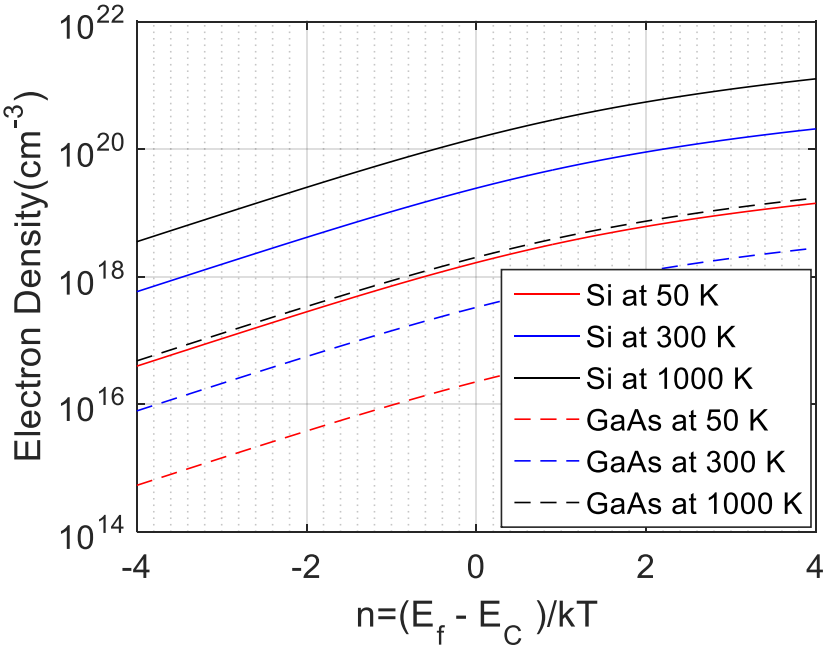

Figure 4.1 Electron Density of Si and GaAs Devices versus the Position of Fermi Level

One of the popular ways to calculate the electron and hole densities is using Boltzmann's distribution, and the equations can be written as follows:

$$n = N_C e^{\frac{E_f - E_C}{kT}} \tag{4.9}$$

$$p = N_V e^{\frac{E_V - E_f}{kT}} \tag{4.10}$$

Nevertheless, these equations are applicable for non-degenerate regions of devices, and at medium temperatures as Figures 4.3 and 4.4 show electron and hole densities of Si and GaAs at $300\ K$. It is observed from Figures 4.3 and 4.4 that Boltzmann's approximation does not give accurate values when $E_f - E_C$ and $E_V - E_f \leq -3kT$ which effectively means that Boltzmann's distribution is only valid for nondegenerate region of electronic devices. Furthermore, for high doping and high temperatures Boltzmann's distribution can lead to erroneous results. As a result, several studies have been conducted to achieve good approximations to be used in electron and hole density equations. These approximations and their impact on density equations can modify other equations such as, current equation and Einstein relation. In the

following paragraph, some studies with electron and hole densities using different approximations of Fermi-Dirac Integrals will be discussed.

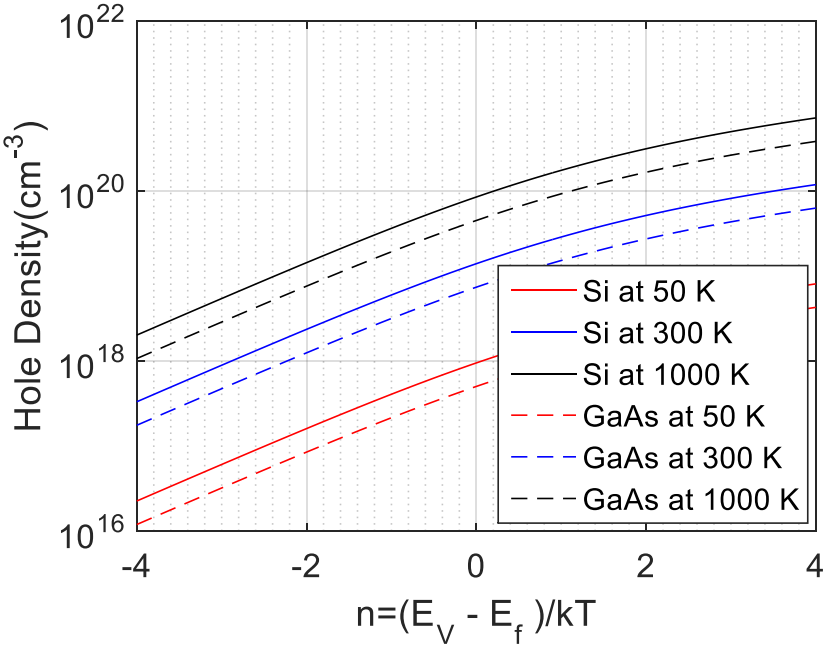

Figure 4.2 Hole Density of Si and GaAs Devices versus the Position of Fermi Level

Next, the electron and hole density equations that use the proposed approximations will be presented. These will be compared to the actual values and the relative error of using the proposed approximation when compared to Boltzmann's distribution.

The relative mean absolute error of electron and hole concentrations, using Boltzmann's distribution compared to the actual values, is 1.2249, so using Boltzmann's distribution to calculate the electron and hole concentrations in heavily doped ($\geq 10^{18}$ cm^{-3}) materials leads to large errors. As a result, a few studies have established a new formula of carrier concentration equation, which is suitable for degenerate regions of devices by using different approaches to the Fermi-Dirac Integrals. Marshak et al. presented a new approximation half-integer of Fermi-Dirac Integrals to be used in carrier concentration [64]. The form of their approximation of Fermi-Dirac Integrals is:

$$f_{\frac{1}{2}}(n) = \frac{e^{\eta}}{1+C(\eta)e^{\eta}} \tag{4.11}$$

where $C(\eta) = -4.4 * 10^{-2} * \eta + 3.1 * 10^{-1}$ for $\eta \leq +2$

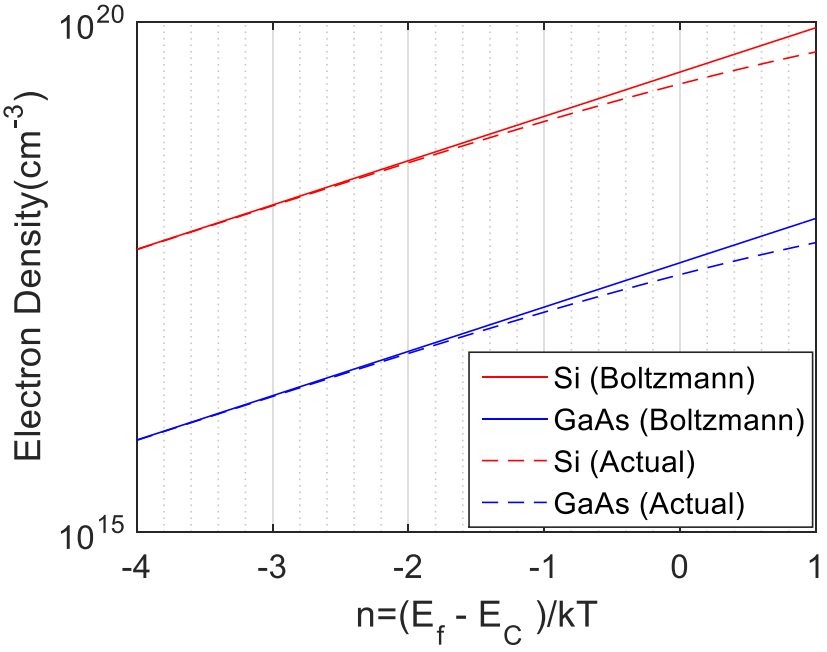

Figure 4.3 Electron Density in Si and GaAs devices using Boltzmann's Distribution and the Actual Values of Fermi-Dirac Integrals

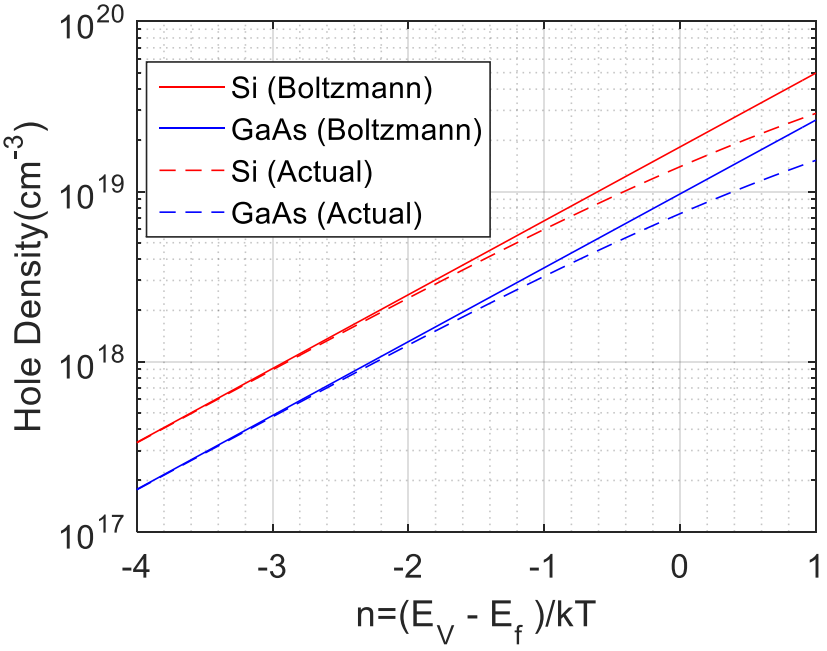

Figure 4.4 Hole Density in Si and GaAs devices using Boltzmann's Distribution and the Actual Values of Fermi-Dirac Integrals

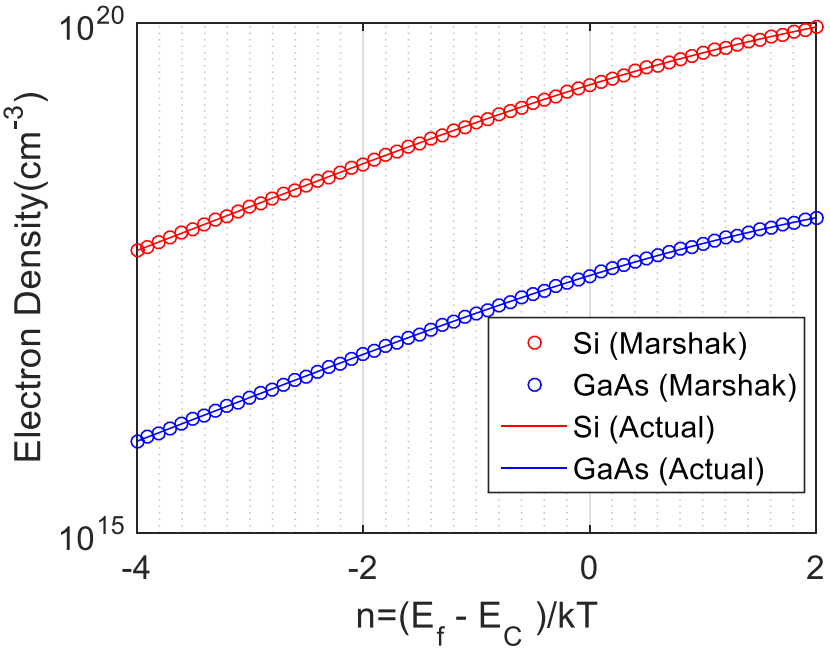

Figure 4.5 Electron Density in Si and GaAs devices using Marshak et al.'s Approximation and the Actual Values of Fermi-Dirac Integrals

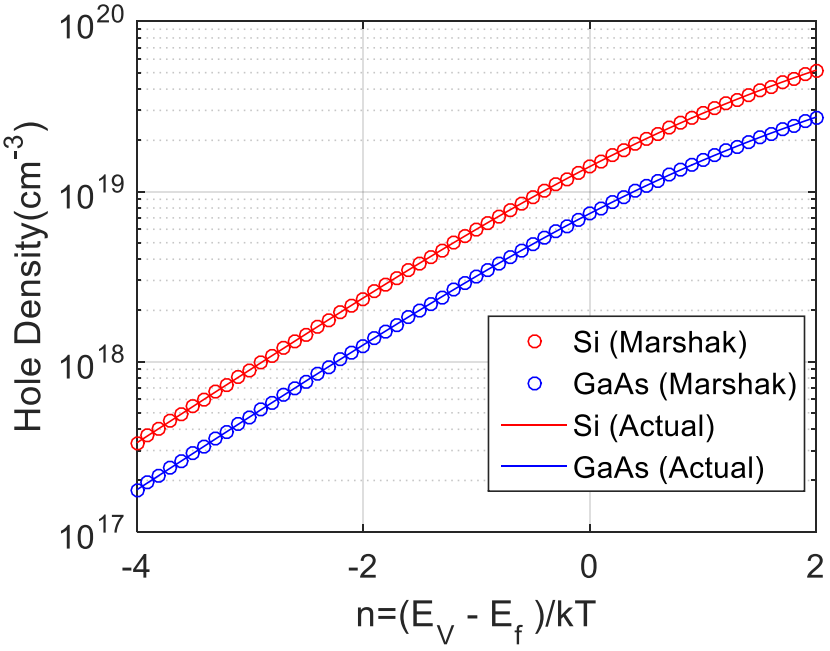

Figure 4.6 Hole Density in Si and GaAs devices using Marshak et al.'s Approximation and the Actual Values of Fermi-Dirac Integrals

Consequently, the carrier concentration equation can be calculated and plotted as shown in Figure 4.5. The relative mean absolute error for this approximation is 0.0043, but this approximation is only valid for values of η below two.

Furthermore, the approximation is not easy to differentiate or integrate in the current density equation and Einstein relation. Figure 4.6 shows the hole concentration in Silicon and Gallium Arsenide at $300\ K$.

Another study that calculates the electron and hole density equations [103] has been conducted by using Aymerich-Humet et al.'s approximation (1983) [8]. The relative mean absolute error is 0.1155, two orders of magnitude bigger than Marshak et al.

Thus, this approximation is not sufficiently suitable to be used in degenerate semiconductors due to its poor accuracy and high complexity to differentiate and to integrate. Figures 4.7 and 4.8 show the electron and hole concentrations in Si and GaAs devices that are determined by Xiao & Wei.

By using a different approach to calculate the electron and hole densities, Das and Khan [30] presented a new approximation for the carrier concentrations based on Van Halen and Pulfrey's approximation of Fermi-Dirac Integrals [97]. Nevertheless, Van Halen and Pulfrey's approximation does not cover any integer of FDI above than $j = +\frac{7}{2}$, so Khan and Das' calculations are hard to be used for the electron density. Moreover, Khan and Das [53] introduced a new approximation to calculate the electron density of degenerate semiconductors with normalized relative Fermi-levels η larger than zero, however most of current degenerate semiconductors have Fermi-levels either below conduction band or into the conduction band.

Thus, the last two approximations cannot be compared to other approximations due to lack of calculating Fermi-Dirac Integrals for the first approximation and non-coverage of an extensive range of values for the second approximation. Previous studies of approximating the carrier concentrations equations still have some issues such as, the complexity of the calculation, poor accuracy, and the limited range of values for the normalized relative Fermi-level position. Therefore, a new simple approximation of carrier concentration is required to obtain an accurate and simple way to calculate the carrier concentration. In the next part of this section, a newly proposed approximation of Fermi-Dirac Integral will be applied to calculate the electron and hole density equations.

The previous chapter explained the new proposed approximation; this part however will show the electron density and hole density with the error at each point of the Fermi-level position thus with different degeneracies.

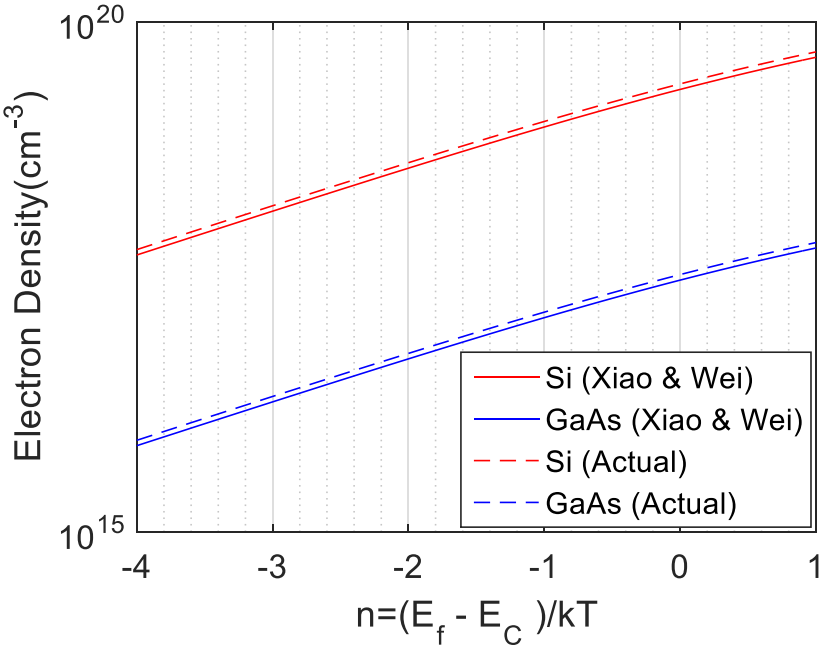

Figure 4.7 Electron Density in Si and GaAs devices using Aymerich-Humet et al.'s Approximation (1983) and the Actual Values of Fermi-Dirac Integrals

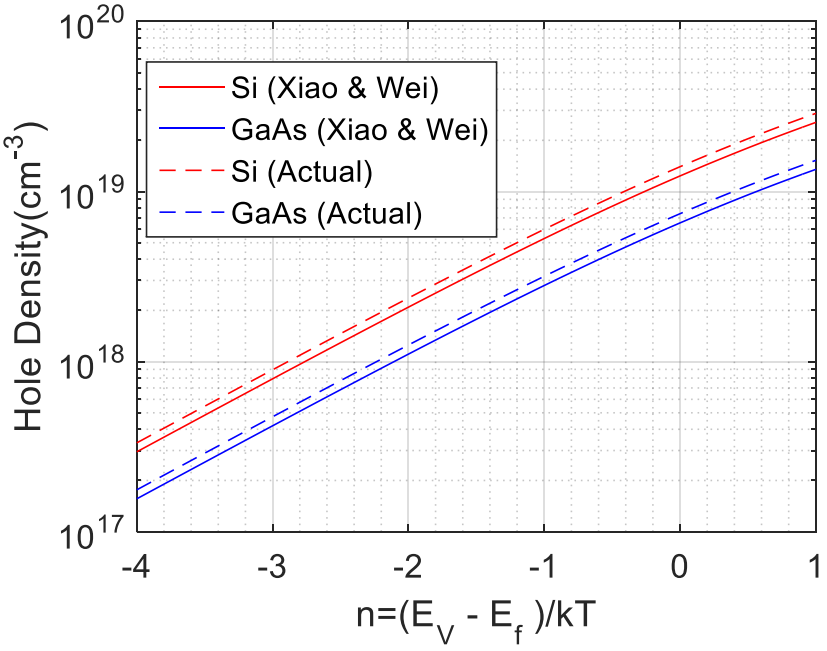

Figure 4.8 Hole Density in Si and GaAs devices using Aymerich-Humet et al.'s Approximation (1983) and the Actual Values of Fermi-Dirac Integrals

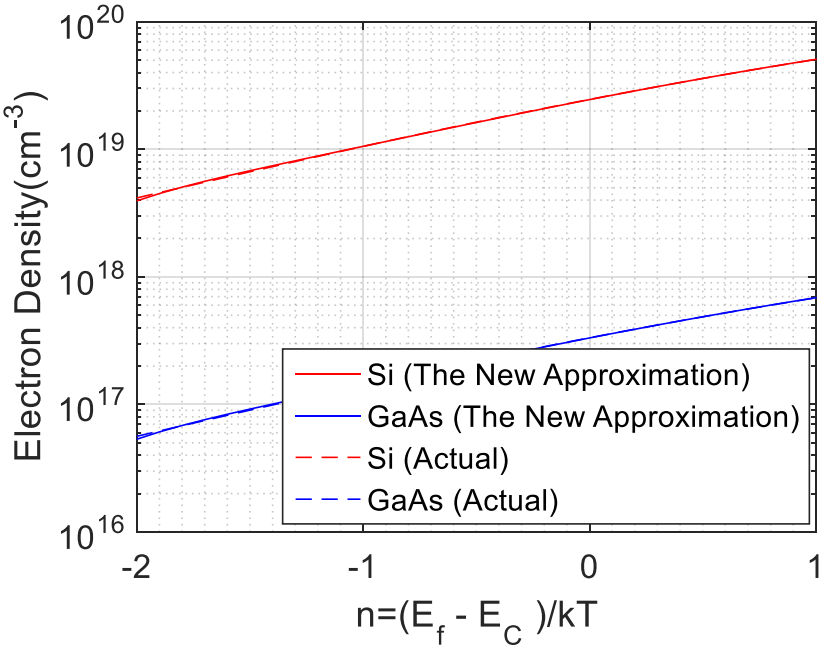

Figure 4.9 Electron Density in Si and GaAs devices using the New Proposed Approximation and the Actual Values of Fermi-Dirac Integrals

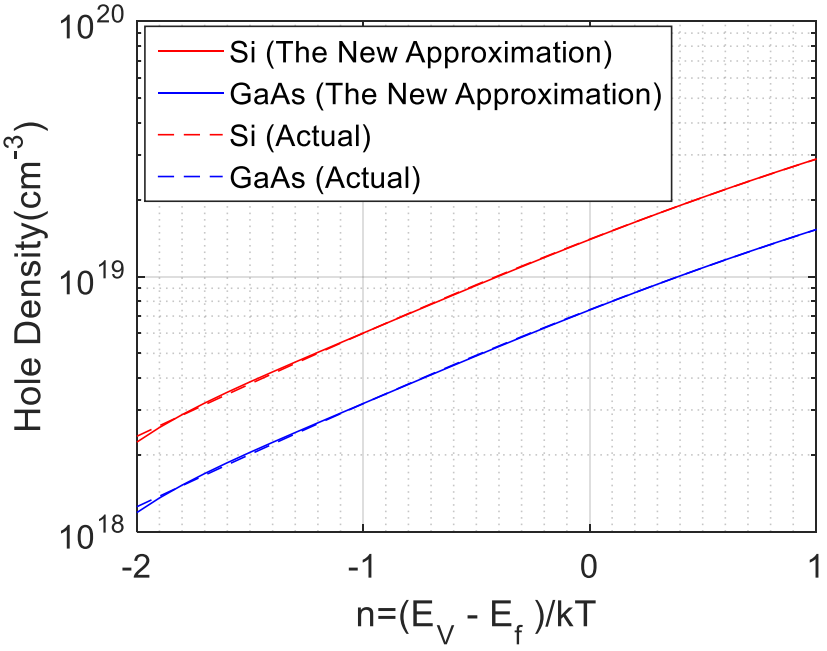

Figure 4.10 Hole Density in Si and GaAs devices using the New Proposed Approximation and the Actual Values of Fermi-Dirac Integrals

As seen Figure 4.9, the range of examined points starts from η of negative two, because Boltzmann's distribution is an accurate enough approximation below negative two. Additionally, the relative mean absolute error is 0.0038; a value comparable to Marshak's relative mean square error. Figure 4.10 shows similarly the hole concentration in Silicon and Gallium Arsenide at 300 K.

The electron and hole densities that have been calculated using the newly proposed approximation can be used efficiently in solving the current density and Einstein relation due to its simplicity to differentiate or to integrate. It has reasonable accuracy. The next section shows different approaches to calculating the Einstein relation compared to the newly proposed approach. Table 4.2 summarizes the studies discussed, above, outlining the errors and issues.

Table 4.2 Summary of Section 4.1

The approximation	**Range η**	**RMAE**	**Issues**
Boltzmann	Below -3	1.2249	Poor accuracy
Marshak [63]	Any value until +2	0.0043	Complexity when used in other equations like Einstein relation
Xiao and Wei [103]	Any value	0.1155	Poor accuracy, complexity when applied to other equations like Einstein relation
Das and Khan [30]	Below zero	0.0367	Dependency on an approximation of Fermi-Dirac Integrals that does not cover all the integers used in their expression
Khan and Das [53]	Above zero	0.0152, 0.2836	Two different ranges , difficult to use in other equations like Einstein relation

4.3 Einstein Relation

The diffusion coefficient and drift mobility are critical parameters in electronic devices which play significant role in the characterization of material quality and electronic transport properties. The Einstein relation describes the ratio between the diffusion coefficient and mobility by using electron and hole concentrations. The general forms of the Einstein relation for electron and hole can be written as follows [56]:

$$\frac{D_n}{\mu_n} = \frac{1}{q}\frac{n}{\frac{dn}{dE_f}} \tag{4.12}$$

$$\frac{D_p}{\mu_p} = \frac{1}{q}\frac{p}{\frac{dp}{dE_f}} \tag{4.13}$$

The Einstein relation depends significantly on Fermi-Dirac Integrals due to the electron and hole. Therefore, many approximations have been used to solve the Einstein relation. The first attempt was made by Landsberg [56], and the resulting form can be expressed as:

$$\frac{D_{n,p}}{\mu_{n,p}} = \frac{kT}{q}\frac{f_{\frac{1}{2}}(\eta)}{f_{-\frac{1}{2}}(\eta)} \tag{4.14}$$

This expression has been plotted by San Li and Lindholm [83] as shown in Figure 4.11. This expression has also been used as a general form of the Einstein relation, and it is being used as a reference to other approximations.

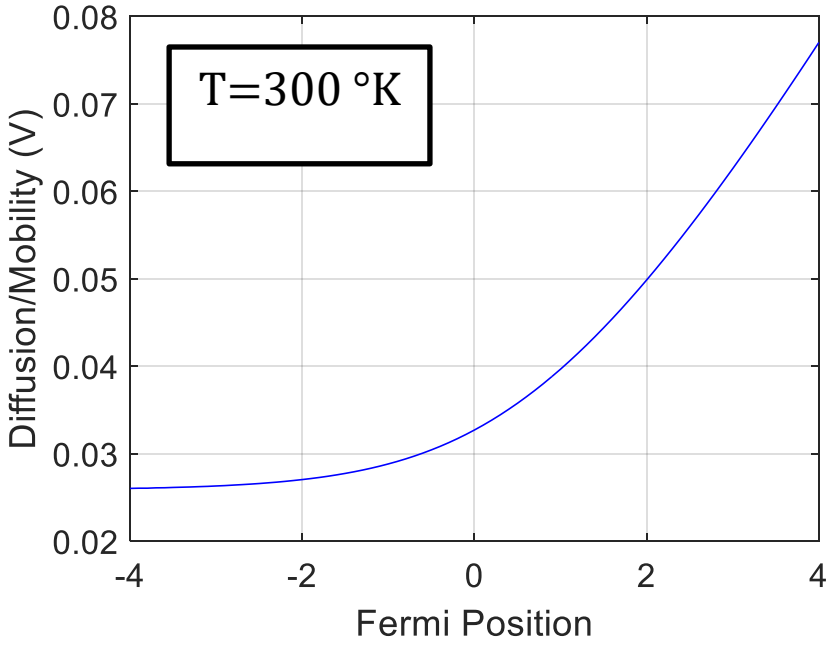

Figure 4.11 Einstein Relation versus the Fermi Level Position

Figure 4.11 shows the diffusion/mobility relation using the previous equation, and it indicates that the relation differs from non-degenerate and degenerate semiconductors. One of the common approaches has used Boltzmann's distribution to calculate the Einstein relation. The form of the relation can be written as:

$$\frac{D_{n,p}}{\mu_{n,p}} = \frac{kT}{q} \tag{4.15}$$

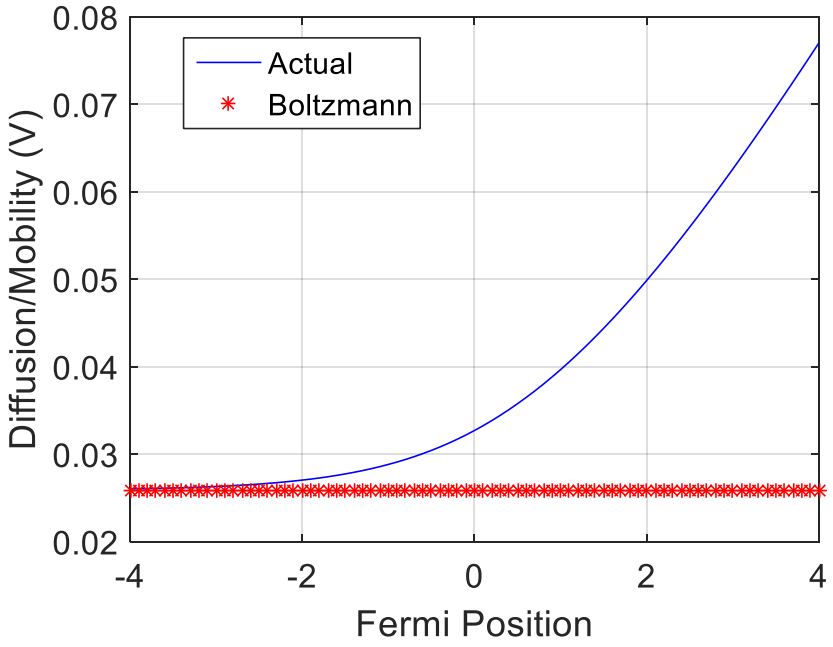

Figure 4.12 Actual Values of Einstein Relation with an Einstein Relation using Boltzmann's Distribution

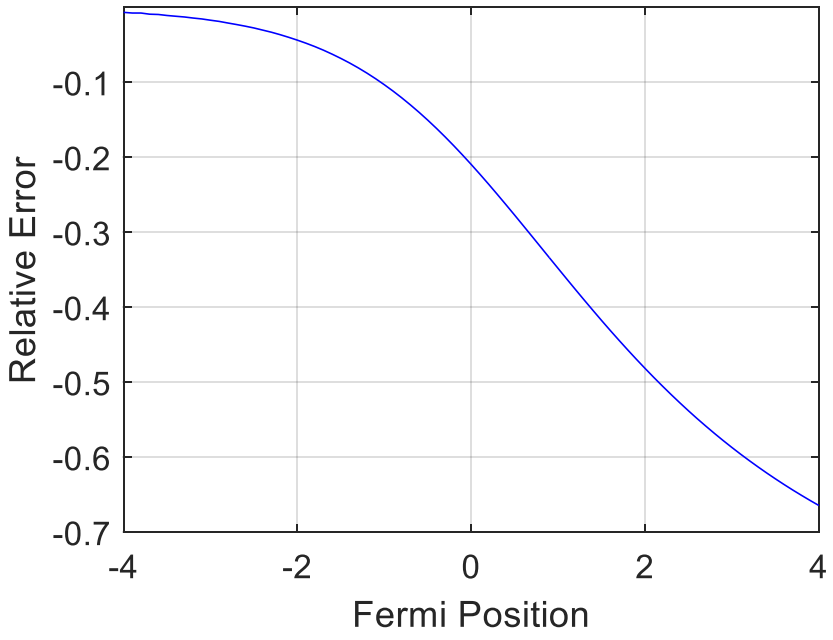

Figure 4.13 Relative Error of Approximated Values of Einstein Relation compared to the Actual Values as a Function of Fermi-Level Position

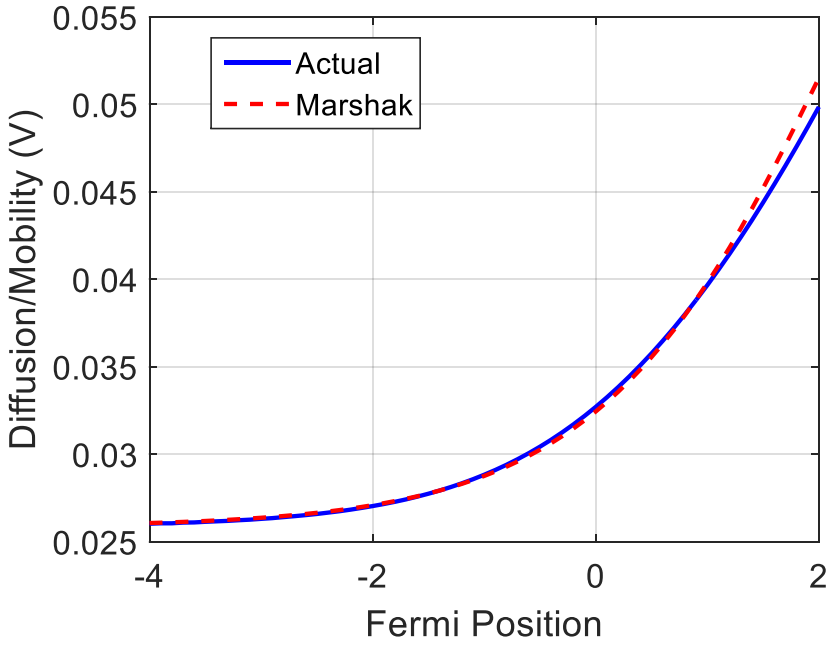

Figure 4.14 Einstein Relation Calculated by Marshak et al. and the Actual Values

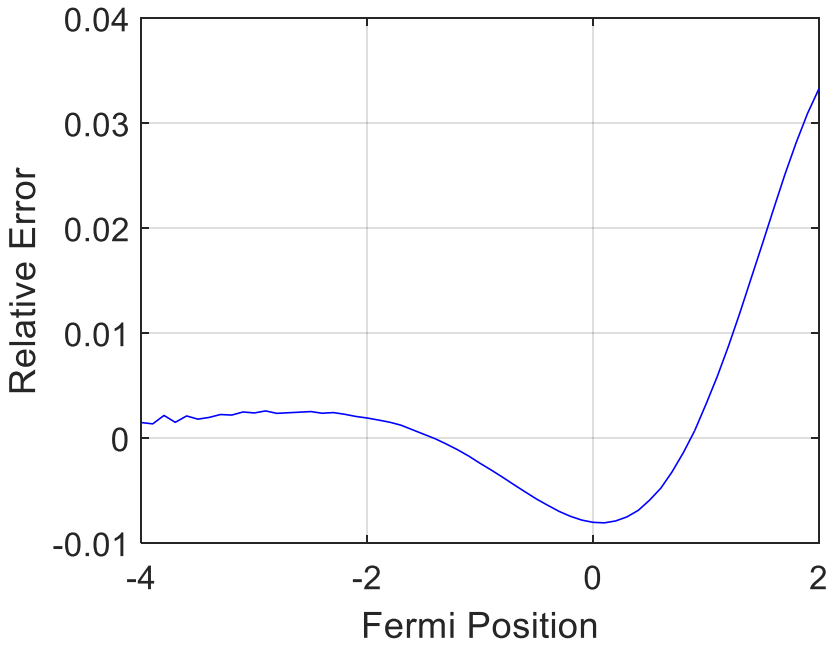

Figure 4.15 Relative Error of the Einstein Relation approximated by Marshak et al. compared to the Actual Values as a Function of Fermi-Level Position

As can be seen in Figure 4.11, it is valid for the normalized relative Fermi-level $\eta<-2$. Thus, equation 4.15 is not valid for degenerate semiconductors since it does not depend on Fermi-Dirac Integrals. Figures 4.12 and 4.13 show the inadequacy of equation (4.15) for degenerate semiconductors. The relative mean absolute error calculated for this approximation is 0.2659. Therefore, this approximation will lead to significant errors when used in heavily doped semiconductors or for high temperature situations. Despite this equation's lack of precision, many studies and books have used it as a general form of the Einstein relation and have calculated Diffusion coefficients based on it [9, 27, 70].

Marshak et al. established another method to calculate the Einstein relation [63], using the same approximation of Fermi-Dirac Integrals. The differentiation of their approximation has been accomplished using a numerical software due to its complexity to differentiate. Figure 4.14 shows the Einstein relation approximated by Marshak compared to the actual values of the Einstein relation.

Though the relative mean absolute error of Marshak et al. is 0.006, the differentiation of their approximation cannot be achieved directly. The relative error profiles of each Fermi-level position can be seen in Figure 4.15. This approximation is only valid for values of η below positive two.

Xiao and Wei [103] assumed that the narrowing bandgap could affect the electron and hole densities, so the diffusion to mobility ratio for electrons can be modified and written as follows::

$$\frac{D_n}{\mu_n} = \frac{kT}{q} * \frac{f_{\frac{1}{2}}(\eta)}{f_{-\frac{1}{2}}(\eta)} * \frac{1}{1+\frac{\lambda_n}{\frac{kT}{N_C f_{-\frac{1}{2}}(\eta)}-\lambda_n}} \tag{4.16}$$

where $\lambda_n = \frac{d\Delta E_{gC}}{dN_D}$ and ΔE_{gC} is the bandgap narrowing of the conduction band due to the effects of high doping.

This approximation can be applied when bandgap narrowing is considered, but it is not considered in this thesis. Furthermore, the electron and hole densities equations would be affected by bandgap narrowing if the bandgap narrowing is taken into account. Khan and Das [30, 53] introduced two new approximations of diffusion-mobility relations that depend on another approximation of Fermi-Dirac Integrals [97]. Their proposed equations can be expressed as follows:

$$\frac{D_n}{\mu_n} = \left(\frac{kT}{q}\right) \frac{\sum_{j=1}^{7} (kT)^{j-1} \Gamma\left(j+\frac{1}{2}\right) \xi_j f_{j-\frac{1}{2}}(\eta_C)}{\sum_{j=1}^{7} (kT)^{j-1} \Gamma\left(j+\frac{1}{2}\right) \xi_j f_{j-\frac{3}{2}}(\eta_C)} \tag{4.17}$$

$$\frac{D_n}{\mu_n} = \left(\frac{kT}{q}\right) \left[\frac{\xi_1 \xi_4}{\xi_1+\xi_2 \xi_3}\right] \frac{f_{\frac{1}{2}}(\eta_C)}{f_{-\frac{1}{2}}(\eta_C)} \tag{4.18}$$

Equation (4.18) calculates the diffusion-mobility ratio due to the bandgap narrowing situation, but equation (4.17) can be a general approximation of diffusion-mobility ratio. However, they have depended on an approximation of Fermi-Dirac Integrals that does not have any approximation for integrals larger than $\frac{3}{2}$, and their equations need an approximation of Fermi-Dirac Integrals of ($j = \frac{9}{2}, \frac{10}{2}, \frac{11}{2}, \frac{12}{2}, \frac{13}{2}$).

Without considering bandgap narrowing, an accurate and simple approximation of diffusion-mobility ratio is required. Therefore, the proposed approximation of Fermi-Dirac Integrals and its first derivative function will be used to calculate the diffusion-mobility ratio. Using the equation of Landsberg [56], the diffusion-mobility ratio can be computed as shown in Figure 4.16.

As seen in Figure 4.16, the Einstein Relation using the new approximation has somewhat large errors around η values of negative two because of the error of the first derivative function of the proposed approximation. The relative mean absolute error of the Einstein relation calculated by the new approximation is 0.0194, which is larger than the Einstein Relation using Marshak et al. approximation [63]. The relation can be solved directly by differentiating the proposed approximation. This shows the simplicity of using the new approximation compared to Marshak et al.'s. Moreover, the proposed approximation covers the range of η values -2 to +4 while Marshak et al. approximation only covers the η values up to positive two. Figure 4.17 shows the relative error of each Fermi-level position.

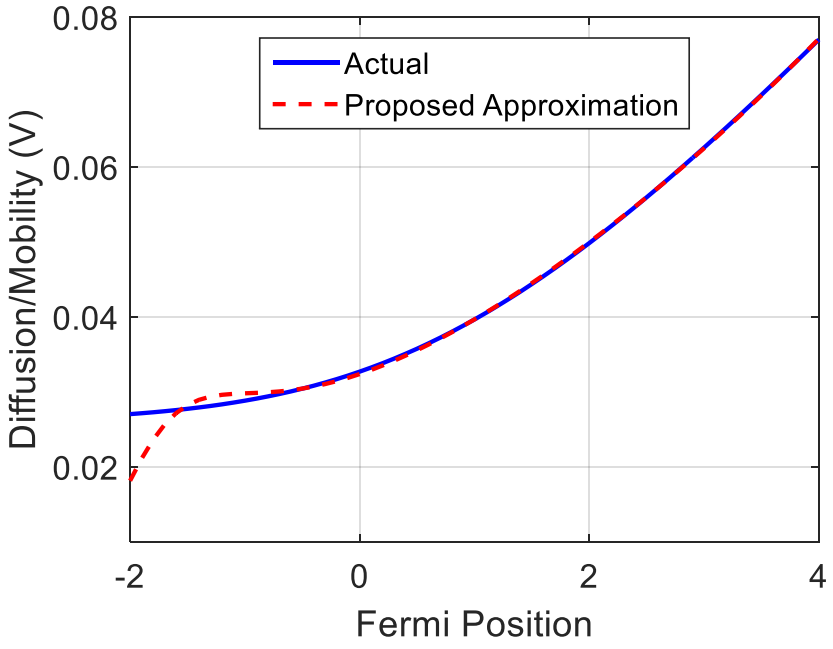

Figure 4.16 Einstein Relation Calculated by the New Proposed Approximation and Actual Values

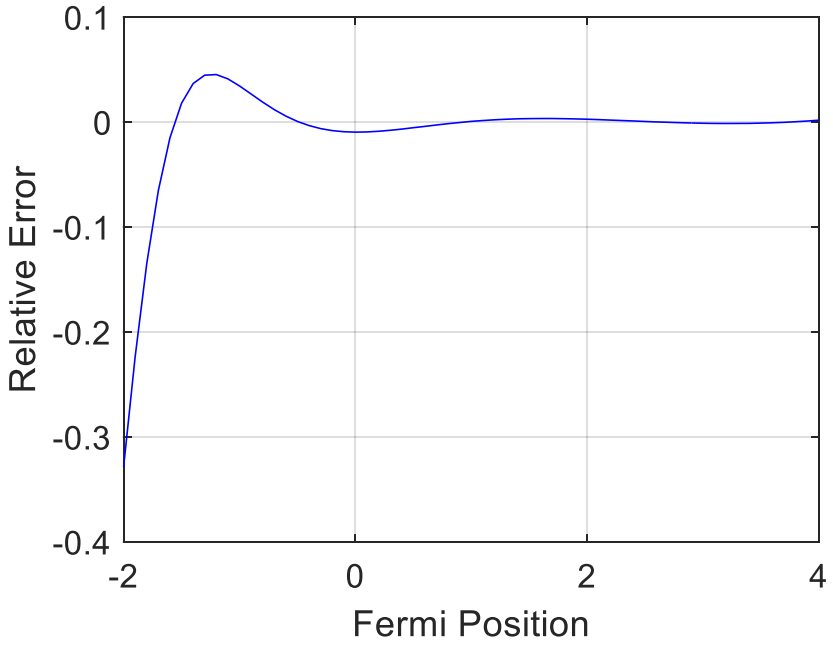

Figure 4.17 Relative Error of Einstein Relation Calculated by the Proposed Approximation compared to the Actual Values as a Function of Fermi-Level Position

In the next section, some electronic devices that have been considered as heavily doped devices such as Junctionless Transistors (JLT) will be studied and discussed. Some aspects of these devices which have been affected by different approximations of Fermi-Dirac Integrals will be presented.

4.4 Junctionless Transistors (JLT)

The junctionless transistor (JLT) is a multigate FET with no PN, N^+N or P^+P junctions, and they act like resistors. Therefore, the gate can adjust the mobile charge density. There are two states for these transistors: ON state and OFF state. In ON state, high doping concentration in the channel region causes large body current, and the surface accumulation current can be added. In Off state, since there is a difference in the workfunction between the semiconductor and the gate material, the depletion region turns off the channel. In addition, two major aspects should be satisfied in Junctionless transistors: high doping to achieve suitable current drive, and small cross section to be able to turn off the device.

Since the Junctionless transistors need to be heavily doped, the Boltzmann's distribution cannot be applied. However, a few research studies based on Boltzmann's distribution have recently been published. Guo et al. introduced a three-dimensional analytical model for short-channel triple-gate junctionless MOSFET, but their hole density was calculated using Boltzmann's approximation [44]. Nevertheless, their doping

concentrations were high, so their calculations should be modified using an approximation that is more accurate and straightforward. Their equations depend on the Quasi-Fermi level, which can be affected by high doping concentrations. In the section below, a few results will be studied using different approximations of Fermi-Dirac Integrals.

Recently, the Double Gate Ferroelectric Junctionless Transistor (DGFJL) has been modeled and simulated using 2D ATLAS software [65]. Figure 4.18 shows the modeled and simulated electron density versus various gate voltages. It should be noted that this study should be compared to an experimental work to observe the difference in the value of electron density at each value of gate voltage. Another study was conducted to optimize nanoscale JLT that can be used for ultra-low power logic applications by varying device design parameters [81] using 2D ATLAS software [87]. However, 2D ATLAS software used FDI approximation using Boltzmann's approximation instead of Fermi-Dirac Integrals for order $\frac{1}{2}$ and Rational Chebyshev approximation for orders $-\frac{3}{2}, -\frac{1}{2}, \frac{3}{2}$ [87]. Though the accuracy of Rational Chebyshev approximation is very high [27], the use of this approximation cannot be performed easily and without computer simulation tools.

Wang et al. developed a high-performance junctionless MOSFET with an asymmetric gate (AG-JL) [102] by conducting experimental and simulated work. They used 2D Sentaurus software [90]. Their results show AG-JL that shows the difference between the experimental and simulated results as can be seen in Figure 4.19. Furthermore, Hosseini analyzed the electrical characteristics of Strained Junctionless Double-Gate MOSFET (Strained JL DG MOSFET) [49] based on quantum model approach that depends on non-equilibrium Green's function (NEGF) method [4]. He used 2D ATLAS software which is not accurate for calculating Fermi-Dirac Integrals of order $\frac{1}{2}$ [87]. There are a few attempts that have tried to model the equations of junctionless transistors to make the calculations simple and easy. A proposed charge-based continuous model for long-channel Symmetric Double-Gate Junctionless Transistors was simulated and validated for high doping concentrations [19], but the mobile charge density was computed based on Boltzmann's distribution as shown in equation (4.19).

$$\rho = qN_D(-e^{\frac{\varphi_s - V}{\varphi_t}} + 1) \tag{4.19}$$

where $\varphi_t = \frac{kT}{q}$, $V = V_D - V_s$, N_D is doping concentration

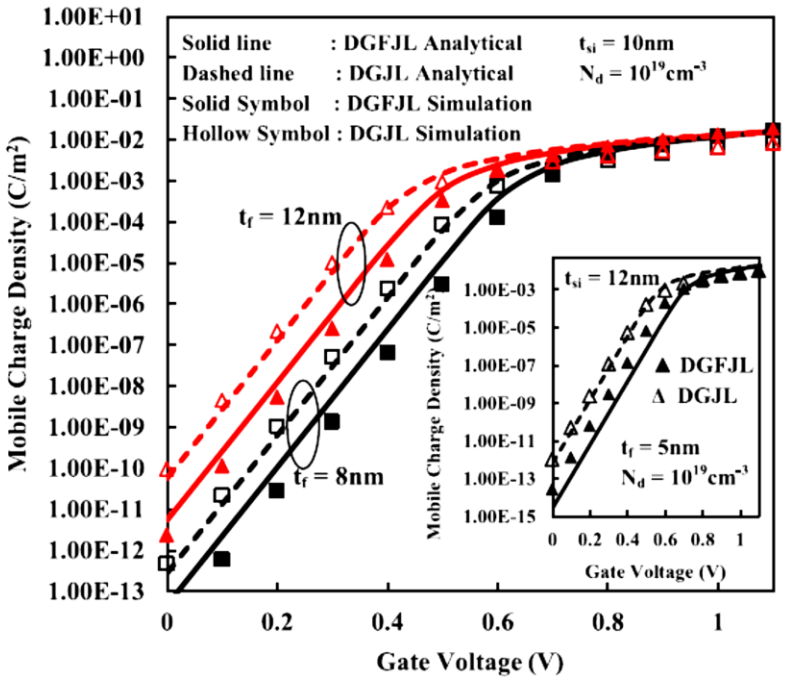

Figure 4.18 Mobile Charge Density of Double Gate Ferroelectric Junctionless Transistor (DGFJL) compared to Double Gate Junctionless Transistor (DGJL) [65]

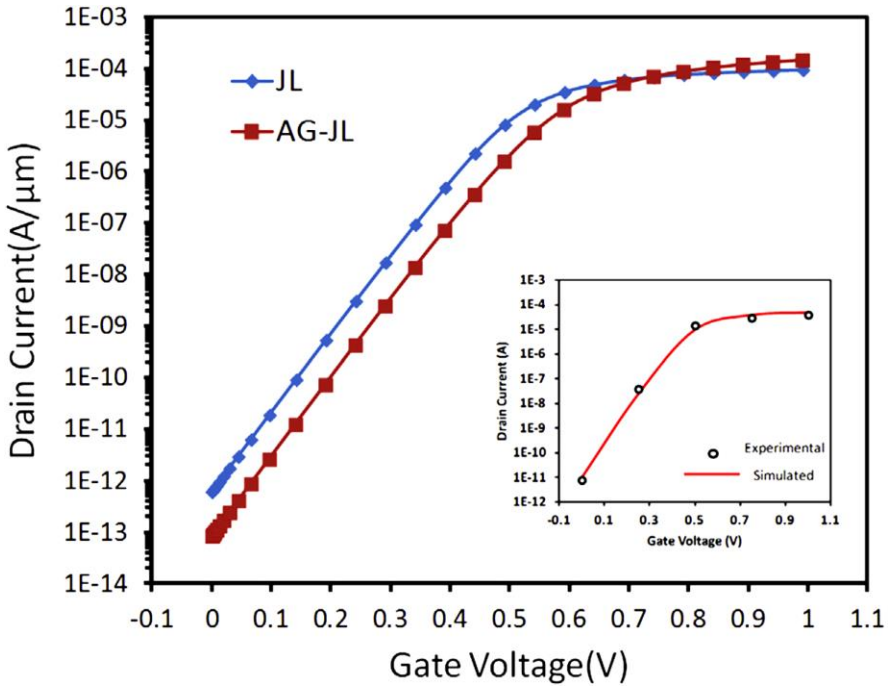

Figure 4.19 Drain Current versus Gate Voltage of JL and AG-JL MOSFET, the inset shows the simulated and experimental results of AG-JL [102]

Thus, the drain current can be calculated by using the following equation

$$I_D = \frac{K\varphi_t}{1+KR(V_g-V_T-nV_d)} \int_{V_s}^{V_d} q_n dV \qquad (4.20)$$

where $K = 2\frac{W}{L}\, C_{ox}\mu_o$, V_T is the threshold voltage, R is the series resistance, q_n is mobile charge density and V_G is the gate voltage.

To calculate the surface potential φ_s, the following equation can be used [82]

$$\varphi_s = \varphi_0 + \frac{Q_b}{8C_s}\,(e^{\frac{\varphi_0-V}{\varphi_t}} - 1) \qquad (4.21)$$

where φ_0 is the potential at the centre of the layer, Q_b is the total fixed charge, $C_s = \frac{\varepsilon_s}{t_s}$.

As can be observed from Figures 4.20 and 4.21, the simulated and modeled values have excellent agreement. Nonetheless, the researchers used the Boltzmann's approximation in their calculations of mobile electron charge even though their doping concentration is high [19]. Moreover, the simulation software that has been used to validate the proposed model, ATLAS, uses the Boltzmann's distribution to determine the mobile charge [61].

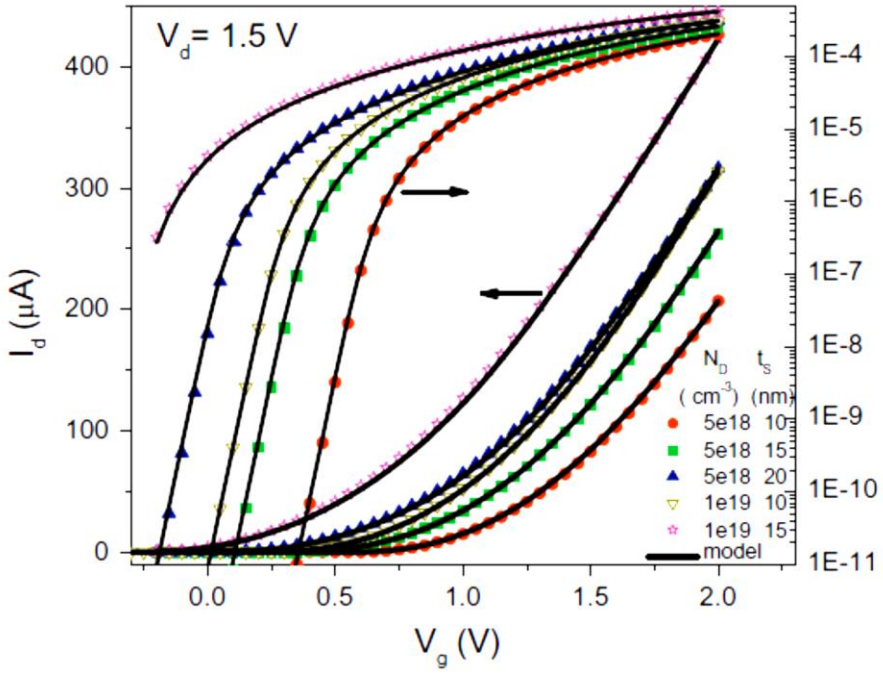

Figure 4.20 The Drain Current versus Gate Voltages of Different Devices with Different Doping Concentrations and Thicknesses Compared to the Modeled Device while $V_D = 1.5$ V [19]

Other studies have been conducted to obtain full-range drain current model with Pao–Sah electrostatic assumptions and by extending the parabolic potential approximation in the subthreshold and the linear

regions [34], while Trevisoli et al. proposed a physically-based definition of threshold voltage in nanowire junctionless transistors analytically and experimentally by using Sentaurus [95].

In order to simplify the calculations of mobile charge density in junctionless transistors to be used in drain current density, Avila-Herrera et al. introduced a new approximation of mobile charge density with its impact on calculations of drain current [6]. Their approximation used Boltzmann's distribution to determine the electron concentration as shown in the following equation:

$$n_{PBz} = F_z(\gamma_C) n_B \tag{4.22}$$

where n_{PBz} is the electron density by Pseudo-Boltzmann continuous, which is their proposed approximation, n_B is the electron density calculated by Boltzmann's approximation, and γ_C is the normalized relative Fermi-level.

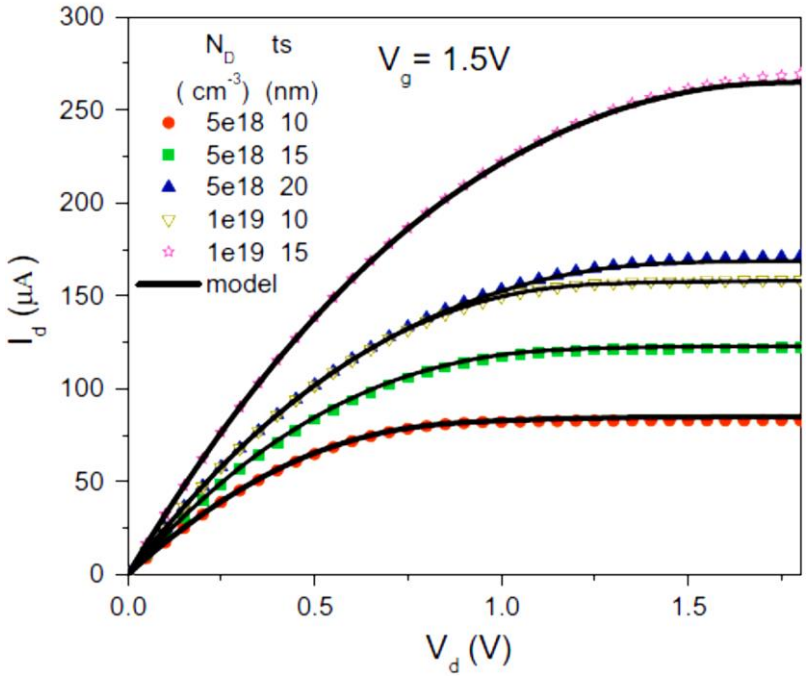

Figure 4.21 The Drain Current versus Drain Voltages of Different Devices with Different Doping Concentrations and Thicknesses Compared to the Modeled Device while $V_G = 1.5$ V [19]

Avila-Herrera et al. proposed an approximation of FDI as shown in equation (4.23):

$$F_z(\gamma_C) \approx \frac{n_{PBz}}{n_B} \approx a_1 e^{(b_1-1)\gamma_C} + \frac{1}{2}\left[\left(1 - a_1 e^{(b_1-1)\gamma_C} + c\right) - \sqrt{(1 - a_1 e^{(b_1-1)\gamma_C} + c)^2 + 4c(a_1 e^{(b_1-1)\gamma_C})}\right] \tag{4.23}$$

$a_1 = 0.7774,$

$b_1 = 0.8127,$

$c = 0.006$

Figure 4.22 shows the calculated electron concentration by Pseudo-Boltzmann continuous model compared to the actual value, and the relative mean absolute error is 0.0486. However, this approximation is valid up to $\gamma_C = 0.5$ because it gives large errors for γ_C values of above 0.5. The relative error profiles can be seen in Figure 4.23. Since the junctionless transistors use heavily doped semiconductor as the active region, this approximation cannot be valid for all the applications of junctionless transistors.

The researchers used their approximation of electron density to calculate drain current of a junctionless Silicon transistor with equation (4.20) while q_n is the calculated mobile charge density by Pseudo-Boltzmann continuous model.

Because the approximation of electron density is complicated and difficult to differentiate or integrate, the equations for solving the drain current equation for different drain and gate voltages cannot be solved without using a simulation tool. Furthermore, the modeled values using Pseudo-Boltzmann's continuous approximation are similar to the values obtained using Boltzmann's distribution as can been seen in Figures 4.24 and 4.25.

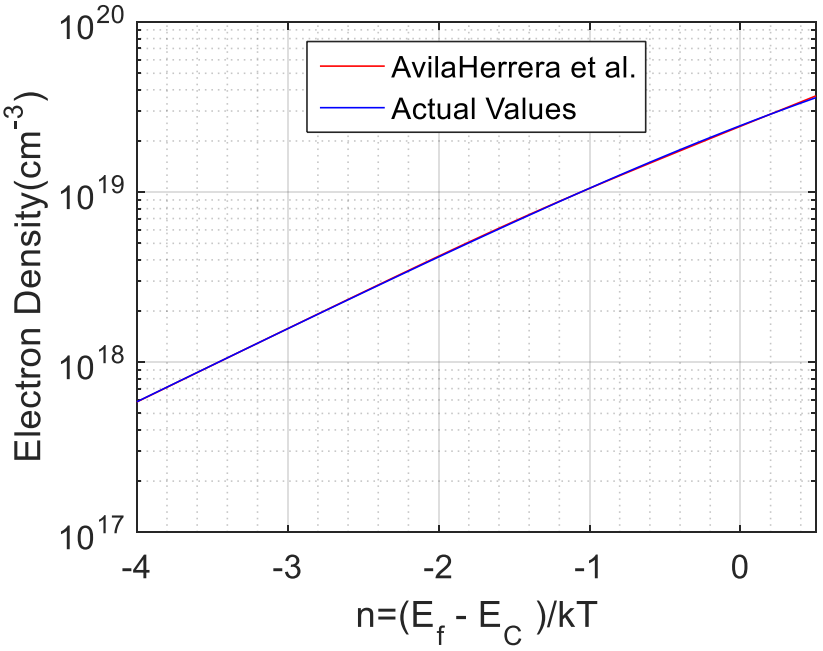

Figure 4.22 Electron Density of Si JLT using Avila-Herrera et al. Approximation and the Actual Values of Fermi-Dirac Integrals

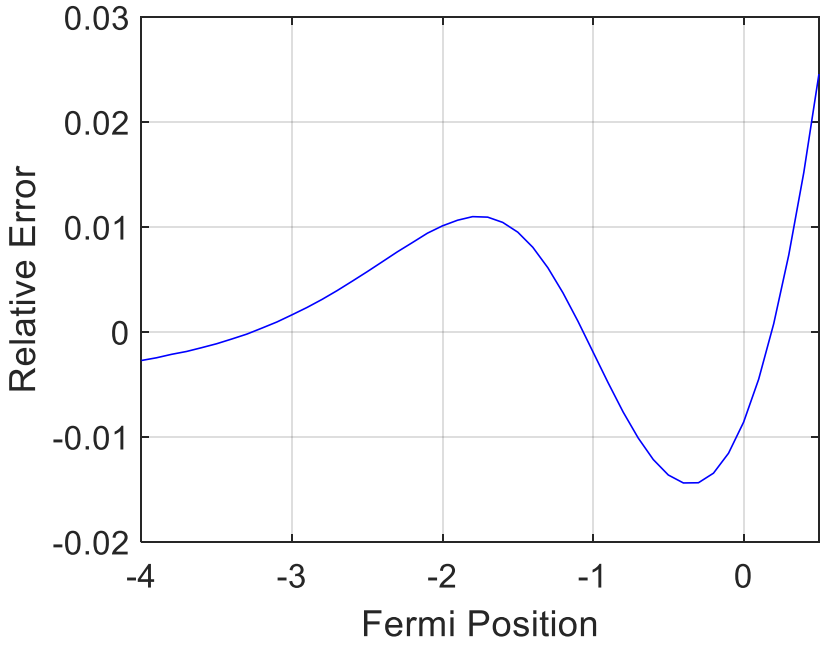

Figure 4.23 Relative Error of Electron Density Approximated by Avila-Herrera et al. compared to the Actual Values as a Function of Fermi-Level Position

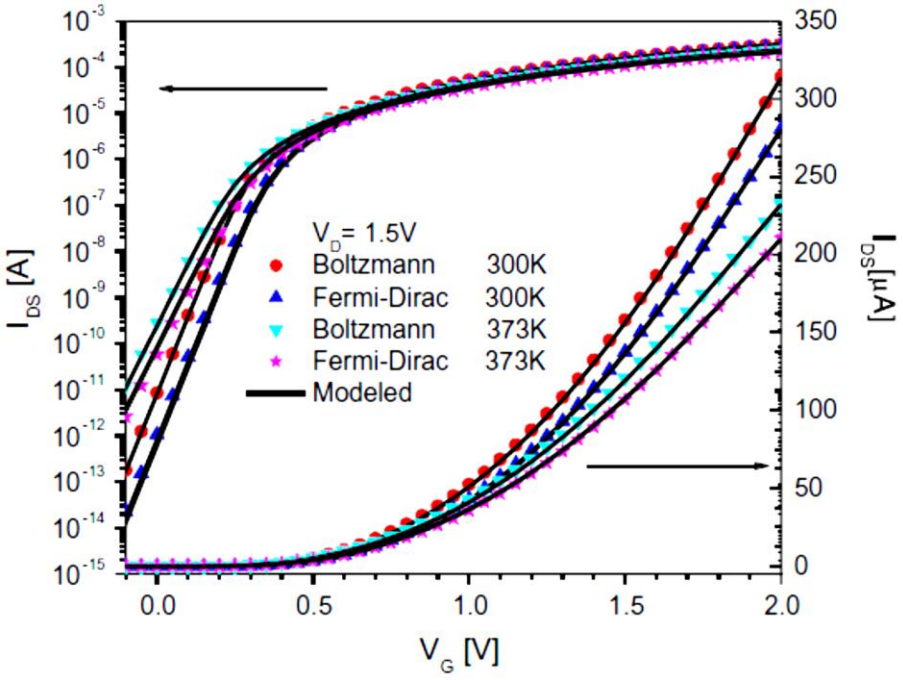

Figure 4.24 Comparison between Different Drain Currents Using Different Approximations of Electron Density with the Actual Fermi-Dirac Values while $V_D = 1.5$ V [6]

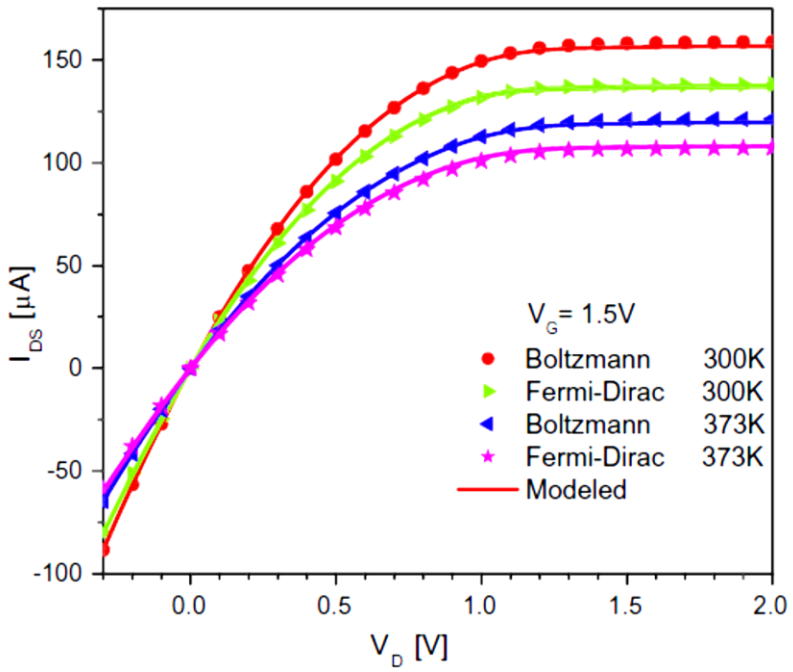

Figure 4.25 Comparison between Different Drain Currents Using Different Approximations of Electron Density with the Actual Fermi-Dirac Values while $V_G = 1.5$ V [6]

They also used Atlas 2D simulation, which depends on Boltzmann's approximation. Therefore, the new proposed approximation of electron density using Prony's method has been applied on mobile charge density to establish a new expression of the current density of junctionless transistors. Firstly, the mobile charge density of N-type Silicon JLT is formed as

$$\rho = q(-n + N_D) \tag{4.24}$$

$$\rho = q\left(-N_C f_{\frac{1}{2}}\left(\frac{\varphi - V}{\varphi_t}\right) + N_D\right) \tag{4.25}$$

Where $f_{\frac{1}{2}}\left(\frac{\varphi-V}{\varphi_t}\right) = \sum_{i=1}^{4} C_i e^{a_i\left(\frac{\varphi-V}{\varphi_t}\right)}$ $N_C = 3.217 * 10^{19} cm^{-3}$ at $T = 300\ K$, $N_D = 10^{19} cm^{-3}$

The potential at center ($\varphi_0 = \varphi(0)$) can be obtained by applying the Poisson's equation then equate it to zero, so the form of Poisson's equation is

$$\nabla^2 \varphi = -\frac{\rho}{\varepsilon_{si}} = -\frac{q}{\varepsilon_{si}}\left(-N_C \sum_{i=1}^{4} C_i e^{a_i\left(\frac{\varphi-V}{\varphi_t}\right)} + N_D\right) = 0 \tag{4.26}$$

$$\frac{N_D}{N_C} = \sum_{i=1}^{4} C_i e^{a_i\left(\frac{\varphi-V}{\varphi_t}\right)} \tag{4.27}$$

By calculating $\frac{N_D}{N_C} = 0.31085$ which is equal to a certain value of the new proposed approximation of Fermi-Dirac Integrals of order $\frac{1}{2}$, the value of $\frac{\varphi_0 - V}{\varphi_t} = -1.06275$. Thus, the equation of φ_0 is

$$\varphi_0 = V - 1.06275\frac{kT}{q} \quad (4.28)$$

Consequently, one can see that the values of drain current and φ_s will be affected due to changes in the form of mobile charge density.

4.5 Other Applications of Fermi-Dirac Integrals

Fermi-Dirac Integrals are not only crucial in semiconducting applications, but they also play an important role in other applications. For instance, Fermi-Dirac Integrals have been used in non-Debye specific heat applications to calculate the difference between entropies [21]. In addition, Charlier, Blase, and Roche used Fermi-Dirac Integrals to determine the current density in nanotube devices [23]. Another research which had used Fermi-dirac Integrals in quantum computer showed that Fermi-Dirac Integral plays a key role in a condition for the onset of chaos [13]. Groß et al. introduced a new model to determine the absorption enthalpies and entropy of the resulting water vapor pressure-hydrogen composition isotherms [43]. As one of the least example I want to cite here, the Fermi-Dirac Integrals has been used to compare results for non-Long Term Evolution (LTE) systems [104].

4.6 Summary

In this chapter, the applications of Fermi-Dirac Integrals in semiconductor devices have been discussed. Firstly, the electron and hole densities in Silicon and Gallium Arsenide devices have been studied with different approximations and actual values of Fermi-Dirac Integrals. Second, the electron and hole concentrations of Si and GaAs devices were determined by using the proposed approximation developed in this thesis, our calculations showed a small RMSE compared to the other approximations. The second application was Einstein relation, and the importance of this relation in electronic devices was presented. The Einstein relation was calculated by using the actual values of Fermi-Dirac Integrals and approximated using various approximations of Fermi-Dirac Integrals. The last application of Fermi-Dirac Integrals in semiconductor devices was junctionless transistors where drain current in junctionless transistors was determined using Boltzmann's distribution. The last section showed other applications of Fermi-Dirac Integrals in non-semiconducting devices. The next chapter will summarize the thesis, indicating future work that can be related to this thesis.

Chapter 5
Conclusion and Future Work

5.1 Conclusion

In this thesis I introduced a new analytical approximation for the Fermi-Dirac Integrals of half order using Prony's method. It was shown that not only that the magnitude of FDI are well approximated, but it predicted as well the rate of change. The exponential series approximation lent itself for easy differentiation and integration. The quality of the approximation for FDI was tested by twice differentiating and integrating the expression of the approximation and comparing them to the actual values. These tests showed how good the approximation is. In order to compare the accuracy of my approximation I surveyed a range of previous approximations and determined their accuracies. I used relative mean absolute error to assess the approximations. Finally I employed the new approximation in a few devices and in Einstein Relation and showed the usefulness.

5.2 Future Work

A careful look at this problem shows that there are a number of potential works that can be done.

- When semiconductors are doped heavily the fundamental bandgap shrinks. This will impact the carrier densities in combination with FDI. This has not been pursued in this thesis but can be done as a future work.
- Investigations of Einstein Relation for heavily doped regions along with the new approximation of FDI would lead to useful results in a tractable way.
- For non-thermal equilibrium situations, the quasi-Fermi level would be impacted by the FDI.
- A study of devices like Junctionless Transistors with this new approximation for FDI would lead to significant corrections or modifications of the computation of its terminal characteristics.
- The impact of this new approximation on the characteristics of MIM devices can be studied.

References

[1] S. Abidi and S. N. Mohammad, "Approximation for the Fermi–Dirac integral with applications to degenerately doped solar cells and other semiconductor devices," *J. Appl. Phys.,* vol. 56, pp. 3341-3343, 1984.

[2] A. Abramo *et al*, "Two-dimensional quantum mechanical simulation of charge distribution in silicon MOSFETs," *IEEE Trans. Electron Devices,* vol. 47, pp. 1858-1863, 2000.

[3] M. T. Abuelma'atti, "Approximations for the Fermi-Dirac integrals Fj (x)," *Solid-State Electronics,* vol. 37, pp. 1367-1369, 1994.

[4] O. M. Alatise *et al*, "Improved analog performance in strained-Si MOSFETs using the thickness of the silicon–germanium strain-relaxed buffer as a design parameter," *IEEE Trans. Electron Devices,* vol. 56, pp. 3041-3048, 2009.

[5] J. M. Aparicio, "A simple and accurate method for the calculation of generalized Fermi functions," *The Astrophysical Journal Supplement Series,* vol. 117, pp. 627, 1998.

[6] F. Avila-Herrera *et al*, "Pseudo-Boltzmann model for modeling the junctionless transistors," *Solid-State Electronics,* vol. 95, pp. 19-22, 2014.

[7] X. Aymerich-Humet, F. Serra-Mestres and J. Millan, "An analytical approximation for the Fermi-Dirac integral F32 (η)," *Solid-State Electronics,* vol. 24, pp. 981-982, 1981.

[8] X. Aymerich-Humet, F. Serra-Mestres and J. Millan, "A generalized approximation of the Fermi–Dirac integrals," *J. Appl. Phys.,* vol. 54, pp. 2850-2851, 1983.

[9] M. Balkanski 1927-, *Semiconductor Physics and Applications.* Oxford ; New York: Oxford University Press, 2000.

[10] J. Batey and S. Wright, "Energy band alignment in GaAs:(Al, Ga) As heterostructures: The dependence on alloy composition," *J. Appl. Phys.,* vol. 59, pp. 200-209, 1986.

[11] H. B. Bebb and C. Ratliff, "Numerical Tabulation of Integrals of Fermi Functions Using k lim→· p lim→ Density of States," *J. Appl. Phys.,* vol. 42, pp. 3189-3194, 1971.

[12] D. Bednarczyk and J. Bednarczyk, "The approximation of the Fermi-Dirac integral F12 (η)," *Physics Letters A,* vol. 64, pp. 409-410, 1978.

[13] G. Benenti, G. Casati and D. L. Shepelyansky, "Emergence of Fermi-Dirac thermalization in the quantum computer core," *The European Physical Journal D-Atomic, Molecular, Optical and Plasma Physics,* vol. 17, pp. 265-272, 2001.

[14] H. S. Bennett, "Majority and minority electron and hole mobilities in heavily doped gallium aluminum arsenide," *J. Appl. Phys.,* vol. 80, pp. 3844-3853, 1996.

[15] V. Bhagat, R. Bhattacharya and D. Roy, "On the evaluation of generalized Bose–Einstein and Fermi–Dirac integrals," *Comput. Phys. Commun.,* vol. 155, pp. 7-20, 2003.

[16] J. S. Blackmore, *Semiconductor Statistics.* Pergamon, 1962.

[17] P. Brounkov, T. Benyattou and G. Guillot, "Simulation of the capacitance–voltage characteristics of a single-quantum-well structure based on the self-consistent solution of the Schrödinger and Poisson equations," *J. Appl. Phys.,* vol. 80, pp. 864-871, 1996.

[18] H. Casey Jr, "Room-temperature threshold-current dependence of GaAs-Al x Ga1− x As double-heterostructure lasers on x and active-layer thickness," *J. Appl. Phys.,* vol. 49, pp. 3684-3692, 1978.

[19] A. Cerdeira *et al*, "Charge-based continuous model for long-channel symmetric double-gate junctionless transistors," *Solid-State Electronics,* vol. 85, pp. 59-63, 2013.

[20] T. Chai and R. R. Draxler, "Root mean square error (RMSE) or mean absolute error (MAE)?–Arguments against avoiding RMSE in the literature," *Geoscientific Model Development,* vol. 7, pp. 1247-1250, 2014.

[21] R. V. Chamberlin and B. F. Davis, "Modified Bose-Einstein and Fermi-Dirac statistics if excitations are localized on an intermediate length scale: Applications to non-Debye specific heat," *Physical Review E,* vol. 88, pp. 042108, 2013.

[22] T. Chang and A. Izabelle, "Full range analytic approximations for Fermi energy and Fermi–Dirac integral F− 1/2 in terms of F 1/2," *J. Appl. Phys.,* vol. 65, pp. 2162-2164, 1989.

[23] J. Charlier, X. Blase and S. Roche, "Electronic and transport properties of nanotubes," *Reviews of Modern Physics,* vol. 79, pp. 677, 2007.

[24] J. Chen, "A circuit-compatible analytical device model for ballistic nanowire transistors," *Microelectron. J.,* vol. 39, pp. 750-755, 2008.

[25] A. C. Chia and R. R. LaPierre, "Analytical model of surface depletion in GaAs nanowires," *J. Appl. Phys.,* vol. 112, pp. 063705, 2012.

[26] K. Chu and D. Pulfrey, "An improved analytic model for the metal-insulator-semiconductor tunnel junction," *IEEE Trans. Electron Devices,* vol. 35, pp. 1656-1663, 1988.

[27] J. Chu, *Device Physics of Narrow Gap Semiconductors.* New York: Springer, 2010.

[28] L. D. Cloutman, "Numerical evaluation of the Fermi-Dirac integrals," *The Astrophysical Journal Supplement Series,* vol. 71, pp. 677, 1989.

[29] W. Cody and H. C. Thacher Jr, "Rational Chebyshev approximations for Fermi-Dirac integrals of orders-1/2, 1/2 and 3/2," *Mathematics of Computation,* vol. 21, pp. 30-40, 1967.

[30] A. Das and A. Khan, "Carrier concentrations in degenerate semiconductors having band gap narrowing," *Zeitschrift Für Naturforschung A,* vol. 63, pp. 193-198, 2008.

[31] S. De *et al*, "Studies on temperature and concentration dependent minority carrier lifetime in heavily doped InGaAsP," *Solid-State Electronics,* vol. 37, pp. 1455-1457, 1994.

[32] A. Dimoulas *et al*, "Electric-field dependence of interband transitions in In0. 53Ga0. 47As/In0. 52Al0. 48As single quantum wells by room-temperature electrotransmittance," *J. Appl. Phys.,* vol. 72, pp. 1912-1917, 1992.

[33] R. Dingle, "The fermi-dirac integrals\ mathcal {F} _p (\ eta)=(p!)^{-1}\ mathop\ smallint\ limits_0^\ infty\ varepsilon^ p (e^{\ varepsilon-\ eta} 1)^{-1} d\ varepsilon," *Applied Scientific Research, Section A,* vol. 6, pp. 225-239, 1957.

[34] J. P. Duarte, S. Choi and Y. Choi, "A full-range drain current model for double-gate junctionless transistors," *IEEE Trans. Electron Devices,* vol. 58, pp. 4219-4225, 2011.

[35] H. Fang *et al*, "High-performance single layered WSe2 p-FETs with chemically doped contacts," *Nano Letters,* vol. 12, pp. 3788-3792, 2012.

[36] T. Fukushima, "Precise and fast computation of Fermi–Dirac integral of integer and half integer order by piecewise minimax rational approximation," *Applied Mathematics and Computation,* vol. 259, pp. 708-729, 2015.

[37] T. Fukushima, "Precise and fast computation of inverse Fermi–Dirac integral of order 1/2 by minimax rational function approximation," *Applied Mathematics and Computation,* vol. 259, pp. 698-707, 2015.

[38] T. Fukushima, "Computation of a general integral of Fermi–Dirac distribution by McDougall–Stoner method," *Applied Mathematics and Computation,* vol. 238, pp. 485-510, 2014.

[39] T. Fukushima, "Analytical computation of generalized Fermi–Dirac integrals by truncated Sommerfeld expansions," *Applied Mathematics and Computation,* vol. 234, pp. 417-433, 2014.

[40] X. Gao *et al*, "Quantum computer aided design simulation and optimization of semiconductor quantum dots," *J. Appl. Phys.,* vol. 114, pp. 164302, 2013.

[41] M. Goano, "Algorithm 745: Computation of the complete and incomplete Fermi-Dirac integral," *ACM Transactions on Mathematical Software (TOMS),* vol. 21, pp. 221-232, 1995.

[42] Z. Gong, W. Däppen and L. Zejda, "MHD equation of state with relativistic electrons," *Astrophys. J.,* vol. 546, pp. 1178, 2001.

[43] B. Groß *et al*, "Dissociative water vapour absorption in BaZr 0.85 Y 0.15 O 2.925/H 2 O: pressure–compositions isotherms in terms of Fermi–Dirac statistics," *Physical Chemistry Chemical Physics,* vol. 2, pp. 297-301, 2000.

[44] Z. Guo *et al*, "3-D Analytical Model for Short-Channel Triple-Gate Junctionless MOSFETs," *IEEE Trans. Electron Devices,* vol. 63, pp. 3857-3863, 2016.

[45] I. Guseinov and B. Mamedov, "Unified treatment for accurate and fast evaluation of the Fermi–Dirac functions," *Chinese Physics B,* vol. 19, pp. 050501, 2010.

[46] G. Halkias and A. Vegiri, "Device parameter optimization of strained Si channel SiGe/Si n-MODFET's using a one-dimensional charge control model," *IEEE Trans. Electron Devices,* vol. 45, pp. 2430-2436, 1998.

[47] C. Harder *et al*, "Noise equivalent circuit of a semiconductor laser diode," *IEEE J. Quant. Electron.,* vol. 18, pp. 333-337, 1982.

[48] F. B. Hildebrand, *Introduction to Numerical Analysis.* Courier Corporation, 1987.

[49] R. Hosseini, "Uncoupled mode space approach for analysis of nanoscale strained junctionless double-gate MOSFET," *Journal of Computational Electronics,* vol. 15, pp. 787-794, 2016.

[50] B. Johnson and J. McCallum, "Dopant-enhanced solid-phase epitaxy in buried amorphous silicon layers," *Physical Review B,* vol. 76, pp. 045216, 2007.

[51] E. Jones, "Rational Chebyshev approximation of the Fermi-Dirac integrals," *Proc IEEE,* vol. 54, pp. 708-709, 1966.

[52] W. Joyce and R. Dixon, "Analytic approximations for the Fermi energy of an ideal Fermi gas," *Appl. Phys. Lett.,* vol. 31, pp. 354-356, 1977.

[53] A. Khan and A. Das, "General Diffusivity-Mobility Relationship for Heavily Doped Semiconductors," *Zeitschrift Für Naturforschung A,* vol. 64, pp. 257-262, 2009.

[54] N. Kozhukhov, B. Oh and H. Shin, "Approximations to field-effect factor and their use in GIDL modeling," in *Physical and Failure Analysis of Integrated Circuits (IPFA), 2011 18th IEEE International Symposium on the,* pp. 1-4, 2011.

[55] J. Lami and C. Hirlimann, "Two-photon excited room-temperature luminescence of CdS in the femtosecond regime," *Physical Review B,* vol. 60, pp. 4763, 1999.

[56] P. Landsberg, "On the diffusion theory of rectification," in *Proceedings of the Royal Society of London A: Mathematical, Physical and Engineering Sciences,* pp. 226-237, 1952.

[57] Z. Li, S. McAlister and C. Hurd, "Use of Fermi statistics in two-dimensional numerical simulation of heterojunction devices," *Semiconductor Science and Technology,* vol. 5, pp. 408, 1990.

[58] L. Lin *et al*, "Pole-based approximation of the Fermi-Dirac function," *Chinese Annals of Mathematics, Series B,* vol. 30, pp. 729, 2009.

[59] P. Loskot and N. C. Beaulieu, "Prony and polynomial approximations for evaluation of the average probability of error over slow-fading channels," *IEEE Transactions on Vehicular Technology,* vol. 58, pp. 1269-1280, 2009.

[60] M. S. Lundstrom and R. J. Schuelke, "Numerical analysis of heterostructure semiconductor devices," *IEEE Trans. Electron Devices,* vol. 30, pp. 1151-1159, 1983.

[61] A. J. MacLeod, "Algorithm 779: Fermi-Dirac functions of order-1/2, 1/2, 3/2, 5/2," *ACM Transactions on Mathematical Software (TOMS),* vol. 24, pp. 1-12, 1998.

[62] B. Mamedov, "Analytical evaluation of the plasma dispersion function for a Fermi Dirac distribution," *Chinese Physics B,* vol. 21, pp. 055204, 2012.

[63] A. H. Marshak *et al*, "Rigid band analysis of heavily doped semiconductor devices," *IEEE Trans. Electron Devices,* vol. 28, pp. 293-298, 1981.

[64] J. McDougall and E. C. Stoner, "The computation of Fermi-Dirac functions," *Philosophical Transactions of the Royal Society of London.Series A, Mathematical and Physical Sciences,* vol. 237, pp. 67-104, 1938.

[65] H. Mehta and H. Kaur, "Modeling and simulation study of novel Double Gate Ferroelectric Junctionless (DGFJL) transistor," *Superlattices and Microstructures,* vol. 97, pp. 536-547, 2016.

[66] D. Melrose and A. Mushtaq, "Plasma dispersion function for a Fermi–Dirac distribution," *Phys Plasmas,* vol. 17, pp. 122103, 2010.

[67] M. I. Miah, "Spin transport in the degenerate and diffusion regimes," *J. Appl. Phys.,* vol. 103, pp. 123711, 2008.

[68] M. I. Miah, "Drift-diffusion crossover and the intrinsic spin diffusion lengths in semiconductors," *J. Appl. Phys.,* vol. 103, pp. 063718, 2008.

[69] M. Miczek *et al*, "Effects of interface states and temperature on the C-V behavior of metal/insulator/AlGaN/GaN heterostructure capacitors," *J. Appl. Phys.,* vol. 103, pp. 104510, 2008.

[70] U. K. Mishra, *Semiconductor Device Physics and Design.* Dordrecht: Springer, 2007.

[71] S. N. Mohammed and S. Abidi, "Current, carrier concentration, Fermi energy, and related properties of binary compound polar semiconductors with nonparabolic energy bands," *J. Appl. Phys.,* vol. 60, pp. 1384-1390, 1986.

[72] N. Mohankumar and A. Natarajan, "On the very accurate numerical evaluation of the Generalized Fermi–Dirac Integrals," *Comput. Phys. Commun.,* vol. 207, pp. 193-201, 2016.

[73] N. Mohankumar and A. Natarajan, "A note on the evaluation of the generalized Fermi-Dirac integral," *Astrophys. J.,* vol. 458, pp. 233, 1996.

[74] N. Mohankumar and A. Natarajan, "The accurate numerical evaluation of half-order Fermi-Dirac Integrals," *Physica Status Solidi (b),* vol. 188, pp. 635-644, 1995.

[75] K. K. Ng, "Appendix D: Physical properties," in Anonymous Wiley Online Library, pp. 671-696, 2010.

[76] B. Pichon, "Numerical calculation of the generalized Fermi-Dirac integrals," *Comput. Phys. Commun.,* vol. 55, pp. 127-136, 1989.

[77] R. Prony, "Essai experimental–,-," *J.De l'Ecole Polytechnique,* 1795.

[78] E. Ramayya and I. Knezevic, "Self-consistent Poisson-Schrödinger-Monte Carlo solver: electron mobility in silicon nanowires," *Journal of Computational Electronics,* vol. 9, pp. 206-210, 2010.

[79] P. Rhodes, "Fermi-dirac functions of integral order," in *Proceedings of the Royal Society of London A: Mathematical, Physical and Engineering Sciences,* pp. 396-405, 1950.

[80] T. Rivlin, "Chebyshev Polynomials. From Approximation Theory to Algebra and Number Theory. 1990," *Pure Appl.Math.(NY),* 1990.

[81] D. Roy and A. Biswas, "Performance optimization of nanoscale junctionless transistors through varying device design parameters for ultra-low power logic applications," *Superlattices and Microstructures,* vol. 97, pp. 140-154, 2016.

[82] J. Sallese *et al*, "Charge-based modeling of junctionless double-gate field-effect transistors," *IEEE Trans. Electron Devices,* vol. 58, pp. 2628-2637, 2011.

[83] S. San Li and F. Lindholm, "Alternative formulation of generalized Einstein relation for degenerate semiconductors," *Proc IEEE,* vol. 56, pp. 1256-1257, 1968.

[84] C. Selvakumar, "Approximations to two-step diffusion process by Prony's method," *Proc IEEE,* vol. 70, pp. 514-516, 1982.

[85] C. Selvakumar, "Approximations to Fermi-Dirac integrals and their use in device analysis," *Proc IEEE,* vol. 70, pp. 516-518, 1982.

[86] M. Sherwin and T. Drummond, "A parametric investigation of AlGaAs/GaAs modulation-doped quantum wires," *J. Appl. Phys.,* vol. 66, pp. 5444-5455, 1989.

[87] I. SILVACO, "ATLAS User's Manual," *Santa Clara, CA, Ver,* vol. 5, 2011.

[88] M. A. Sobhan and S. NoorMohammad, "Approximation for the Fermi–Dirac integral with applications to the modeling of charge transport in heavily doped semiconductors," *J. Appl. Phys.,* vol. 58, pp. 2634-2637, 1985.

[89] A. Sommerfeld, "Zur elektronentheorie der metalle auf grund der fermischen statistik," *Zeitschrift Für Physik,* vol. 47, pp. 1-32, 1928.

[90] Synopsys, "Sentaurus Device User Manual," June 2012.

[91] D. Szmyd, M. Hanna and A. Majerfeld, "Heavily doped GaAs: Se. II. Electron mobility," *J. Appl. Phys.,* vol. 68, pp. 2376-2381, 1990.

[92] D. Szmyd *et al*, "Heavily doped GaAs: Se. I. Photoluminescence determination of the electron effective mass," *J. Appl. Phys.,* vol. 68, pp. 2367-2375, 1990.

[93] M. Taher, "Approximations for fermi-dirac integrals Fj (x)," *Solid-State Electronics,* vol. 37, pp. 1677-1679, 1994.

[94] A. Trellakis, A. Galick and U. Ravaioli, "Rational Chebyshev approximation for the Fermi-Dirac integral F− 32 (x)," *Solid-State Electronics,* vol. 41, pp. 771-773, 1997.

[95] R. D. Trevisoli *et al*, "A physically-based threshold voltage definition, extraction and analytical model for junctionless nanowire transistors," *Solid-State Electronics,* vol. 90, pp. 12-17, 2013.

[96] H. Van Cong and B. Doan-Khanh, "Simple accurate general expression of the Fermi-Dirac integral Fj (a) for arbitrary a and j>− 1," *Solid-State Electronics,* vol. 35, pp. 949-951, 1992.

[97] P. Van Halen and D. Pulfrey, "Accurate, short series approximations to Fermi–Dirac integrals of order− 1/2, 1/2, 1, 3/2, 2, 5/2, 3, and 7/2," *J. Appl. Phys.,* vol. 57, pp. 5271-5274, 1985.

[98] R. Venugopal *et al*, "Simulating quantum transport in nanoscale transistors: Real versus mode-space approaches," *J. Appl. Phys.,* vol. 92, pp. 3730-3739, 2002.

[99] X. Wan *et al*, "Enhanced performance and fermi-level estimation of coronene-derived graphene transistors on self-assembled monolayer modified substrates in large areas," *The Journal of Physical Chemistry C,* vol. 117, pp. 4800-4807, 2013.

[100] A. Wang, M. Tadjer and F. Calle, "Simulation of thermal management in AlGaN/GaN HEMTs with integrated diamond heat spreaders," *Semiconductor Science and Technology,* vol. 28, pp. 055010, 2013.

[101] M. Wang *et al*, "n-CdSe/p-ZnTe based wide band-gap light emitters: Numerical simulation and design," *J. Appl. Phys.,* vol. 73, pp. 4660-4668, 1993.

[102] Y. Wang *et al*, "High performance of junctionless MOSFET with asymmetric gate," *Superlattices and Microstructures,* vol. 97, pp. 8-14, 2016.

[103] Z. Xiao and T. Wei, "Modification of the Einstein equations of majority-and minority-carriers with band gap narrowing effect in n-type degenerate silicon with degenerate approximation and with non-parabolic energy bands," *IEEE Trans. Electron Devices,* vol. 44, pp. 913-914, 1997.

[104] W. Ze-Qing, L. Shi-Chang and H. Guo-Xing, "Opacity calculations for a non-LTE system with the three-temperature model," *Journal of Quantitative Spectroscopy and Radiative Transfer,* vol. 56, pp. 623-627, 1996.

[105] L. Zhang and M. Chan, "SPICE modeling of double-gate tunnel-FETs including channel transports," *IEEE Trans. Electron Devices,* vol. 61, pp. 300-307, 2014.

Appendix A

Blakemore Tables

The Table A.1 in this appendix shows the "actual values" of the FDI as tabulated by Blakemore. These are the actual values which have been used in this thesis.

Table A.1 Blakemore's Tabulated Values

η	$F_{-\frac{3}{2}}(\eta)$	$F_{-\frac{1}{2}}(\eta)$	$F_{\frac{1}{2}}(\eta)$	$F_{\frac{3}{2}}(\eta)$	$F_{\frac{5}{2}}(\eta)$	$F_{\frac{7}{2}}(\eta)$
-4	0.0178	0.01808	0.018199	0.018256	0.018287	0.018301
-3.9	0.0196	0.01995	0.020099	0.02017	0.020206	0.020224
-3.8	0.0217	0.02203	0.022195	0.022283	0.022327	0.022349
-3.7	0.0238	0.02429	0.02451	0.024617	0.02467	0.024697
-3.6	0.0263	0.02681	0.027063	0.027193	0.027259	0.027291
-3.5	0.0289	0.02956	0.02988	0.030037	0.030118	0.030158
-3.4	0.0318	0.0326	0.032986	0.033179	0.033276	0.033325
-3.3	0.035	0.03595	0.036412	0.036645	0.036764	0.036824
-3.2	0.0385	0.03962	0.040187	0.040473	0.040617	0.04069
-3.1	0.0423	0.04367	0.044349	0.044696	0.044872	0.044961
-3	0.0465	0.0481	0.048933	0.049356	0.049571	0.049679
-2.9	0.051	0.05298	0.053984	0.054498	0.054759	0.054891
-2.8	0.056	0.05831	0.059545	0.06017	0.060488	0.060649
-2.7	0.0613	0.06417	0.065665	0.066425	0.066813	0.067009
-2.6	0.0671	0.07059	0.072398	0.073323	0.073795	0.074033
-2.5	0.0735	0.07762	0.079804	0.080927	0.081501	0.081791
-2.4	0.0802	0.08529	0.087944	0.089309	0.090006	0.09036
-2.3	0.0876	0.09369	0.096887	0.098544	0.099391	0.099822
-2.2	0.0955	0.10284	0.10671	0.10872	0.10975	0.11027
-2.1	0.104	0.1128	0.11748	0.11992	0.12117	0.12181
-2	0.1132	0.12366	0.1293	0.13225	0.13377	0.13454
-1.9	0.1229	0.13546	0.14225	0.14581	0.14766	0.1486
-1.8	0.1331	0.14826	0.15642	0.16074	0.16297	0.16412
-1.7	0.1442	0.16213	0.17193	0.17714	0.17986	0.18125

η	$F_{-\frac{3}{2}}(\eta)$	$F_{-\frac{1}{2}}(\eta)$	$F_{\frac{1}{2}}(\eta)$	$F_{\frac{3}{2}}(\eta)$	$F_{\frac{5}{2}}(\eta)$	$F_{\frac{7}{2}}(\eta)$
-1.6	0.1558	0.17712	0.18889	0.19517	0.19846	0.20015
-1.5	0.168	0.1933	0.2074	0.21497	0.21895	0.22099
-1.4	0.1808	0.21074	0.22759	0.23671	0.24152	0.24401
-1.3	0.1941	0.22948	0.24959	0.26055	0.26636	0.26938
-1.2	0.208	0.24958	0.27353	0.28669	0.2937	0.29736
-1.1	0.2222	0.27108	0.29955	0.31533	0.32378	0.32822
-1	0.2367	0.29402	0.3278	0.34667	0.35686	0.36222
-0.9	0.2517	0.31845	0.35841	0.38096	0.39321	0.3997
-0.8	0.2667	0.34438	0.39154	0.41844	0.43316	0.44098
-0.7	0.282	0.37181	0.42733	0.45936	0.47702	0.48646
-0.6	0.2971	0.40077	0.46595	0.504	0.52515	0.53653
-0.5	0.3121	0.43123	0.50754	0.55265	0.57795	0.59164
-0.4	0.3268	0.46318	0.55224	0.60561	0.63583	0.65229
-0.3	0.341	0.49657	0.60022	0.66321	0.69923	0.71899
-0.2	0.3548	0.53137	0.65161	0.72577	0.76863	0.79234
-0.1	0.3677	0.5675	0.70654	0.79365	0.84455	0.87294
0	0.38	0.6049	0.76515	0.8672	0.92755	0.96148
0.1	0.3915	0.64348	0.82756	0.9468	1.0182	1.0587
0.2	0.4019	0.68317	0.89388	1.0328	1.1171	1.1654
0.3	0.4114	0.72384	0.96422	1.1257	1.225	1.2824
0.4	0.4196	0.7654	1.0387	1.2258	1.3425	1.4107
0.5	0.4269	0.80774	1.1173	1.3336	1.4704	1.5513
0.6	0.4328	0.85074	1.2003	1.4494	1.6095	1.7052
0.7	0.4378	0.89429	1.2875	1.5738	1.7606	1.8736
0.8	0.4415	0.93826	1.3791	1.7071	1.9246	2.0577
0.9	0.4441	0.98255	1.4752	1.8497	2.1023	2.2589
1	0.4457	1.0271	1.5756	2.0023	2.2948	2.4787
1.1	0.4463	1.0717	1.6806	2.165	2.5031	2.7184
1.2	0.4459	1.1163	1.79	2.3385	2.7282	2.9799

η	$F_{-\frac{3}{2}}(\eta)$	$F_{-\frac{1}{2}}(\eta)$	$F_{\frac{1}{2}}(\eta)$	$F_{\frac{3}{2}}(\eta)$	$F_{\frac{5}{2}}(\eta)$	$F_{\frac{7}{2}}(\eta)$
1.3	0.4447	1.1608	1.9038	2.5232	2.9712	3.2647
1.4	0.4427	1.2052	2.0221	2.7194	3.2332	3.5747
1.5	0.4398	1.2493	2.1449	2.9278	3.5155	3.912
1.6	0.4365	1.2931	2.272	3.1486	3.8192	4.2786
1.7	0.4325	1.3366	2.4035	3.3823	4.1456	4.6766
1.8	0.4281	1.3796	2.5393	3.6294	4.4961	5.1085
1.9	0.4233	1.4222	2.6794	3.8903	4.8719	5.5767
2	0.4182	1.4643	2.8237	4.1654	5.2746	6.0838
2.1	0.4126	1.5058	2.9722	4.4552	5.7055	6.6325
2.2	0.407	1.5468	3.1249	4.76	6.1662	7.2258
2.3	0.4013	1.5872	3.2816	5.0803	6.658	7.8668
2.4	0.3954	1.6271	3.4423	5.4164	7.1827	8.5585
2.5	0.3893	1.6663	3.607	5.7689	7.7419	9.3044
2.6	0.3833	1.7049	3.7755	6.138	8.3371	10.108
2.7	0.3772	1.743	3.948	6.5241	8.97	10.973
2.8	0.3712	1.7804	4.1241	6.9277	9.6425	11.903
2.9	0.3654	1.8172	4.304	7.3491	10.356	12.903
3	0.3595	1.8535	4.4876	7.7886	11.113	13.976
3.1	0.3537	1.8891	4.6747	8.2467	11.915	15.127
3.2	0.3481	1.9242	4.8653	8.7237	12.763	16.36
3.3	0.3425	1.9588	5.0595	9.2199	13.66	17.681
3.4	0.337	1.9927	5.2571	9.7357	14.608	19.094
3.5	0.3319	2.0262	5.458	10.271	15.608	20.605
3.6	0.3267	2.0591	5.6623	10.827	16.662	22.218
3.7	0.3216	2.0915	5.8699	11.404	17.774	23.939
3.8	0.3167	2.1235	6.0806	12.001	18.944	25.774
3.9	0.312	2.1549	6.2945	12.62	20.175	27.73
4	0.3075	2.1859	6.5115	13.26	21.469	29.812